UNIVERSIDADE ESTADUAL PAULISTA
"JULIO DE MESQUITA FILHO"
FACULDADE DE CIÊNCIAS
Programa de Pós-Graduação em Ciência e Tecnologia de Materiais

MULTICOMPONENT SOLID FORMS OF NIMESULIDE: SYNTHESIS, CHARACTERIZATION AND EVALUATION OF PHYSICOCHEMICAL PROPERTIES

Amanda Cosmo de Almeida

BAURU
2025

AMANDA COSMO DE ALMEIDA

MULTICOMPONENT SOLID FORMS OF NIMESULIDE: SYNTHESIS, CHARACTERIZATION AND EVALUATION OF PHYSICOCHEMICAL PROPERTIES

Doctoral thesis presented to the Postgraduate Program in Materials Science and Technology (POSMAT), at the São Paulo State University (UNESP), as a partial requirement to obtain the title of Doctor in Science and Materials Technology, concentration area Materials Chemistry.

Advisor: Prof. Dr. Flávio Junior Caires
Co-advisor: Profa. Dra. M. Ermelinda S. Eusébio

Bauru
2025

D279m

Almeida, Amanda Cosmo de

Multicomponent solid forms of nimesulide : Synthesis, characterization and evaluation of physicochemical properties / Amanda Cosmo de Almeida. -- Bauru, 2025

107 f. : il., tabs.

Tese (doutorado) - Universidade Estadual Paulista (UNESP), Faculdade de Ciências, Bauru

Orientador: Flávio Junior Caires

Coorientadora: Maria Ermelinda da Silva Eusébio

1. Multicomponent solid forms. 2. Virtual-experimental screening. 3. Phase diagrams. 4. Dissolution rate. 5. Non-steroidal anti-inflammatory drugs. I. Título.

Sistema de geração automática de fichas catalográficas da Unesp. Dados fornecidos pelo autor(a).

ATA DA DEFESA PÚBLICA DA TESE DE DOUTORADO DE AMANDA COSMO DE ALMEIDA, DISCENTE DO PROGRAMA DE PÓS-GRADUAÇÃO EM CIÊNCIA E TECNOLOGIA DE MATERIAIS, DA FACULDADE DE CIÊNCIAS - CÂMPUS DE BAURU.

Aos 24 dias do mês de outubro do ano de 2025, às 9h, por meio de Videoconferência, realizou-se a defesa de TESE DE DOUTORADO de AMANDA COSMO DE ALMEIDA, intitulada **Multicomponent solid forms of nimesulide: Synthesis, characterization and evaluation of physicochemical properties**, sob orientação do Prof. Dr. Flavio Junior Caires. A Comissão Examinadora foi constituída pelos seguintes membros: Prof. Dr. FLAVIO JUNIOR CAIRES (Orientador(a) - Participação Virtual) do(a) Departamento de Química / Faculdade de Ciências - Unesp/Câmpus de Bauru, Prof. Dr. MÁRIO TÚLIO DOS SANTOS ROSADO (Participação Virtual) do(a) Departamento de Química / Universidade de Coimbra - UC - Coimbra, Prof. Dr. AROLDO GERALDO MAGDALENA (Participação Virtual) do(a) Departamento de Química / Faculdade de Ciências - Unesp/Câmpus de Bauru, Prof. Dr. FENELON MARTINHO LIMA PONTES (Participação Virtual) do(a) Departamento de Química / Faculdade de Ciências - Unesp/Câmpus de Bauru, Profa. Dra. ANA CARINA SOBRAL CARVALHO (Participação Virtual) do(a) Centro de Química Estrutural / Instituto Superior Técnico, Universidade de Lisboa. Após a exposição pela doutoranda e arguição pelos membros da Comissão Examinadora que participaram do ato, de forma presencial e/ou virtual, a discente recebeu o conceito final:_ _Aprovado_ _ _ _ _ _ _ . Nada mais havendo, foi lavrada a presente ata, que após lida e aprovada, foi assinada pelo(a) Presidente(a) da Comissão Examinadora.

Prof. Dr. FLAVIO JUNIOR CAIRES

gov.br Documento assinado digitalmente
FLAVIO JUNIOR CAIRES
Data: 10/11/2025 14:08:01-0300
Verifique em https://validar.iti.gov.br

ACKNOWLEDGEMENTS

Apesar de toda a minha tese de doutorado estar escrita em inglês, sinto que meus agradecimentos precisam ser expressos em minha língua materna, para que eu possa expressar os meus reais sentimentos de gratidão.

Gratidão é uma palavra muito pequena frente a todo sentimento que sinto neste momento em que escrevo. É muito difícil agradecer apenas com palavras a todas as pessoas e entidades que de algum modo me proporcionaram chegar até aqui.

Em primeiro lugar e sempre, à Deus e aos meus protetores espirituais. Esse doutorado como um todo foi a realização de muitas orações minhas, de meus pais e de meus ancestrais. Gratidão por toda força, sabedoria e proteção durante esses anos. Obrigada por colocarem tantas pessoas e oportunidades maravilhosas em meu caminho.

Agradeço aos meus pais, Rosângela e Pedro, por me incentivarem a seguir meus sonhos, por serem exemplo de garra e determinação, por todo suporte que sempre recebi. Obrigada por me amarem tanto e por renunciarem de seus sonhos em prol dos meus. Eu os amo e espero um dia retribuir tudo o que fizeram e fazem por mim.

Ao meu marido e companheiro de aventuras, Rafael, que por vezes abdicou de suas coisas para me auxiliar nessa caminhada, que topou cruzar o oceano comigo e viver em terras lusitanas, que me incentivou e incentiva todos os dias a ir em busca dos meus objetivos. Obrigada por seu amor, eu te amo.

Ao meu irmão, Guilherme, por demonstrar seu amor por mim de forma singular e por sempre acreditar em mim. Aos meus sobrinhos Davi e Isis, meu afilhado Luís Fernando e minhas “primas-irmãs” Maria Eugênia, Franciele e Elena. Obrigada por simplesmente existirem e trazerem brilho para minha vida.

Quero agradecer ainda, todos os meus familiares, principalmente meus avós, Irene, Aparecida (em memória), José “Baté” (em memória) e Pedro (em memória), por depositarem em mim a esperança de um futuro melhor. Muito obrigada por estarem sempre zelando por mim onde quer que estejam.

Ao meu orientador, Prof. Dr. Flávio Junior Caires, por toda orientação e conselhos desde 2016. Agradeço por acreditar no meu potencial, por me impulsionar sempre para ser cada vez melhor e até pelos “puxões de orelha”.

Obrigada pela confiança que deposita em mim. Obrigada por esses anos de parceria, hoje sei que finalizo esta etapa levando comigo um amigo.

Outra peça-chave desse doutorado, com certeza foi a minha querida coorientadora Professora Ermelinda Eusébio. Quanto amor e dedicação podem caber dentro deste ser humano? Eu só sei agradecer imensamente pelas trocas, pelas risadas e pelos momentos que eu jamais me esquecerei, sem contar todo o conhecimento compartilhado comigo. Muitíssimo obrigada!

Além disso, existem pessoas com as quais compartilhamos momentos de alegria, tristeza, choros, conquistas, mas que não temos laços sanguíneos. Esses podemos chamar de amigos. Pessoas especiais que são colocadas em nossas vidas. Algumas há anos, outras nem tanto. Ainda assim, necessito de agradecê-los por tornarem essa caminhada mais leve e amena. Muito obrigada aos meus amigos do Laboratório de Análise Térmica e Química do Estado Sólido (LATQES), Laura, Aniele, Giovanna, Mavi e Giulia. E também amigos do estimado “LATIG Araraquara”, em especial à querida Ana Carina (Aninha).

Um agradecimento especial minha parceira e “irmã” Patrícia Osório. O que seria de mim sem essa mulher? Obrigada por toda ajuda, por ser apoio nos momentos difíceis, pela cumplicidade, pelos momentos memoráveis. Obrigada por ser meu braço direito durante esses anos.

Aos amigos e Professores do Laboratório de Termodinâmica e Química do Estado Sólido (LTQES) da Universidade de Coimbra – Portugal. À querida Joseany Almeida, que se tornou uma amiga muito especial, que me ajudou passar pelo período de intercâmbio de uma forma muito mais leve e agradável. Que nossa amizade perdure por muito anos, independente da distância.

Aos meus melhores amigos de vida, João Henrique Pelissari, Murilo Cruciol Pamela de Melo, Maria Carolina. Muito obrigada por tantos anos de amizade, por aguentarem meu jeitinho de ser, por me apoiarem e por estarem sempre comigo, mesmo com a correria do dia a dia.

À querida Rosinéia Aredes por ser um instrumento de Deus em minha vida. Por me guiar e cuidar espiritualmente, me dando conselhos e palavras de sabedoria nos momentos que eu mais precisei.

Agradeço aos Professores e laboratórios parceiros por concederem a utilização de seus equipamentos para a realização de minhas análises, e aos seus alunos pela disponibilidade e auxílio.

Agradeço à Coordenação de Aperfeiçoamento de Pessoal de Nível Superior (CAPES) pelo financiamento de minha pesquisa de doutorado (Processos n° 88887.495148/2020-00 e n° 88887.817528/2022-00), bem como a bolsa de doutorado sanduíche recebida no escopo do Programa Capes-PrInt/UNESP (Processo n° 88887.684961/2022-00).

Por fim, agradeço à todas as pessoas que, direta ou indiretamente, contribuíram para meu crescimento pessoal e profissional, resultando na realização deste trabalho. Finalizá-lo, é de fato um momento muito sonhado e esperado.

Com amor e gratidão, Amanda Cosmo de Almeida

"*To everything there is a season, and a time to every purpose under the heaven*"

(Ecclesiastes 3:1)

DE ALMEIDA, Amanda Cosmo. **Multicomponent solid forms of nimesulide: Synthesis, characterization and evaluation of physicochemical properties**. 2025. 107p. Thesis (PhD in Science and Technology of Materials) – UNESP, School of Sciences, Bauru, 2025.

ABSTRACT

One of the main problems faced by the pharmaceutical industry in the search for new drugs is related to the low aqueous solubility of active pharmaceutical ingredients (APIs), which limits the oral bioavailability, efficacy, and clinical safety of an API. The development of multicomponent solid forms, such as salts, cocrystals, eutectic mixtures, and coamorphous systems, has been a widely used strategy to modulate the physicochemical properties of these compounds. In this sense, this work aimed to develop new multicomponent solid forms of nimesulide (NMS), a widely used non-steroidal anti-inflammatory drug that exhibits low aqueous solubility. The virtual screening of cocrystals was performed using the COSMOquick software, from which 30 coformers with adjuvant potential were selected, and experimental screening was carried out using the mechanochemical method. Coamorphous systems between two APIs (drug-drug) were also investigated using quench cooling and/or cryogenic milling processes. Through these strategies, piperazine-NMS cocrystal (NMS-PPZ), two new eutectic mixtures of gentisic acid (NMS-GSA) and isoniazid (NMS-INH), as well as new dual-drug coamorphous systems (with *para*-aminobenzoic acid, bicalutamide, isoniazid, metoclopramide, omeprazole, piracetam, and tenoxicam) were obtained. All solid samples were characterized using differential scanning calorimetry (DSC), powder X-ray diffraction (PXRD), and infrared spectroscopy (FTIR). Eutectic compositions were determined by constructing

binary solid-liquid phase diagrams and Tamman triangles. Among the compounds, the coamorphous NMS-omeprazole (NMS-OMP) proved to be stable for at least 120 days under dry conditions (stored in a desiccator at room temperature). The coamorphous system with bicalutamide (NMS-BICA) prepared by quench cooling is more stable than by cryomilling. The results demonstrate the potential to improve the aqueous solubility of drugs through the development of multicomponent nimesulide systems.

Keywords: Multicomponent solid forms; Virtual-experimental screening; Phase diagrams; Dissolution rate; Non-steroidal anti-inflammatory drugs.

DE ALMEIDA, Amanda Cosmo. **Formas sólidas multicomponentes de nimesulida: Síntese, caracterização e avaliação de propriedades físico-químicas**. 2025. 107f. Tese (Doutora em Ciência e Tecnologia de Materiais) – UNESP, Faculdade de Ciências, Bauru, 2025.

RESUMO

Um dos principais problemas enfrentados pela indústria farmacêutica na prospecção de novos fármacos está relacionada à baixa solubilidade aquosa de insumos farmacêuticos ativos (APIs, do inglês *Active Pharmaceutical Ingredients*), que limitam a biodisponibilidade oral, eficácia e segurança clínica de um API. O desenvolvimento de formas sólidas multicomponentes, tais como sais, cocristais, misturas eutéticas e coamorfos, tem sido uma estratégia amplamente utilizada para modular as propriedades físico-químicas destes compostos. Neste sentido, este trabalho teve como objetivo o desenvolvimento de novas formas sólidas multicomponentes de nimesulida (NMS), um fármaco anti-inflamatório não esteroide amplamente utilizado que apresenta baixa solubilidade aquosa. A triagem virtual de cocristais foi feito por meio do software COSMOquick, dos quais foram selecionados 30 coformadores com potencial coadjuvante, e a triagem experimental foi feita através do método mecanoquímico. Também foram investigados sistemas coamorfos entre dois APIs (*drug-drug*) por processos de resfriamento rápido (*quench cooling*) e/ou moagem criogênica. Por meio destas estratégias, foram obtidos um cocristal de NMS-piperazina (NMS-PPZ), duas novas misturas eutéticas de NMS-ácido gentísico (NMS-GSA) e NMS-isoniazida (NMS-INH), bem como novos sistemas coamorfos dual-drug (com ácido para-amminobenzóico, bicalutamida, isoniazida, metoclopramida, omeprazol, piracetam e tenoxicam). Todas as

amostras sólidas foram caracterizadas utilizando calorimetria exploratória diferencial (DSC), difração de raios-X de pó (PXRD) e espectroscopia de infravermelho (FTIR). As composições eutéticas foram determinadas pela construção de diagramas de fase binário sólido-líquido e triângulos de Tamman. Dentre os compostos, o sistema coamorfo NMS-omeprazol (NMS-OMP) revelou-se estável por pelo menos 120 dias em condições secas (armazenadas em dessecador à temperatura ambiente). O sistema coamorfo com bicalutamida (NMS-BICA) preparado por *quench cooling* é mais estável do que por criomoagem. Os resultados demostram potencialidade de melhorar a solubilidade aquosa de fármacos por meio do desenvolvimento de sistemas multicomponentes de nimesulida.

Palavras-chave: Sistemas sólidos multicomponentes; Triagem virtual-experimental; Diagramas de fase; Taxa de dissolução; Anti-inflamatórios não-esteroides.

LIST OF FIGURES

Figure 1 – Molecular structure of nimesulide. 25
Figure 2 – Explored coformers in the virtual-experimental screening methodology. 28
Figure 3 – Percentage distribution of drugs according to the Biopharmaceutics Classification System (BCS). Adapted from (BABU; NANGIA, 2011). 31
Figure 4 – Schematic representation of pharmaceutical solid forms. Adapted from (CHERUKUVADA; NANGIA, 2014). 32
Figure 5 – Schematic representation of the formation of multicomponent salt, (molecular) cocrystal or ionic cocrystal. Reproduced from (SOLARES-BRIONES et al., 2021). 34
Figure 6 – Supramolecular homosynthons (acid-acid (a) and amide-amide (b)) and heterosynthons (acid-amide (c) and acid-pyridine (d)). Reproduced from (DUGGIRALA et al., 2016). 35
Figure 7 – Schematic representation of coamorphous, polymer-based and mesoporous particle-based amorphous systems. Adapted from (SHI; MOINUDDIN; CAI, 2019)..... 37
Figure 8 – Schematic representation of eutectic mixture, cocrystal and solid solution based on intermolecular interactions. Adapted from (BAZZO; PEZZINI; STULZER, 2020)..... 39
Figure 9 – Examples of coformer screening methods. 40
Figure 10 – Classification of various methods for preparing multicomponent systems. 44
Figure 11 – The scale of η parameter. Adapted from (FRIŠČIĆ; MOTTILLO; TITI, 2020). 44
Figure 12 – Schematic representation of congruent (a) and incongruent (b) ternary phase diagrams. Reproduced from (KARIMI-JAFARI et al., 2018). 45
Figure 13 – Representation of binary phase diagrams with a simple eutectic mixture (a) and cocrystal with congruent melting (b). 50
Figure 14 – Various in-vitro and in-vivo parameters studied during performance evaluation step of multicomponent system development process. 51

Figure 15 – Chemical structures of NMS and selected coformers explored in this study. 55
Figure 16 – TG-DTA-DTG (a) and DSC (b) curves of pure nimesulide. 63
Figure 17 – PXRD pattern (a) and FTIR spectrum (b) of pure nimesulide. 64
Figure 18 – DSC heating curves of NMS-PPZ equimolar system and pure compounds. 66
Figure 19 – PXRD pattern (a) and FTIR spectra (b) of NMS-PPZ equimolar system and pure compounds. 67
Figure 20 – DSC heating curves of NMS-GSA (a) and NMS-INH (b) equimolar systems and pure compounds, prepared by NG and by LAG. 70
Figure 21 – DSC heating curves (a), binary solid-liquid phase diagram (b) and Tamman's triangle (c) of NMS-GSA system for different compositions. In the phase diagram, the dashed lines, correspond to the prediction of Schroder-van Laar equation (PRIGOGINE; DEFAY, 1954). 71
Figure 22 – DSC heating curves (a), binary solid-liquid phase diagram (b) and Tamman's triangle (c) of NMS-INH system for different compositions. In the phase diagram, the dashed lines, correspond to the prediction of Schroder-van Laar equation (PRIGOGINE; DEFAY, 1954). 72
Figure 23 – DSC heating curves of NMS-OMP equimolar mixture and pure compounds, prepared by NG and by LAG. 74
Figure 24 – PXRD pattern of NMS-OMP equimolar mixture and pure compounds, prepared by NG and by LAG. 75
Figure 25 – DSC heating curves of coamorphized NMS-OMP equimolar system and pure compounds. 76
Figure 26 – PXRD pattern of coamorphized NMS-OMP equimolar system and pure compounds. 77
Figure 27 – PXRD pattern of NMS-BICA equimolar mixture and pure compounds. 78
Figure 28 – DSC curves of quench cooled NMS-BICA equimolar mixture and pure compounds. 79
Figure 29 – Dissolution profile of pure NMS and selected multicomponent solid systems. 80

APPENDIX

Figure A.1 – Selectivity essay of NMS, BICA, GSA and INH in phosphate buffer pH 7.4 with 2% (v/v) of tween 80.……103
Figure A.2 – Calibration curves of pure NMS in phosphate buffer pH 7.4 with 2% (v/v) of tween 80 (prepared at 397 nm)..……103
Figure A.3 – PXRD pattern (a) and FTIR spectra (b) of NMS-GSA equimolar system and pure compounds……..……..…….104
Figure A.4 – PXRD pattern (a) and FTIR spectra (b) of NMS-INH equimolar system and pure compounds……..……..105
Figure A.5 – DSC curves of NMS coamorphous systems obtained via quench cooling (QC), cryomilling (Cryo) and/or "cold NG"……..……106
Figure A.6 – FTIR spectra of NMS-OMP equimolar system and pure compounds……..107
Figure A.7 – FTIR spectra of NMS-BICA equimolar mixture and pure compounds.……..……107

LIST OF TABLES

Table 1 – Summary of commercially available pharmaceutical cocrystals. Adapted from (KAVANAGH et al., 2019). 33
Table 2 – Classification of solid dispersions based on solid phase. A: amorphous, C: crystalline. Adapted from (DENGALE et al., 2016; SABERI et al., 2023). ... 37
Table 3 – USP and BP solubility criteria. Reproduced from (SAVJANI; GAJJAR; SAVJANI, 2012). 52
Table 4 – Main FTIR vibrational modes of NMS-PPZ equimolar system and pure compounds. 68

APPENDIX

Table A.1 – Materials, and respective abbreviation, supplier, molecular weight, purity and CAS number. ……100
Table A.2 – Virtual-experimental screening results…….102

LIST OF ABBREVIATIONS AND SYMBOLS

°	Degree
β	Heating rate
δ	Bending (*delta* from Greek alphabet)
Δ	Variation (*delta* from Greek alphabet)
ΔH	Enthalpy variation
ΔH_{excess}	Excess enthalpy or mixing enthalpy
θ	X-ray diffraction angle (*theta* from the Greek alphabet)
λ	Wavelength (*lambda* from the Greek alphabet)
η	Volume of solvent in μL divided by the total sample mass in mg (*eta* from the Greek alphabet)
ν	Stretching (*nu* from the Greek alphabet)
ν_{Asym}	Asymmetric stretching
ν_{Sym}	Symmetric stretching
Abs.	Absorbance
ANVISA	from Portuguese "*Agência Nacional de Vigilância Sanitária*"
API	Active Pharmaceutical Ingredient
ART	Artesunate
BA	Benzamide
BCS	Biopharmaceutics Classification System
BICA	Bicalutamide
BPDCN	[1,1'-biphenyl]-4,4'-dicarbonitrile
BPE	trans-1,2-bis(4-pyridyl)ethene
BZA	Benzoic acid
CAF	Caffeine
CCDC	Cambridge Crystallographic Data Centre
CIP	Ciprofloxacin
CMBN	4-(cyanomethyl)benzonitrile
COSMO	COnductor-like Screening MOdel
COX	Cyclooxygenase enzyme
Cryo	Cryomilling
CSD	Cambridge Structural Database

DITFB	1,4-diiodotetrafluorobenzene
DSC	Differential Scanning Calorimetry
DTA	Differential Thermal Analysis
DTG	Derivative Thermogravimetry
EAFUS	Everything Added to Foods in the United States
EMA	European Medicine Agency
EtOH	Ethanol
FDA	Food and Drug Administration
F_{fit}	Flexibility parameter
FTIR	Infrared spectroscopy
GC	Glucocorticoid
GRAS	“Generally Regarded as Safe”
GSA	Gentisic acid
IDR	Intrinsic dissolution rate
INCA	Isonicotinic acid
INH	Isoniazid
IUPAC	International Union of Pure and Applied Chemistry
LAG	Liquid assisted grinding
MET	Metoclopramide
MNCT	Methyl nicotinate
NA	Nicotinic acid
NG	Neat grinding
NMS	Nimesulide
NOR	Norfloxacin
NSAID	Nonsteroidal anti-inflammatory drug
OMP	Omeprazole
PABA	*p*-Aminobenzoic acid
PIRA	Piracetam
PHEN	4,7-phenanthroline
PPZ	Piperazine
PRO	Proline
PZCA	Pyrazinoic acid
PXRD	Powder X-ray diffraction

QC	Quench cooling
SAC	Saccharin
SDZ	Sulfadiazine
SLA	Salicylamide
SMILES	Simplified Molecular Input Line Entry System
TBM	Theobromine
***T*g**	Glass transition temperature
TG	Thermogravimetry
TG-DTA	Simultaneous Thermogravimetry and Differential Thermal Analysis
THEO	Theophylline
TNX	Tenoxicam
T_{onset}	Onset temperature
T_{peak}	Peak temperature
TRYP	Tryptophan
UV-Vis	Ultraviolet and visible Spectrophotometry

TABLE OF CONTENTS

CHAPTER 1 23

1.1 INTRODUCTION 24

1.2 OBJECTIVES 27

1.2.1 Specific objectives 27

CHAPTER 2 29

2.1 LITERATURE REVIEW 30

2.1.1 Multicomponent solid forms 31

2.1.1.1 Cocrystals 33

2.1.1.2 Coamorphous systems 36

2.1.1.3 Eutectic mixtures 38

2.1.2 Screening and coformer selection methods 40

2.1.2.1 Cambridge Structural Database (CSD) tool 41

2.1.2.2 pKa approach 42

2.1.2.3 COnductor-like Screening MOdel (COSMO) theory 42

2.1.3 Preparation methods 43

2.1.3.1 Solvent evaporation method 44

2.1.3.2 Slurry method 46

2.1.3.3 Mechanochemical methods 46

2.1.3.4 Quench cooling 47

2.1.4 Characterization techniques 48

2.1.4.1 Thermal analysis 48

2.1.4.2 Structural analyses 50

2.1.5 Physical-chemical and performance evaluation 51

CHAPTER 3 54

3.1 INTRODUCTION 55

3.2 MATERIALS AND METHODS 57
3.2.1 List of chemicals used 57
3.2.2 Virtual-experimental cocrystal screening approach 57
3.2.2.1 Mechanochemical synthesis 58
3.2.2.2 Slurry 58
3.2.3 Coamorphous preparation 59
3.2.3.1 Cryomilling (Cryo) and “cold NG” 59
3.2.3.2 Quench cooling (QC) 59
3.2.4 Characterization 60
3.2.4.1 Simultaneous Thermogravimetry and Differential Scanning Calorimetry (TG-DTA) 60
3.2.4.2 Differential scanning calorimetry (DSC) 60
3.2.4.3 Binary solid-liquid phase diagrams and Tamman’s triangle construction 61
3.2.4.4 Infrared spectroscopy (FTIR) 61
3.2.4.5 Powder X-ray diffraction (PXRD) 62
3.2.5 Dissolution rate study 62
3.3 RESULTS AND DISCUSSION 63
3.3.1 Nimesulide characterization 63
3.3.2. Virtual-experimental cocrystal screening and coformers selection 65
3.3.3 Nimesulide cocrystals 66
3.3.4 Nimesulide eutectic mixtures 69
3.3.5 Nimesulide coamorphous systems 72
3.3.5.2 Nimesulide–omeprazole system 73
3.3.5.3 Nimesulide-bicalutamide 77
3.3.6 Dissolution rate study 79
3.4 CONCLUSIONS 81

CHAPTER 4 82
4.1 GENERAL CONCLUSIONS 83
4.2 SCIENTIFIC CONTRIBUTIONS 84
4.2.1 Periodical Peer-Reviewed Publications 84
4.2.2 Event Participations 85
4.2.3 Scholarship and internship 86
REFERENCES 87
Appendix section 100

CHAPTER 1

GENERAL INTRODUCTION AND OBJECTIVES

1.1 INTRODUCTION

Inflammation is a cellular response to numerous stimuli associated with the release of many inflammatory mediators, like oxidative stress, infectious agents, and antigen-antibody interactions genes (ALVES et al., 2020; ASSALI et al., 2018). These stimuli induce pain, fever and general sense of illness. There are two main classes of anti-inflammatory drugs: the glucocorticoids (GCs) and the non-steroidal anti-inflammatory drugs (NSAIDs). The NSAIDs control the inflammatory condition by inhibiting the cyclooxygenase enzymes (COX-1 and COX-2), while the GCs – also called corticosteroids or simply steroids – act through interactions with GC receptors in the cell nucleus, repressing several inflammatory genes (ALVES et al., 2020; ASSALI et al., 2018; BARNES, 2006).

Corticosteroids are steroid hormones released by the adrenal cortex commonly used in the treatment of inflammatory bowel diseases, rheumatoid arthritis, multiple sclerosis, allergic reactions and asthma (ALVES et al., 2020; RAMAMOORTHY; CIDLOWSKI, 2016). Although corticosteroids, such as dexamethasone, prednisone and hydrocortisone, are effective in the treatment of several inflammatory diseases, they have a short half-life, requiring more frequent doses, which is not favorable to the patient. Another problem is the high dose administration or continuous treatment, as they lead to serious adverse effects, like cataracts, glaucoma, muscle weakness, disturbed sleep, skin atrophy, weight gain, diabetes, hypertension, growth retardation, osteoporosis and psychiatric symptoms (ALVES et al., 2020; RAMAMOORTHY; CIDLOWSKI, 2016; SARDANA et al., 2018).

In the case of NSAIDs, every day, about 30 million people take them around the world (BADRI et al., 2016; SZABÓ-RÉVÉSZ, 2018). NSAIDs are among the most widely used therapeutic agents globally, not only by prescription, but also because many of them are available as over-the-counter drugs, allowing self-medication (BADRI et al., 2016; MANRIQUE-MORENO et al., 2016; STAREK; KRZEK, 2009). Moreover, this class of drugs is made up of a numerous and heterogeneous group of compounds. They have the same mechanism of action, inhibiting the COX-enzyme and present anti-inflammatory, analgesic and antipyretic properties. They are very effective for the treatment of diseases accompanied by excessive inflammatory responses, such as rheumatoid arthritis,

osteoarthritis, musculoskeletal disorders, in postoperative conditions and various types of pain attributed to inflammation (MANRIQUE-MORENO et al., 2016; PSOMAS, 2020; RODRÍGUEZ-BARRIENTOS et al., 2009; TASAKI et al., 2012). Furthermore, NSAIDs present a lower health risk when compared to GCs (BADRI et al., 2016).

Despite its wide use, most NSAIDs are classified as class-II drugs in the Biopharmaceutics Classification System (BCS), presenting low solubility and high permeability, exhibiting absorption limited by solubility (SZABÓ-RÉVÉSZ, 2018). In this sense, several approaches have emerged in order to achieve improved physicochemical properties of APIs, solving these solubility problems. These approaches are typically based on altering their solid form, which include polymorphic forms, amorphous solids, solvates or hydrates, cocrystals, and salts (BERRY; STEED, 2017; BOLLA; SANPHUI; NANGIA, 2013; DUGGIRALA et al., 2020; GOPI; BANIK; DESIRAJU, 2017; LI et al., 2020b; SATHISARAN; DALVI, 2018; UPPALA et al., 2022).

Nimesulide (NMS), is shown in Figure 1. NMS is an NSAID classified as a BCS-class II, presenting aqueous solubility of about 0.01 mg mL^{-1} at 25 °C (PATEL et al., 2019; WANG et al., 2020). According to the "*Anuário Estatístico do Mercado Farmacêutico de 2017*" published by *Agência Nacional de Vigilância Sanitária* (ANVISA), NMS was ranked as the 10th best-selling active ingredient (ANVISA, 2018). The increase in consumption of this NSAID in recent years in Brazil made the NMS rise to the 5th position in 2018, remaining there until today (ANVISA, 2019a, 2023).

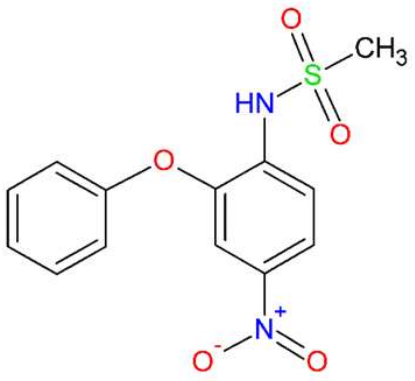


Figure 1 – Molecular structure of nimesulide.

Multicomponent solid forms of NMS with improved physicochemical properties are reported in the literature (ABDELKADER et al., 2014; GEORGESCU et al., 2021; ISMAIL; EL-MAHDY; AL-KUBATI, 2009; PATEL et al., 2019; WANG et al., 2020, 2021b; ZHANG et al., 2021). One example is demonstrated by Patel and co-authors (PATEL et al., 2019). They described the preparation of a eutectic mixture between NMS and nicotinamide, with solubility and dissolution 14 and 2 times greater than pure NMS, respectively.

Given the context, altering the solid form of NMS becomes important to explore the potential of multicomponent approaches in improving its aqueous solubility and dissolution rate. Thus, the overall objective of this study was the virtual-experimental screening, synthesis, characterization, and evaluation of physicochemical properties of multicomponent solid forms of NMS. Some unprecedented cocrystals, coamorphous and eutectic mixtures were obtained and investigated throughout this study, as is reported in the following sections.

1.2 OBJECTIVES

The aim of this work was the screening, preparation, characterization, and evaluation of nimesulide multicomponent solid forms, focusing on improving its physicochemical properties.

1.2.1 Specific objectives

Specific aims of the study are as follows:

- Use a virtual screening methodology to rank the cocrystal formation propensity of nimesulide with selected coformers (chosen with different functional groups, structurally related, or potentially useful as dual-drugs with NMS, Figure 2).
- Evaluate the virtual screening outcomes by performing experimental screening by mechanochemical and slurry methodologies.
- Synthesize novel NMS multicomponent solid forms through different solid-based methods;
- Characterize the API, coformers and multicomponent solid systems through spectroscopic (FTIR), diffractometric (PXRD) and thermal analyses (DSC and TG-DTA) techniques;
- Construct solid-liquid binary phase diagrams and Tamman's triangle of eutectic mixtures to determine their stoichiometric composition;
- Investigate physicochemical properties of selected samples and compare with the pure API.

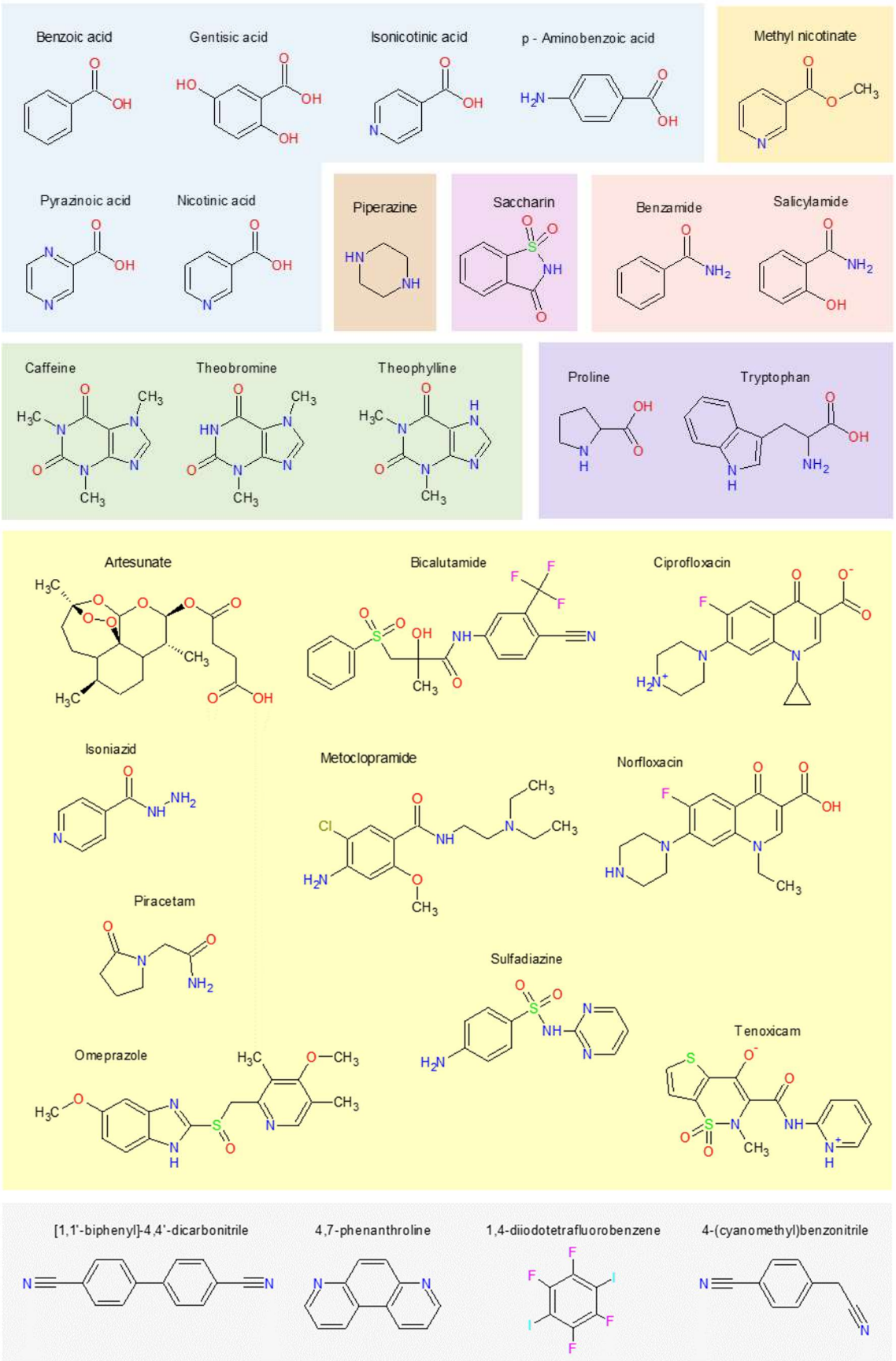


Figure 2 – Explored coformers in the virtual-experimental screening methodology.

CHAPTER 2

LITERATURE REVIEW

2.1 LITERATURE REVIEW

In the drug research and development process, many newly discovered compounds fails to reach into the market due to their poor physicochemical properties. Among them, the low aqueous solubility is the major issue faced by the pharmaceutical industry (PATEL et al., 2019).

As shown in Figure 3, it is estimated that up to 90% of new active pharmaceutical ingredients (APIs) and almost 40% of marketed drugs are poorly soluble in water (KARIMI-JAFARI et al., 2018; RAJPUT; SANPHUI; DESIRAJU, 2013), resulting in problems related to their dissolution, inconsistent bioavailability and consequent inaccurate efficacy in patients, especially when administered orally (BLAGDEN et al., 2007; CHADHA et al., 2016; KOTBANTAO; CHAROENCHAITRAKOOL, 2017).

Since aqueous solubility and permeability in biological membranes are fundamental parameters that control drug absorption, Amidon et al. (1995) developed a scheme of classification correlating them to the *in vitro* dissolution and *in vivo* bioavailability. The Biopharmaceutics Classification System (BCS), a guide provided by Food and Drug Administration (FDA), categorizes drugs into four groups taking in account their solubility and permeability. Classes II and IV encompass poorly soluble drugs (AMIDON et al., 1995; TSUME et al., 2014). Consequently, numerous attempts have been made to overcome low-solubility drug issues, such as the use of cyclodextrin complexes, lipid formulations, drug-carrier formulations, prodrugs, and multicomponent solid forms (BAZZO; PEZZINI; STULZER, 2020; MOHAMMAD et al., 2019; SAVJANI; GAJJAR; SAVJANI, 2012).

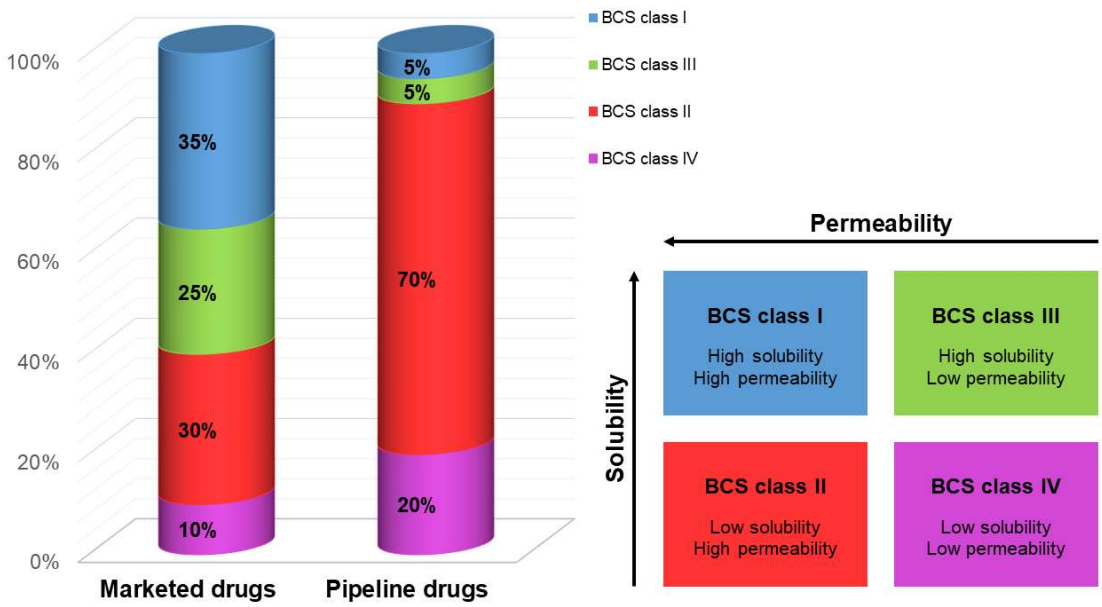


Figure 3 – Percentage distribution of drugs according to the Biopharmaceutics Classification System (BCS). Adapted from (BABU; NANGIA, 2011).

2.1.1 Multicomponent solid forms

In recent decades, multicomponent systems have been developed aiming to alter physicochemical properties of APIs, such as stability, melting point, solubility, dissolution rate and bioavailability, without affecting its pharmacological properties (KOTBANTAO; CHAROENCHAITRAKOOL, 2017; SATHISARAN; DALVI, 2018; SU et al., 2015), as well as to improve other essential properties of APIs, such as flowability, hygroscopicity and compressibility (QIAO et al., 2011). In the case of dual-drug multicomponent systems, in addition to pharmacokinetic improvement, there may be an increase in its synergistic actions, therapeutic combination and reduction of side effects (BOLLA; NANGIA, 2016; LI et al., 2020a).

Thus, considering the scenario of drug solubility and how it can affect their therapeutic efficacy, it is of utmost importance to study pharmaceutical multicomponent forms, like cocrystals, coamorphous, and salts (BERRY; STEED, 2017; BOLLA; SANPHUI; NANGIA, 2013; DUGGIRALA et al., 2020; GOPI; BANIK; DESIRAJU, 2017; LI et al., 2020b; SATHISARAN; DALVI, 2018; UPPALA et al., 2022). Some of these approaches are presented in Figure 4.

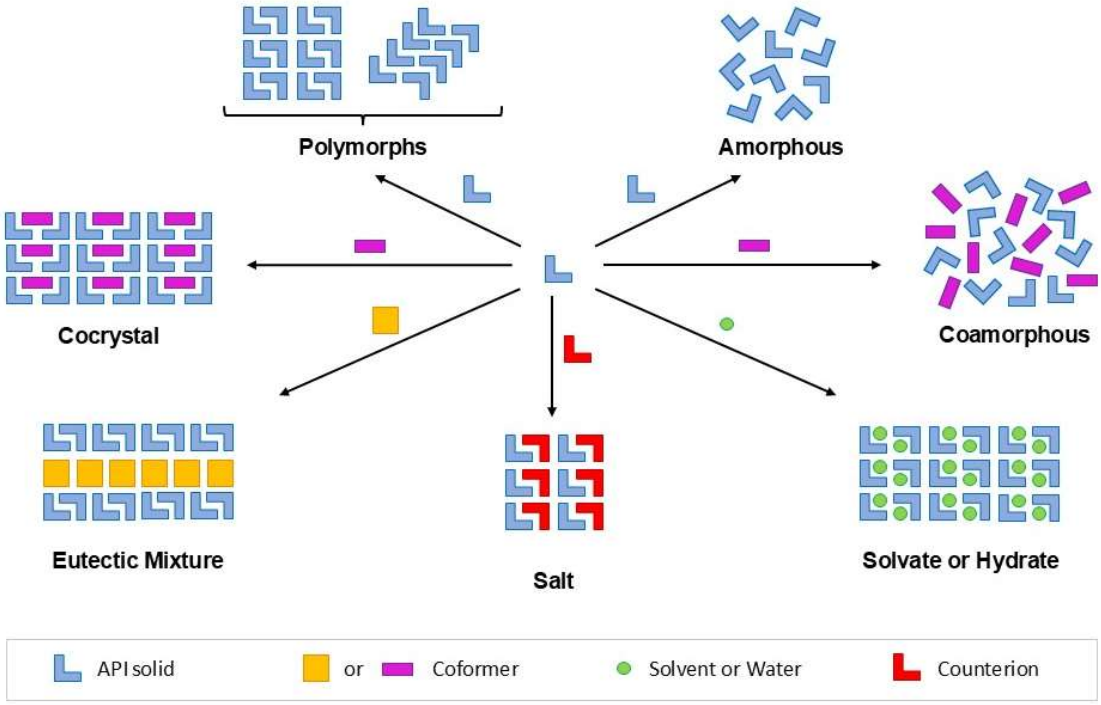


Figure 4 – Schematic representation of pharmaceutical solid forms. Adapted from (CHERUKUVADA; NANGIA, 2014).

Pharmaceutical solids can broadly be divided into crystalline and amorphous forms, in a single or multicomponent system. In the crystalline solids the components are arranged in a regular order, repeating pattern in three dimensions, while amorphous materials do not have a long-range order. The polymorphism of a given compound is attributed to its ability to present two or more distinct crystalline forms (AITIPAMULA et al., 2012; D'ANGELO et al., 2018; DESIRAJU, 2001; MALAMATARI et al., 2017). Coamorphous systems are single-phase multicomponent amorphous systems, in which a small molecule (also called as coformer) kinetically stabilizes the amorphous drug state through intermolecular interactions, such as hydrogen bonding, π-π stacking, proton transfer or mixing effects (HATANAKA et al., 2021; SABERI et al., 2023).

In eutectic mixtures, two solids result in a mixture with a lower melting point than the precursors, being miscible in the liquid state and immiscible in the solid state, maintaining the crystalline structure of the starting materials (BAZZO; PEZZINI; STULZER, 2020; CHERUKUVADA; NANGIA, 2014). On the other hand, cocrystals are single phase multicomponent crystalline forms, in which an API and one or more coformers interact. In the cocrystal, the precursors are in a defined stoichiometry and are linked by non-covalent and non-ionic

intermolecular interactions, such as hydrogen bonding, van der Waals forces and π-π stacking (KARIMI-JAFARI et al., 2018; PINDELSKA; SOKAL; KOLODZIEJSKI, 2017; VISHWESHWAR et al., 2006). If the coformer is a liquid at room temperature, then the crystal is designated as a hydrate or solvate, when incorporating water or solvent molecules, respectively (ALLESØ et al., 2010; HEALY et al., 2017). Salts are distinguished from cocrystals as they are species that are formed by the exchange of protons between molecules that have ionizable groups (CAVANAGH; MAHESHWARI; RODRÍGUEZ-HORNEDO, 2018; PINDELSKA; SOKAL; KOLODZIEJSKI, 2017).

2.1.1.1 Cocrystals

Over the last two decades, cocrystals have attracted significant attention from academia and pharmaceutical industries due to the potential to improve physicochemical properties of APIs, without compromising their therapeutic benefit. This is evident from the number of cocrystals approved for commercialization, as described in Table 1.

Table 1 – Summary of commercially available pharmaceutical cocrystals. Adapted from (KAVANAGH et al., 2019).

Commercial name	FDA approval	Components	Indication
Beta-Chlor®	1963	Chloral hydrate···betaine	Sedation
Depakote®	1983	Valproic acid···[valproate sodium]	Epilepsy
Cafcit®	1999	Caffeine···[citric acid]	Infantile apnoea
Lexapro®	2002	[Escitalopram oxalate] ···Oxalic acid	Depression
Suglat®	2014	Ipraglifozin···L-proline	Diabetes
Entresto®	2015	[Valsartan sodium]···[sacubitril sodium]	Heart failure
Odomzo®	2015	[Sonidegib monophosphate] ···phosphoric acid	Basal cell carcinoma
Steglatro®	2017	Ertuglifozin···L-pyroglutamic acid	Diabetes

It should be mentioned that there is considerable debate surrounding the definition of cocrystals. According to the FDA, cocrystals are defined as “solids which are crystalline materials composed of two or more molecules in the same crystal lattice”. Additionally, according to the European Medicine Agency (EMA),

cocrystals are “homogenous (single phase) crystalline structures made up of two or more components in a definite stoichiometric ratio where the arrangement in the crystal lattice is not based on ionic bonds (as with salts)” (AITIPAMULA et al., 2012; SATHISARAN; DALVI, 2018). Another definition generally accepted was stated by Aitipamula and co-workers (2012): “cocrystals are solids that are crystalline single phase materials composed of two or more different molecular and/or ionic compounds generally in a stoichiometric ratio which are neither solvates nor simple salts” (AITIPAMULA et al., 2012).

In this regard, cocrystals can be classified as “molecular” or “ionic” depending of the coformer nature (Figure 5). Most pharmaceutical cocrystals fit into the category of molecular cocrystals – here mentioned simply as cocrystals. They are typically composed by API and a neutral coformer, but not exclusively, sustained by hydrogen bonds (DUGGIRALA et al., 2016). The ionic cocrystals have recently emerged and are typically sustained by charge assisted hydrogen bonds and/or coordination bonds (if metal cations are present). Families of ionic cocrystals, as Entresto, include acid salts (cocrystals containing carboxylic acids and carboxylate salt) and conjugate acid-base cocrystals (containing an ion and its neutral counterpart) (DUGGIRALA et al., 2016). Then, in general, the distinction between cocrystals and salts is that the proton is shared between an acid and a base in cocrystals while it is transferred in salts (Figure 5) (MALAMATARI et al., 2017; SATHISARAN; DALVI, 2018).

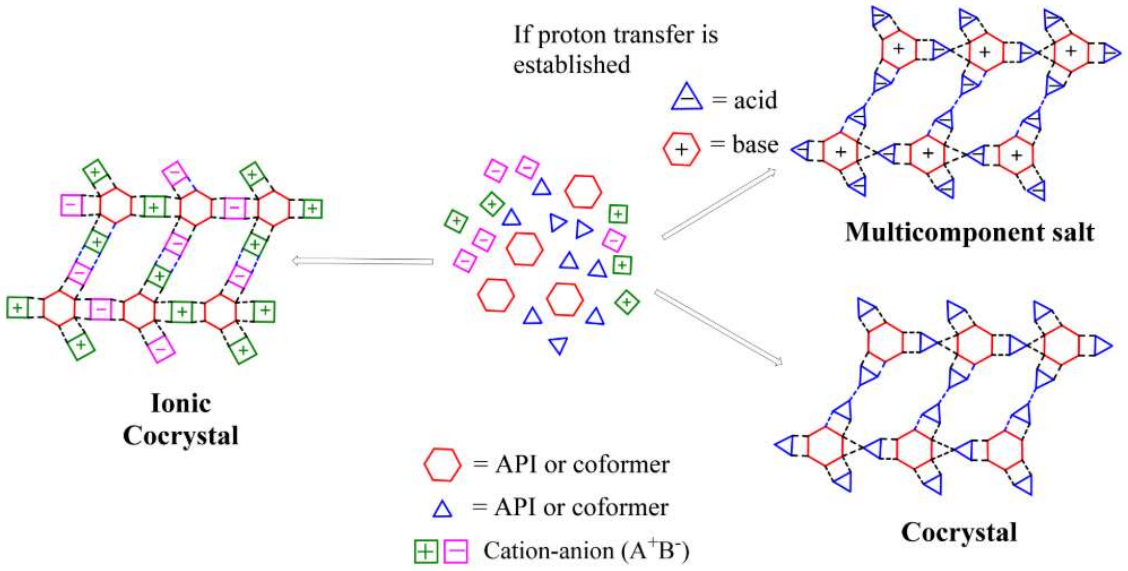


Figure 5 – Schematic representation of the formation of multicomponent salt, (molecular) cocrystal or ionic cocrystal. Reproduced from (SOLARES-BRIONES et al., 2021).

Cocrystals are stabilized by strong intermolecular non-covalent adhesive interactions of short-range order that exist between the API and coformer, such as hydrogen bonding, van der Waals forces and π-π stacking (KARIMI-JAFARI et al., 2018; PINDELSKA; SOKAL; KOLODZIEJSKI, 2017; VISHWESHWAR et al., 2006). The API and coformer are held together by "supramolecular synthons" – a Crystal Engineering concept introduced by Desiraju in 1995 – to mean "structural units in the supramolecule which can be formed or assembled by known or possible intra-/intermolecular interactions" (DESIRAJU, 1995; SATHISARAN; DALVI, 2018). The supramolecular synthons are spatial arrangements of intermolecular interactions that incorporate the chemical and geometrical recognition features of molecules. They are designated as homosynthons or heterosynthons when formed by the same or different functional groups, respectively. Figure 6 shows some supramolecular synthons commonly found in cocrystals.

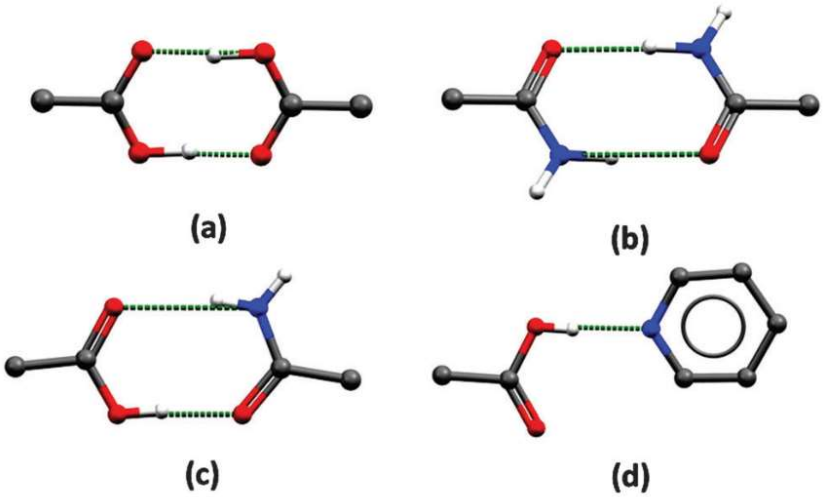


Figure 6 – Supramolecular homosynthons (acid-acid (a) and amide-amide (b)) and heterosynthons (acid-amide (c) and acid-pyridine (d)). Reproduced from (DUGGIRALA et al., 2016).

Various advantages of pharmaceutical cocrystals are mentioned in the literature as (1) the bulk material and physical-chemical properties of the API can be modified while still maintaining the intrinsic activity of the drug, (2) all types of drugs, in theory, have the capability to form cocrystals, including weakly ionizable and non-ionizable APIs, (3) possibility of achieving a high dissolution rate comparable to that of the amorphous form while maintaining the long-term chemical and physical stability provided by crystalline forms, (4) in terms of intellectual property, these materials are patentable or eligible for rights

extension. The process for accepting these patents is simpler than for new drugs, given the prior knowledge of the pharmaceutical properties of the API (GADADE; PEKAMWAR, 2016; QIAO et al., 2011; THAKURIA et al., 2013).

According to Friscic and Jones (2009), in mechanochemical processes, widely used for cocrystal synthesis, the cocrystal formation may involve at least three different mechanistic processes through the presence of an intermediate bulk phase: (1) molecular diffusion (2) eutectic formation, and (3) mediation by an amorphous phase (FRIŠČIČ; JONES, 2009; SOLARES-BRIONES et al., 2021). So, even if an attempt at cocrystallization “fails”, different solid forms can be produced in this process, such as a drug polymorph, salts, solvates/hydrates, coamorphous systems and eutectic mixtures (SATHISARAN; DALVI, 2018).

2.1.1.2 Coamorphous systems

Compared to cocrystals (or crystalline salts), amorphous drugs present long-range disorder along with the large unit surface free energy, thereby improving solubility, dissolution rate and bioavailability of the drugs. On the other hand, single component amorphous is a thermodynamically high energy state, then, the solid is more unstable than its crystalline counterparts and tends to recrystallize over time (SABERI et al., 2023; SHI; MOINUDDIN; CAI, 2019; SILVA; ROSADO; EUSÉBIO, 2021; WANG et al., 2020). An alternative to prevent the drug molecules aggregation is preparing multicomponent amorphized forms, such as coamorphous systems.

Polymer-based and coamorphous forms (Figure 7) come under the term glass solutions, which itself is a subcategory of solid dispersions. A solid dispersion can be defined as ‘one or more active ingredients dispersed in an inert carrier in the solid state prepared by the melting, solvent or melting-solvent method’ (DENGALE et al., 2016; SABERI et al., 2023). As presented in Table 2, solid dispersions are categorized according to their physical state and number of solid phases, which can be diverse, including eutectic mixtures, solid solutions, glass solutions and glass suspensions. In turn, the glass solutions can be divided by the type of excipient used to stabilize the amorphous drug (DENGALE et al., 2016; SABERI et al., 2023).

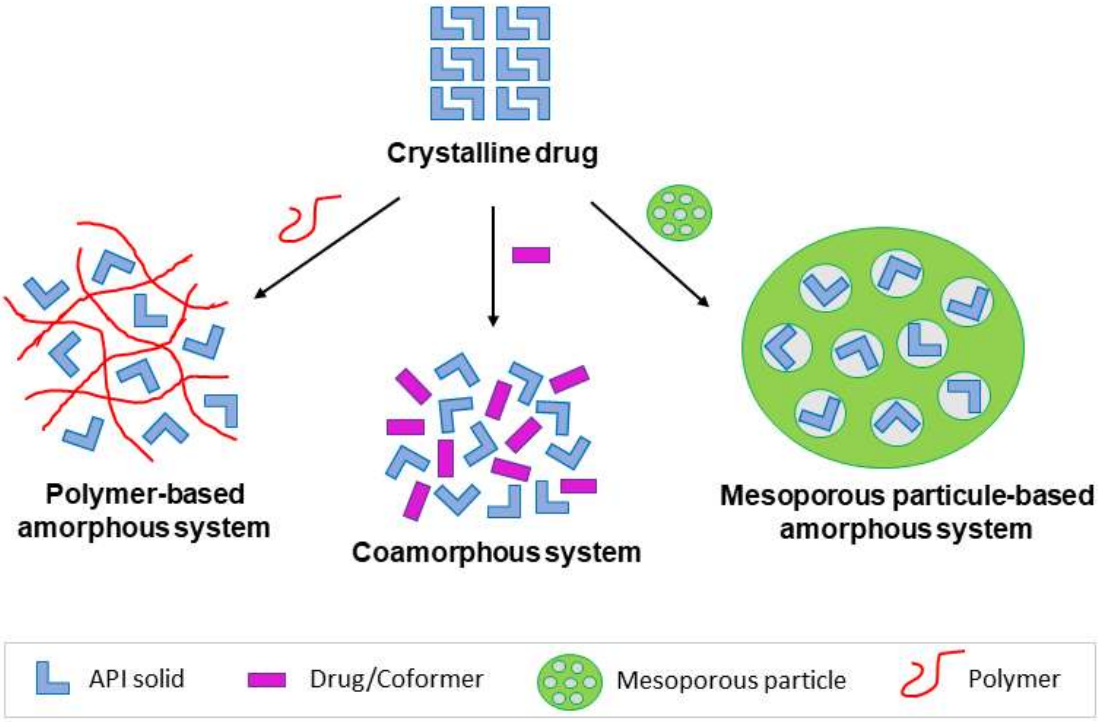


Figure 7 – Schematic representation of coamorphous, polymer-based and mesoporous particle-based amorphous systems. Adapted from (SHI; MOINUDDIN; CAI, 2019).

Table 2 – Classification of solid dispersions based on solid phase. A: amorphous, C: crystalline. Adapted from (DENGALE et al., 2016; SABERI et al., 2023).

Solid dispersion	Number of phases	Physical state of phase(s)
Eutectic mixture	2	C/C
Solid solution	1	C
Glass solution	1	A
Glass suspension	2	A/A or A/C

The term “coamorphous” was first coined by Chieng et al. in 2009. Thereafter, the number of published research articles on this topic expanded. Coamorphous systems are single-phase multicomponent amorphous systems, in which a small molecule kinetically stabilizes the amorphous drug state through intermolecular interactions, such as hydrogen bonding, π-π stacking, proton transfer or intimate mixing effects (DENGALE et al., 2016; HATANAKA et al., 2021; SABERI et al., 2023). These multicomponent systems present a single glass-transition temperature (*T*g) indicating the complete miscibility/interaction of components. The enhanced physical stability of coamorphous systems is always

associated with a decrease in molecular mobility, as suggested by an increase of relaxation time measured by dielectric spectroscopy or differential scanning calorimetry (DSC) (HATANAKA et al., 2021; WANG et al., 2020; ZHANG et al., 2021).

Aiming to make coamorphous mixtures efficient, reliable, and adaptable to large-scale processing, different types of excipients are explored, including amino acids, organic acids, sugars and pharmacologically relevant second drugs. In terms of properties, the coamorphization can improve physical stability, apparent solubility, dissolution rate and, consequently improve bioavailability of drugs. Also, the synergistic combination of two drugs can improve clinical efficacy and reduce the side effects (SABERI et al., 2023; WANG et al., 2020)

2.1.1.3 Eutectic mixtures

Eutectic mixtures are another interesting group of pharmaceutical solids. Different definitions are used to describe eutectic mixtures based on their composition and low melting point. An eutectic mixture is the combination of substances that melts at a single temperature, which is lower than the melting points of the isolated compounds. This mixture is completely miscible in the liquid state but only to a very limited extent in the solid state. Their formation occurs via homomeric interaction (cohesive forces) between parent compounds. In eutectic mixtures, as they are formed by non-isomorphous solids (having mismatched size and shape), the adhesive forces (heteromeric interactions) are relatively weak. On the other hand, in a cocrystal, the adhesive forces dominate, while in a solid solution, adhesive and cohesive interactions are balanced due to the matching size/shape of precursors (ABDELQUADER et al., 2023; ARAYA-SIBAJA et al., 2019; BAZZO; PEZZINI; STULZER, 2020; CHERUKUVADA; NANGIA, 2014). A schematic representation is shown in Figure 8.

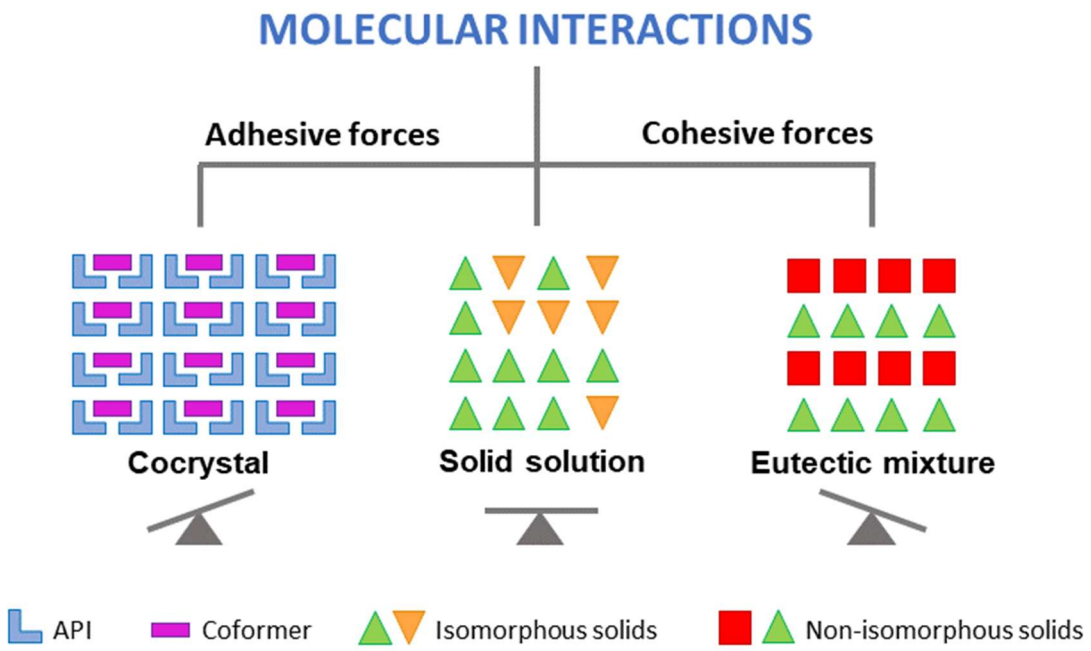


Figure 8 – Schematic representation of eutectic mixture, cocrystal and solid solution based on intermolecular interactions. Adapted from (BAZZO; PEZZINI; STULZER, 2020)

Eutectics are crystalline mixtures where both components exist in the crystalline state. Thus, they have some of the identical characteristics of each isolated component, but other properties like dissolution rate, solubility and chemical stability may be different (ARAYA-SIBAJA et al., 2019; BAZZO; PEZZINI; STULZER, 2020; CHERUKUVADA; NANGIA, 2014).

The lower melting point of the eutectic is due to its heterogeneous crystalline arrangements consisting of an alternating lamellar microstructure held by weak interphase interactions, which in turn is responsible for its high thermodynamic functions, such as free energy, enthalpy and entropy, which also may provide both solubility and dissolution enhancements (ARAYA-SIBAJA et al., 2019; BAZZO; PEZZINI; STULZER, 2020; CHERUKUVADA; NANGIA, 2014).

The main advantages of eutectic mixtures in the pharmaceutical field include (1) the cost-effective and easy producing and scaling up procedures, (2) they are not considered new chemical entities, or a new crystal form like cocrystals, and consequently do not require clinical trials, and (3) since the drug and coformer exist as crystalline compounds, the mixture is highly stable compared to amorphous materials (ARAYA-SIBAJA et al., 2019; YANG et al., 2022).

2.1.2 Screening and coformer selection methods

Frequently, when preparing multicomponent solid forms, substances presented on the “Generally Regarded as Safe” (GRAS) and “Everything Added to Foods in the United States” (EAFUS) lists – such as flavonoids, nutraceuticals, vitamins, minerals, excipients, amino acids, biomolecules and even other APIs – are employed as coformers (ARENAS-GARCÍA et al., 2017; QIAO et al., 2011; SABERI et al., 2023; THAKURIA et al., 2013). Suitable coformer candidates can be also selected, in a rational way, using experimental and/or computational approaches, like crystal engineering principles, pKa rule, Cambridge Structure Database (CSD) tool, COnductor-like Screening MOdel (COSMO) theory (ABRAMOV; LOSCHEN; KLAMT, 2012; KUMAR; NANDA, 2021). Some of these screening methods are presented in Figure 9.

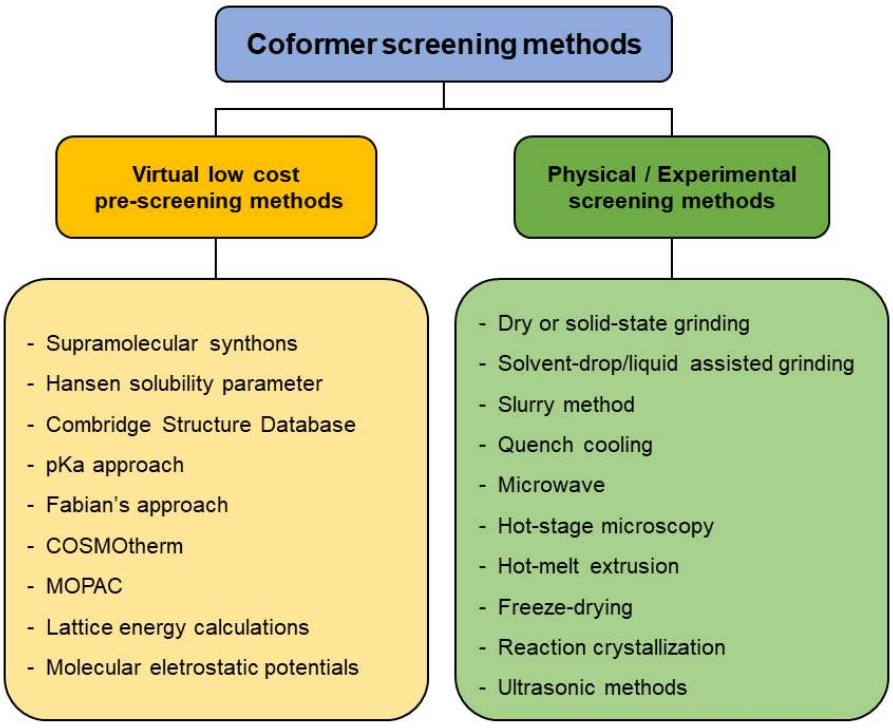


Figure 9 – Examples of coformer screening methods.

Various experimental techniques are currently employed for multicomponent systems screening, including grinding, crystallization from solutions attaining solution supersaturation by solvent evaporation, cooling or

antisolvent addition, slurry crystallization, and so on. These experimental methodologies are typically time-consuming, expensive and practically not feasible to carry out for a large set of coformers (ABRAMOV; LOSCHEN; KLAMT, 2012; KUMAR; NANDA, 2021; SATHISARAN; DALVI, 2018).

In this sense, virtual screening tools play an important role when predicting the propensity of different coformers to form multicomponent systems with a given API. Some of the methods take advantage of the use of computer systems, making it possible to perform screening studies to predict the best coformer with a vast library of different molecules in a short period of time (ABRAMOV; LOSCHEN; KLAMT, 2012; KUMAR; NANDA, 2021; SATHISARAN; DALVI, 2018). Some low-cost virtual screening methods are detailed in the following sections, as examples, including that used in this work.

2.1.2.1 Cambridge Structural Database (CSD) tool

The CSD is a continuously growing repository of accurate tree-dimensional structures of organic and metal-organic compounds, created by Cambridge Crystallographic Data Centre (CCDC) in 1965. Each CSD entry contain chemical and crystallographic data, crystal packing, molecular geometry, stereochemistry, molecular dimensions, conformational analysis, and structure representation (ABRAMOV; LOSCHEN; KLAMT, 2012; DUGGIRALA et al., 2016; KUMAR; NANDA, 2021).

CSD is a validated and valuable tool to facilitate the statistical analysis of intermolecular interactions between functional groups. It is used to provide information about molecular association of drug and coformers based on molecular complementarity that engage into supramolecular synthons. A library of suitable coformers can be prepared by CSD for an API based on the hydrogen bond propensity. Thus, this approach can find appropriate cocrystal forming pairs, and reduces the research time and experimental cost (ABRAMOV; LOSCHEN; KLAMT, 2012; DUGGIRALA et al., 2016; KUMAR; NANDA, 2021).

2.1.2.2 pKa approach

The pKa approach has been used to assess the ability of a given API and coformer to form a salt, cocrystal or salt-cocrystal. The negative logarithm of dissociation constant (pKa value) indicates the ability of an acid molecule to give up a proton. When the difference between pKa value of the API and the coformer (∆pKa) ranges in negative values, there will be no proton transfer, and cocrystal formation is expected. Salt formation is predicted when ∆pKa value is greater than 3, due to a high propensity for a complete proton transfer. On the other hand, when the ∆pKa value ranges between 0 and 3, it is not reliable to predict whether the resultant solid form will be a salt or cocrystal, or if partially ionized states will be formed in a salt-cocrystal continuum. Although it can be an interesting, simple and less time-consuming tool, an ∆pKa value cannot always be used to predict/confirm the nature of the multicomponent solid accurately (KUMAR; NANDA, 2021; SATHISARAN; DALVI, 2018).

2.1.2.3 COnductor-like Screening MOdel (COSMO) theory

The COnductor-like Screening MOdel for Real Solvents (COSMO-RS) is a statistical liquid phase thermodynamic theory used in several fields like solubility prediction, solvent screening, coformer ranking, pKa prediction, for instance. This theory simulates the miscibility and affinity of the API and coformer under supercooled liquid conditions. The intermolecular interactions in COSMO-RS are calculated as polarization charge densities (σ-profile) of surface segments, employing quantum-chemical calculation, usually density functional theory (DFT). It is assumed that the supercooled liquid interactions are similar in the crystal (GUIDETTI et al., 2023; KUMAR; NANDA, 2021; NUNES COSTA et al., 2020).

The COSMOquick software, used in this work, is a tool based on the COSMO-RS theory, that contains a database of already compiled σ-profiles of several compounds and avoids the time-consuming and costly quantum-chemical calculations (KUMAR; NANDA, 2021; LOSCHEN; KLAMT, 2015). The method calculates the excess enthalpy (ΔH_{excess}) of an undercooled liquid mixture

of the components, reflecting the interaction strength of the API and coformer, intimately connected to the free energy of cocrystaliization. Another important parameter in the cocrystal formation prediction is the flexibility parameter (F_{fit}) that combines the molecular interactions (ΔH_{excess}) with the number of rotatable bonds in the molecules (GUIDETTI et al., 2023; KUMAR; NANDA, 2021; LOSCHEN; KLAMT, 2015).

2.1.3 Preparation methods

The preparation of new solid forms may be performed through several methodologies, that can be divided basically between solid-based methods and solution-based methods (Figure 10). The solvent-based approaches involve a large amount of solvent request a subsequent step to separate the crystalline product, as in the case of crystallization by solvent evaporation, precipitation from solution, anti-solvent addition, cooling crystallization, slurry conversion methods. Moreover, the solid state methods comprise that using very little or no solvent in the preparation route, such as the hot melt extrusion, sonochemical method, resonant acoustic mixing, melt quenching, and mechanochemical grinding (BAZZO; PEZZINI; STULZER, 2020; DENGALE et al., 2016; GAJDA et al., 2019; GUO et al., 2021; KARIMI-JAFARI et al., 2018; SATHISARAN; DALVI, 2018; YADAV et al., 2009).

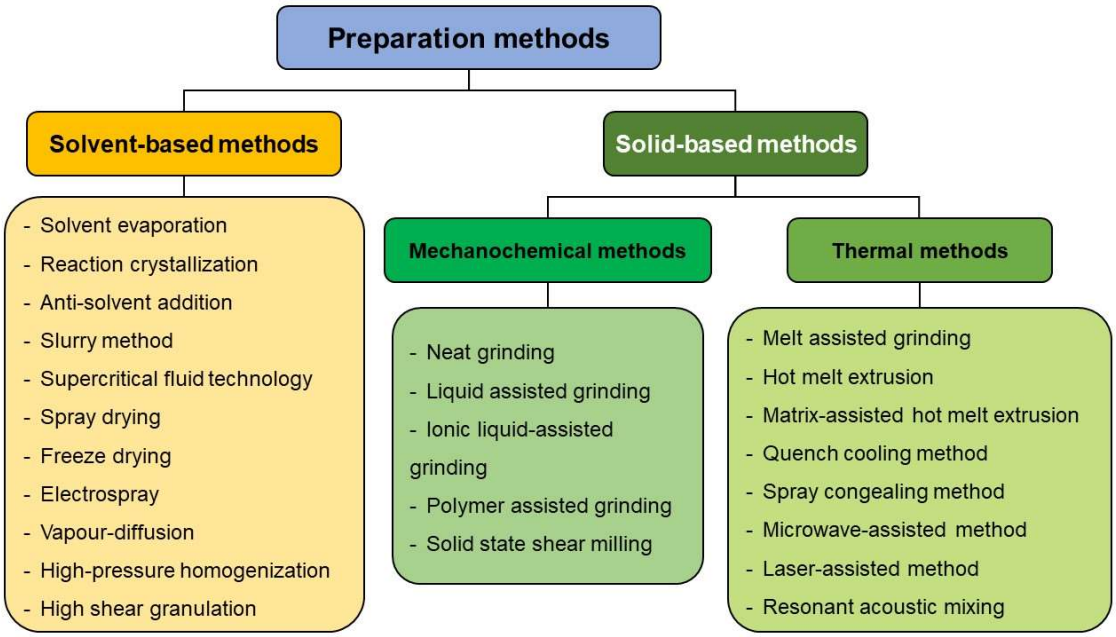


Figure 10 – Classification of various methods for preparing multicomponent systems.

Since each preparation method requires different amounts of solvents, the parameter *η* was introduced by Friščić in 2009 to correlate the ratio of the volume of liquid phase (in μL) to the amount of solid (in mg) used in the synthetic process, as shown in Figure 11. This parameter allows the classification of synthesis methods according to the amount of solvent: neat grinding (NG) (η=0), liquid-assisted grinding (LAG) (0-2 μL mg^{-1}), slurrying (2-12 μL mg^{-1}), and solution reactions (≈12 μL mg^{-1} or more) (FRIŠČIĆ et al., 2009).

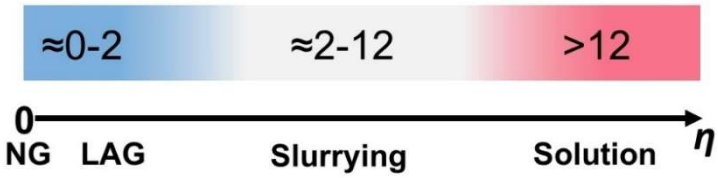


Figure 11 – The scale of *η* parameter. Adapted from (FRIŠČIĆ; MOTTILLO; TITI, 2020).

2.1.3.1 Solvent evaporation method

Solvent-based methods are most frequently used at laboratory scale, because of their simplicity, possibility of process monitoring, for example changing the solvent and/or temperature, and control of final product properties. The solvent selection is an important step in these methods, as it potentially impacts the solubility of the precursors, and should be carefully and rationally

done. Usually, crystallization by solvent evaporation method is employed to generate single crystals suitable for structural elucidation. Single crystal is prepared from a supersaturated solution via slow evaporation, involving the nucleation and growth of the crystalline material (GUO et al., 2021; KARIMI-JAFARI et al., 2018; SATHISARAN; DALVI, 2018).

Some tools as ternary phase diagrams (Figure 12) can be used to identify the ideal crystallization conditions, both at laboratorial level and for scale-up purposes. This type of diagrams describes the phase behavior of a multicomponent system (API, coformer and solvent) in a given solvent at a fixed temperature and pressure. It identifies regions of stability for different solid phases, being able to predict the cocrystal formation pathway. In a given solvent, if the cocrystal components have similar solubilities, the phase diagram with cocrystal formation, with congruent behavior, exhibits a more symmetrical trend. If the two precursors present dissimilar solubilities, then the cocrystallization process occurs incongruently, the less soluble component precipitates preferentially, leading to a solid mixture of cocrystal and starting materials, or a failure of forming cocrystals (GUO et al., 2021; KARIMI-JAFARI et al., 2018; SATHISARAN; DALVI, 2018).

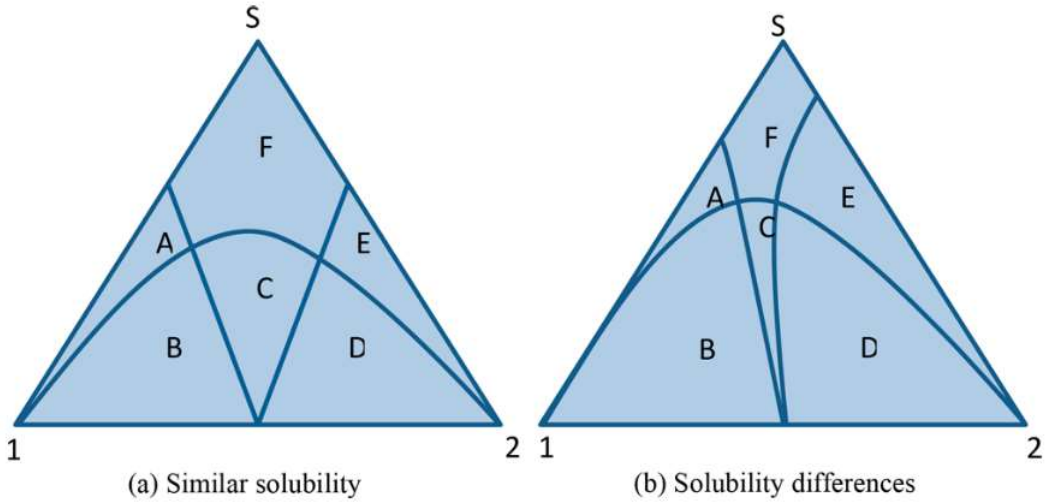


Figure 12 – Schematic representation of congruent (a) and incongruent (b) ternary phase diagrams. Reproduced from (KARIMI-JAFARI et al., 2018).

As shown in Figure 12, the ternary phase diagram is represented by an equilateral triangle, where each vertex corresponds to pure compounds (API and coformer = 1 and 2; solvent = S) and each side corresponds to binary diagrams.

Additionally, the diagram can be divided into several areas with different combinations, bringing information about components solubility and thermodynamic equilibrium between the phases. The top area (F) usually represents the solution/liquid phase. The regions A and E represent the equilibrium between the solvent and component 1 and 2, respectively. In turn, B and D regions respectively correspond the area where the cocrystal equilibrates with the components 1 and 2, while the region C represents the area where is possible to obtain the cocrystal in the solvent (GUO et al., 2021; KARIMI-JAFARI et al., 2018).

2.1.3.2 Slurry method

In this method, solvent-mediated phase transformation occurs. Although it is a solution-based method, it does not require large amounts of solvents to generate a clear (fully dissolved) solution. Thus, the slurry technique involves the suspension of the target molecule and coformer, usually at a fixed molar ratio, in a solvent with the solid fraction remaining in excess. During the slurry, each component gradually dissolves and forms a complex to promote the nucleation and growth of a cocrystal, for example (GUO et al., 2021; HASKINS; ZAWOROTKO, 2021; KARIMI-JAFARI et al., 2018).

The choice of solvent for synthesis is crucial, as the individual components must have intermediate solubility in a given solvent to ensure that both can be in suspension. In this way, the most soluble form in the solvent (least stable) dissolves and the least soluble form (most stable) precipitates from the solution under constant stirring. Thus, the conversion rate in the slurry depends on the driving force of solubility, the relative amounts of the starting compounds, and also on the kinetics of nucleation and growth of the system (GUO et al., 2021; HASKINS; ZAWOROTKO, 2021; KARIMI-JAFARI et al., 2018).

2.1.3.3 Mechanochemical methods

Solvent-free methods for cocrystal synthesis have attracted considerable attention over the last decades due to the benefits associated with such methods. Some of the advantages of these methods are the use of no or very lower amount

of solvent(s), the exceptional purity and quality of produced cocrystal, large yield and the short reaction times (BAZZO; PEZZINI; STULZER, 2020; KARIMI-JAFARI et al., 2018; QIAO et al., 2011; SOLARES-BRIONES et al., 2021).

The term mechanochemistry refers to any physical process or chemical reaction, involving solids, induced by mechanical energy (typically by friction, impact, collision, grinding stimuli). The mechanical action results in a reduction in particle size, as well as the creation of active sites for chemical reactivity, or the generation of new active surfaces, therefore activating the physical or chemical process (CARNEIRO et al., 2022; KARIMI-JAFARI et al., 2018; KAUPP, 2009; QIAO et al., 2011; SOLARES-BRIONES et al., 2021).

Grinding synthesis is a green or ecofriendly method that eliminates (neat grinding – NG) or reduces to few drops (liquid assisted grinding – LAG) the use of solvents by grinding of two or more solid reagents through manual (mortar and pestle) or non-manual practices (ball milling or extrusion). It is worthy mention that the low amount of solvent in LAG experiments can reveal a catalytic effect, often resulting in cleaner physical processes or chemical reactions with high yields and selectivity. (CARNEIRO et al., 2022; KARIMI-JAFARI et al., 2018; KAUPP, 2009; QIAO et al., 2011; SOLARES-BRIONES et al., 2021).

Additionally, milling process can generates significant heat. In the case of coamorphous systems, the conventional grinding may induce the recrystallization of amorphous drug or thermal degradation. So, in this regard, cryogenic milling is an alternative, being performed under liquid nitrogen – used as a coolant – while avoiding the build-up of excess heat produced during the milling process (MESALLATI; MUGHEIRBI; TAJBER, 2016; MOINUDDIN et al., 2017).

2.1.3.4 Quench cooling

The production of amorphous material can be divided into two types depending on the mechanism involved, the kinetic or thermodynamic disordering processes. The kinetic involves the direct conversion of a solid crystalline API to its amorphous form, while the thermodynamic pathway starts from a thermodynamically stable non-crystalline form, that is, the drug as a melt or in solution (DENGALE et al., 2016; SHI; MOINUDDIN; CAI, 2019).

The quench cooling (or melt quenching) technique is one of the most common method of coamorphous preparation. In general, the API and the coformers are heated to a molten liquid state that is, subsequently, vitrified by a rapidly cooling, a process called quenching, to avoid the compounds crystallization. The rapid cooling rate prevents the nucleation and crystal growth, facilitating the amorphous solid formation (DENGALE et al., 2016; SHI; MOINUDDIN; CAI, 2019).

Considering the laboratory scale, the quench cooling process is attractive for screening purposes. As the coamorphous system can be prepared and analyzed directly in situ within a DSC calorimeter, then the quenching also offers the possibility to assess important physico-chemical parameters, like the glass transition temperature (*T*g), miscibility and recrystallization behavior (DENGALE et al., 2016; SHI; MOINUDDIN; CAI, 2019).

2.1.4 Characterization techniques

After preparation, the multicomponent systems are commonly characterized in what concerns their structure and physical properties. Structural characterization may involve Fourier Transform Infrared Spectroscopy (FTIR), Raman Spectroscopy, Solid-State Nuclear Magnetic Resonance Spectroscopy (ssNMR), Powder X-ray Diffraction (PXRD) and Single Crystal X-ray Diffraction (SXRD). For the physical properties determination techniques such as Thermogravimetry analysis (TG), Differential Thermal Analysis (DTA), Differential Scanning Calorimetry (DSC) and Scanning Electron Microscopy (SEM) have been used (FRIŠČIĆ; JONES, 2010; QIAO et al., 2011; SATHISARAN; DALVI, 2018; SHAIKH et al., 2018).

2.1.4.1 Thermal analysis

Thermal analysis encompasses a group of techniques that monitor a sample property, while it is submitted to a controlled temperature program, that may include isothermal and heating/cooling steps, in a controlled atmosphere. Different thermal events can be detected such as melting, crystallization, sublimation, decomposition, solid-state transitions, glass transitions and volatile component quantification (IONASHIRO; CAIRES; GOMES, 2014; QIAO et al.,

2011; SATHISARAN; DALVI, 2018; SHAIKH et al., 2018; SOARES; CARNEIRO, 2014).

Thermogravimetry (TG) is a technique in which the mass of a sample is measured as a function of temperature, while the Differential Thermal Analysis (DTA) measures the temperature difference between a sample and a reference material. On the other hand, the Differential Scanning Calorimetry (DSC) is a technique in which the enthalpy changes of the sample are monitored relative to a thermally inert reference material, while both are maintained under a controlled temperature program. It is very common the conjugation of these thermal analysis techniques (TG-DTA or TG-DSC), then, providing more accurate thermal information (IONASHIRO; CAIRES; GOMES, 2014; QIAO et al., 2011; SATHISARAN; DALVI, 2018; SHAIKH et al., 2018; SOARES; CARNEIRO, 2014).

Moreover, through thermal analytical data it is possible to construct the binary solid-liquid phase diagram and Tamman's triangle, which are tools used for eutectic and cocrystal checking composition. The Tamman's triangle is constructed by plotting the eutectics enthalpy correlated to the sample composition, while binary phase diagrams are constructed by taking the *solidus* and *liquidus* temperatures – the onset temperature (T_{onset}) of first DSC melting event and peak temperature (T_{peak}) of second event that corresponds to the complete melting, respectively – of each sample. When a eutectic mixture is formed, the binary phase diagram presents a "V" shape, while a "W" shape is observed when a cocrystal is formed with congruent melting (Figure 13) (AGAFONOVA; MOSHCHENSKIY; TKACHENKO, 2014; BAZZO; PEZZINI; STULZER, 2020; CHERUKUVADA; GURU ROW, 2014; LORENZ; SEIDEL-MORGENSTERN, 2002; PATEL et al., 2019).

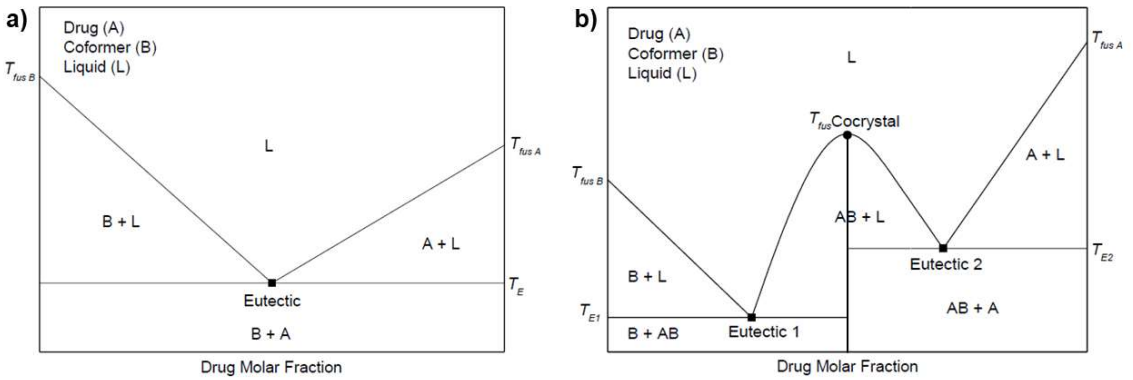


Figure 13 – Representation of binary phase diagrams with a simple eutectic mixture (a) and cocrystal with congruent melting (b).

2.1.4.2 Structural analyses

X-ray diffraction is one of the most used techniques to determine different crystalline structures. This non-destructive technique can distinguish the presence of a new crystallographic pattern, which is unique for each structure. In this sense, Powder X-ray Diffraction (PXRD) can be used to characterize and distinguish polymorphs, multicomponent solid system formation and to identify phase transitions. The Single Crystal X-ray Diffraction (SCXRD) also allow to determine the structure of single crystals at an atomic level, although obtaining single crystals is somewhat challenging (PRASAD; RAKESH, 2012; QIAO et al., 2011; SOARES; CARNEIRO, 2014).

Infrared Spectroscopy (FTIR), as well as Raman Spectroscopy, presents a great quantity of information about the chemical bonds and interaction. The characteristics of vibrational modes act as molecular fingerprints. Through the spectral comparison is possible to identify functional groups and suggest intermolecular interactions, distinguishing cocrystals from salts, for example. It is a non-destructive and rapid analysis, and when coupled with attenuated total reflectance (ATR) accessory do not need sample preparation (PRASAD; RAKESH, 2012; QIAO et al., 2011; SOARES; CARNEIRO, 2014).

In the case of completely amorphized materials, no Bragg peaks are observed in the PXRD diffractograms due to the lack of long-range order of molecular packing. Additionally, the FTIR of coamorphous usually present broadening and shift of vibrational bands (CHAVAN et al., 2016; HEALY et al.,

2017; MOINUDDIN et al., 2017; SABERI et al., 2023; SHI; MOINUDDIN; CAI, 2019).

2.1.5 Physical-chemical and performance evaluation

The therapeutic effectiveness of an API is impacted by physicochemical properties, such as the stability, particle size, powder flowability, hygroscopicity and solubility. In oral administration, the gastrointestinal absorption depends on the solubility and dissolution rate of molecules (GUO et al., 2021; KOTBANTAO; CHAROENCHAITRAKOOL, 2017; QIAO et al., 2011).

In the solid state, several structural possibilities of an API may influence the physical, chemical and biopharmaceutical properties. Then, one important step after the multicomponent system characterization is the performance evaluation. For better understanding, various parameters studied during this step can be classified as presented in Figure 14.

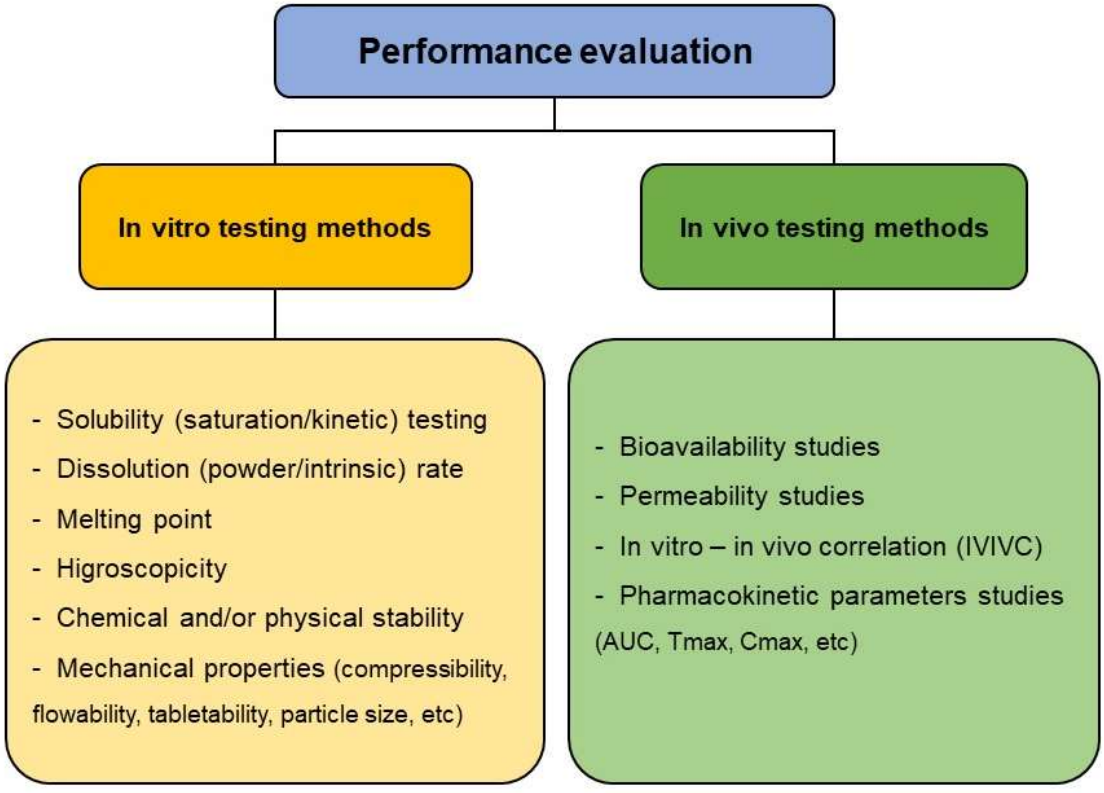


Figure 14 – Various *in-vitro* and *in-vivo* parameters studied during performance evaluation step of multicomponent system development process.

The melting point of a compound is a fundamental physical property that is measured by the temperature at which the solid phase is at equilibrium with the liquid phase. DSC is the favored method to getting complete melting point data, over a standard melting point apparatus. In general, the melting point determination can be used as a means of purity assessment or characterization. In addition, within the pharmaceutical sciences, the melting point also presents correlations to the aqueous solubility and vapor pressure (IONASHIRO; CAIRES; GOMES, 2014; SCHULTHEISS; NEWMAN, 2009).

Mechanical properties of drugs are important for the bulk powder flow, compaction and tableting due to its numerous technical and economic advantages. Low manufacturing costs, high production throughput, and ease of consumption, storage and handling are some of these benefits. The traditional mechanical deformation mechanisms of solid materials include elastic, plastic, viscoelastic, and fragmentation. Thus understanding and improving the relationship between crystal structure and mechanical properties can solve drug formulation problems (ISSA, 2011; KARIMI-JAFARI et al., 2018; LIU et al., 2016).

According to the International Union of Pure and Applied Chemistry (IUPAC), solubility of a solute can be defined as “the analytical composition of a saturated solution expressed in terms of proportion of a designated solute in a designated solvent”, stated as concentration, mole fraction, mole ratio, and other units (IUPAC, 2014; SAVJANI; GAJJAR; SAVJANI, 2012).The United States Pharmacopeia (USP) and British Pharmacopeia (BP) classify the solubility in terms of quantification, regardless of the solvent used, dividing the compounds according to the criteria given in Table 3 (SAVJANI; GAJJAR; SAVJANI, 2012).

Table 3 – USP and BP solubility criteria. Reproduced from (SAVJANI; GAJJAR; SAVJANI, 2012).

Descriptive term	Part of solvent required per part of solute
Very soluble	Less than 1
Freely soluble	From 1 to 10
Soluble	From 10 to 30
Sparingly soluble	From 30 to 100
Slightly soluble	From 100 to 1000
Very slightly soluble	From 1000 to 10,000
Practically insoluble	10,000 and over

As previously mentioned, multicomponent solid systems are usually developed to beat the solubility problem of poorly soluble drugs (BCS-class II and class IV), so solubility testing is done to check whether the desired feature has been achieved or not. The kinetic (or apparent) solubility measures the amount of drug dissolved at various time-points, while the equilibrium solubility measure total amount of drug dissolved at equilibrium condition (SAVJANI; GAJJAR; SAVJANI, 2012; THAKURIA et al., 2013).

Dissolution refers to the amount of solute which dissolves in an aqueous medium at a specific time interval. The rate at which the solute dissolves in the aqueous medium to reach its equilibrium state is called as the dissolution rate Dissolution rate has a major impact on the performance and bioavailability of poorly water-soluble APIs. The intrinsic dissolution rate (IDR) testing encompasses the measurement of rate of dissolution per unit area of a cocrystal, for example. Hence measurement of intrinsic dissolution rate of cocrystals may be better assessment of this parameter as this method eliminates influence of particle size on dissolution, since the sample used in the IDR test is pressed into a disk or pellet (SATHISARAN; DALVI, 2018; SCHULTHEISS; NEWMAN, 2009).

Bioavailability is a measurement of the rate and extent to which a drug reaches the systemic circulation. In a relative or comparative bioavailability study, the amount of drug in the blood is measured after oral administration of the original form and then the multicomponent system. In general, the ultimate purpose of multicomponent preparation is to improve the bioavailability of an active drug (GUO et al., 2021; SCHULTHEISS; NEWMAN, 2009). Therefore, the multicomponent systems can have a positive impact on the pharmaceutical field, improving drug solubility thereby its oral bioavailability, which may lead to lower doses to reach therapeutic plasma concentrations after oral administration (SAVJANI; GAJJAR; SAVJANI, 2012).

CHAPTER 3

NIMESULIDE MULTICOMPONENT SOLID FORMS

The present chapter encompass the complete material published at Journal of Thermal Analysis and Calorimetry:

de Almeida, A. C.; Ferreira, P. O.; Porto, M. V.; Canotilho, J.; Castro, R. A. E.; Caires, F. J; Eusébio, M. E. S. *Novel nimesulide multicomponent solid forms: Screening, synthesis, thermoanalytical study and characterization.* Journal of Thermal Analysis and Calorimetry, 2024. https://doi.org/10.1007/s10973-024-13189-2

3.1 INTRODUCTION

Nimesulide (NMS), shown in Figure 15, is a non-steroidal anti-inflammatory drug (NSAID) that is extensively used worldwide, especially in Brazil, due to its therapeutic properties against pain, fever and inflammation, and also its availability as over-the-counter drug, allowing self-medication (ANVISA, 2023; BADRI et al., 2016; MACEDO et al., 2021). Typically, a NMS dosage of 100 mg twice daily is orally administered, but the dose can vary from 100 to 400 mg per day depending on the disorders (CAIAZZO; IALENTI; CICALA, 2019; CATARRO et al., 2019; WARD; BROGDEN, 1988). NMS belongs to the group of NSAIDs that present preferential selective inhibition of the enzyme cyclooxygenase-2 (COX-2), therefore presenting a low incidence of side effects (GÜNGÖR et al., 2021; TUBIČ et al., 2016). However, NMS has low aqueous solubility (about 0.01 mg mL^{-1} at 25 °C) (NASCIMENTO et al., 2021; PATEL et al., 2019; WANG et al., 2020).

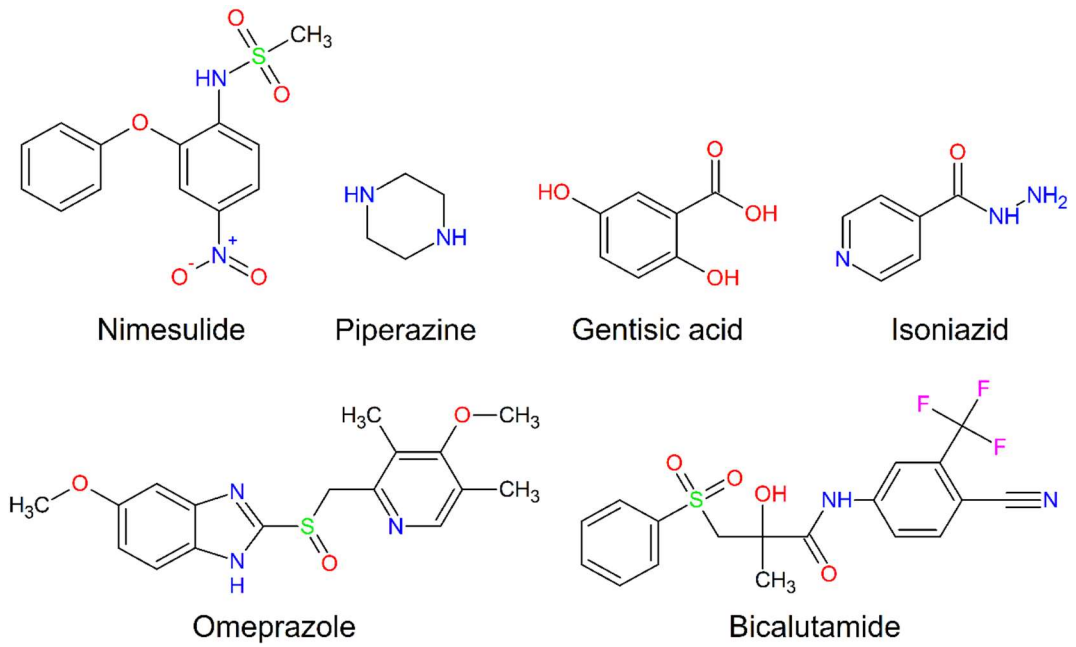


Figure 15 – Chemical structures of NMS and selected coformers explored in this study.

The low aqueous solubility of active pharmaceutical ingredients (APIs) compromises the desired plasmatic concentration and, consequently, limits their oral bioavailability and clinical efficacy (BLAGDEN et al., 2007; CHADHA et al., 2016; KOTBANTAO; CHAROENCHAITRAKOOL, 2017). Nimesulide, as well as

other NSAIDs, is categorized as a BCS-class II drug, corresponding to those that present high permeability and low aqueous solubility (NASCIMENTO et al., 2021; PATEL et al., 2019; WANG et al., 2020).

Several strategies have been used to overcome the solubility issue. One of them is the use of multicomponent solid forms, like salts, cocrystals, eutectic mixtures and coamorphous systems, which are capable of altering the physicochemical properties of drugs without affecting the pharmacological ones (BERRY; STEED, 2017; BOLLA; SANPHUI; NANGIA, 2013; DUGGIRALA et al., 2020; GOPI; BANIK; DESIRAJU, 2017; LI et al., 2020b; SATHISARAN; DALVI, 2018; UPPALA et al., 2022). In the case of dual-drug multicomponent solid forms, in addition to pharmacokinetic improvement, there may be an increase in its activities synergistically, therapeutic combination and/or reduction of side effects (BOLLA; NANGIA, 2016; LI et al., 2020a; NASCIMENTO et al., 2021).

Pharmaceutical cocrystals are multicomponent crystalline forms, in which an API and one or more coformers are linked in a defined stoichiometry by non-covalent and non-ionic intermolecular interactions, such as hydrogen bonding, van der Waals forces and π-π stacking. Commonly, the cocrystal-forming components are neutral and solids at ambient conditions (KARIMI-JAFARI et al., 2018; PINDELSKA; SOKAL; KOLODZIEJSKI, 2017; QIAO et al., 2011; VISHWESHWAR et al., 2006). Meanwhile eutectic mixtures comprise two (or more) solids that result in a mixture with lower melting point than the precursors, being miscible in the liquid state and immiscible in the solid state. They maintain the crystal structure of the starting materials (BAZZO; PEZZINI; STULZER, 2020; CHERUKUVADA; NANGIA, 2014).

The conversion of a crystalline API to its amorphous phase could achieve an increased solubility and dissolution rate. However, amorphous drugs present higher energy and entropy due to the lack of long-range order, the solid is more unstable than its crystalline counterparts and tends to crystallize over time (SABERI et al., 2023; SHI; MOINUDDIN; CAI, 2019; SILVA; ROSADO; EUSÉBIO, 2021). Alternatively, coamorphous systems mix small coformers with the API preventing the drug molecules aggregation, therefore increasing the kinetic stability. They are homogeneous multicomponent amorphous phases characterized by a single glass-transition temperature (*T*g) and are stabilized by

intermolecular interactions and/or mixing effects (SABERI et al., 2023; WANG et al., 2020; ZHANG et al., 2021).

Considering that few papers report obtaining of NMS multicomponent solid forms (ABDELKADER et al., 2014; GEORGESCU et al., 2021; PATEL et al., 2019; WANG et al., 2020, 2021a; ZHANG et al., 2021), the present work focused in prospecting new NMS multicomponent solid systems, using coformers with different functional groups, systematic molecular diversity, and/or with potential for desired therapeutic combination with NMS. A set of 30 coformers was selected, as presented in Figure 2 and Table A.2 (Appendix section). A deeper investigation was performed concerning the coformers piperazine, gentisic acid, isoniazid, omeprazole and bicalutamide, Figure 15.

3.2 MATERIALS AND METHODS

3.2.1 List of chemicals used

A detailed list of all chemicals employed in this study is displaced in Table A.1, on the Appendix section.

3.2.2 Virtual-experimental cocrystal screening approach

The virtual cocrystal screening of NMS was performed using COSMOquick software (Biovia version 2021, Dassault Systèmes, Germany). The method calculates the excess enthalpy (ΔH_{excess}) of an undercooled liquid mixture of the components, reflecting the interaction strength of the API and coformer, and the flexibility parameter (F_{fit}) that combines the molecular interactions (ΔH_{excess}) with the number of rotatable bonds in the molecules, allowing the prediction of cocrystal formation (GUIDETTI et al., 2023; KUMAR; NANDA, 2021; LOSCHEN; KLAMT, 2015).

A set of 30 coformers was chosen to explore diverse functional groups that could be compatible with NMS ones and/or in a dual-drug perspective (see Table A.2 in the Appendix section) and submitted to the “cocrystal and solvate screening” tool. The Simplified Molecular Input Line Entry System (SMILES) notation, for each compound was employed as input data. The output result generated a list which could be compiled by excess enthalpy (ΔH_{excess}) and

flexibility parameter (F_{fit}). In parallel to the virtual screening, NMS + coformer mixtures were submitted to an experimental cocrystal screening through a mechanochemical approach. Some were also slurried in ethyl acetate and/or acetonitrile as mentioned below.

3.2.2.1 Mechanochemical synthesis

Equimolar mixtures of starting materials (approximately 100 mg in total) were milled in a MM400 Retsch ball mil (Retsch GmbH & Co., Germany) at an operating frequency of 15 and/or 30 Hz for 30 minutes. The samples were placed in a 10 mL stainless steel jar with one 7 mm stainless steel ball. A small amount of ethanol (η = 0.25 µL mg^{-1}) was employed in the liquid assisted grinding (LAG) process (FRIŠČIĆ et al., 2009). Some samples were ground in a neat (NG) condition. All the resultant solid products were collected and stored in hermetically sealed containers till further characterization and evaluation.

It is worth pointing out that all the precursors employed in this step of experimental cocrystal screening were submitted to LAG experiments – and subsequently characterized by DSC, PXRD and FTIR techniques – to ensure that this process does not alter their structural characteristics. Furthermore, other binary compositions were prepared at 15Hz for NMS-GSA and NMS-INH systems and analyzed by DSC.

3.2.2.2 Slurry

In a first batch, NMS binary equimolar solid mixtures with caffeine (CAF), ciprofloxacin (CIP), norfloxacin (NOR), piperazine (PPZ), theobromine (TBM) and theophylline (THEO) were slurried overnight in ethyl acetate (η = 5 µL mg^{-1}) (FRIŠČIČ; JONES, 2009; FRIŠČIĆ; MOTTILLO; TITI, 2020). On a second batch, the selected coformers (except PPZ) were slurried with NMS for 72 h in acetonitrile. The wet paste was stirred at 400 rpm using a magnetic stirrer under 25 °C (controlled using a thermostatic bath). After the experiments, all samples were analyzed by PXRD.

3.2.3 Coamorphous preparation

The coamorphous systems preparation was conducted through three different approaches, cryomilling, “cold NG” and/or quench cooling, as detailed bellow.

3.2.3.1 Cryomilling (Cryo) and “cold NG”

Cryogenic milling experiments were performed using a MM400 Retsch ball mil (Retsch GmbH & Co., Germany), a 10 mL stainless steel jar with two 7 mm stainless steel balls and liquid nitrogen as coolant. The anti-inflammatory NMS and the selected coformers were mixed in a 1-1 molar ratio (100 mg sample in total). The cryo process was conducted at 30 Hz for 4 cooling cycles, with total milling time of 60 min. Each cycle consisted of immersion of the jars containing the mixtures in liquid nitrogen for approximately 2.5 min, followed by milling for 15 minutes. The samples were collected and stored in a desiccator at room temperature until further characterization and evaluation.

For the NMS-OMP system, additional experiments were carried out that are identified as “cold NG”: the jars containing the solid mixture were pre-cooled in the freezer at $T \approx$ -20 °C, for 1.5 hour prior to milling (30 Hz, 30 min).

3.2.3.2 Quench cooling (QC)

Quench cooling processes were performed *in situ* using a PerkinElmer Pyris1 calorimeter (PerkinElmer, USA) with liquid nitrogen cryofill cooling unit. In such analysis, about 2.5 mg of sample was placed in 50 µL aluminum crucibles with perforated lid and submitted to a nitrogen atmosphere (20 mL min^{-1}). An empty similar aluminum pan was used as a reference. The samples were equilibrated at 25 °C and heated until complete melting (with 10 °C min^{-1} heating rate) to erase the solid history of the samples and ensure mixing of components. After melting, the samples were quickly cooled to -35 ºC at a cooling rate of 50°C min^{-1}. The second heating (10 °C min^{-1}) was carried out to analyze the propensity of conversion of the crystalline material into amorphous state, and then, the *T*g temperatures were recorded (midpoints of the characteristic baseline step changes).

3.2.3.2.1 Quench cooling scale-up procedure

This procedure was performed to obtain enough sample for dissolution rate tests for the NMS-BICA system. An equimolar mixture was heated in a sealed container to complete melting in an oven (185 °C) and rapidly cooled in an ice bath. Prior to dissolution rate tests, the obtained QC sample was grinded gently using a mortar and pestle, and DSC and PXRD analyses were carried out to ensure complete coamorphization of the mixture.

3.2.4 Characterization

3.2.4.1 Simultaneous Thermogravimetry and Differential Scanning Calorimetry (TG-DTA)

Samples grinded at 15 Hz were analyzed through a TG-DTA equipment, model STA 449 Jupiter (NETZSCH GmbH & Co. Holding KG, Germany). Approximately 5 mg of sample was weighed and placed in a α-Al_2O_3 crucible (70 µL) as sample holder and an empty similar crucible as reference. The temperature program had a heating rate 10 °C min^{-1} from 30 to 800 °C. Dry air atmosphere with flow rate of 50 mL min^{-1} was used as purge gas.

3.2.4.2 Differential scanning calorimetry (DSC)

Samples grinded at 15 Hz were analyzed through the Mettler Toledo DSC1 Stare System equipment (Mettler Toledo, Switzerland). The solid material was heated at a heating rate of 10 °C min^{-1} from 25 °C until the thermal stability of each sample under synthetic air atmosphere with a flow rate of 50 mL min^{-1}. The sample mass was kept in the range of 2.5 mg and aluminum crucibles (40 µL) with perforated lid was used as reference and sample holder. Additionally, the DSC data of the NMS-GSA and NMS-INH systems were used to construct the binary solid-liquid phase diagrams and Tamman's triangle plot.

The DSC curves from 30 Hz samples were obtained using a PerkinElmer DSC7 calorimeter (PerkinElmer, USA) with an intracooler unit at -20 °C (ethyleneglycol-water, 1:1, V/V) and nitrogen purge (20 mL min^{-1}) at a heating rate β = 10 °C min^{-1}. Approximately 2.5 mg of sample were sealed in 50 µL

aluminum crucibles with a single hole punched in the lid. An empty pan of the same type was employed as a reference.

All the instruments were calibrated using indium as a standard, following the manufacturer's instructions.

3.2.4.3 Binary solid-liquid phase diagrams and Tamman's triangle construction

NMS-GSA and NMS-INH mixtures of different compositions were analyzed by DSC. The Tamman's triangle was constructed by plotting the eutectics enthalpy correlated to the sample composition, while binary phase diagrams were constructed by taking the *solidus* and *liquidus* temperatures – the onset temperature (T_{onset}) of first DSC melting event and peak temperature (T_{peak}) of second event that corresponds to the complete melting, respectively – of each sample (AGAFONOVA; MOSHCHENSKIY; TKACHENKO, 2014; BAZZO; PEZZINI; STULZER, 2020; PATEL et al., 2019). For several mixtures, for the determination of the eutectic melting enthalpy, deconvolution of the complex melting peak was carried out using the peak fitting module in the Origin 7 software (version 7.0300, from OriginLab Corporation). A theoretical diagram (represented by calculated *liquidus* temperatures) was estimated using the Schröder-van Laar equation, that assumes solid-liquid ideal mixture equilibrium (AGAFONOVA; MOSHCHENSKIY; TKACHENKO, 2014; IVASHENKO; TITOV; KOVSHEV, 1976; LORENZ; SEIDEL-MORGENSTERN, 2002; PRIGOGINE; DEFAY, 1954).

3.2.4.4 Infrared spectroscopy (FTIR)

The FTIR spectra were obtained in the Nicolet 380 IR spectrophotometer (Thermo Scientific, USA), using an accessory of attenuated total reflectance with diamond crystal, in the range of 4000 cm^{-1} to 400 cm^{-1}, resolution of 2 cm^{-1} and 32 scans per spectrum.

3.2.4.5 Powder X-ray diffraction (PXRD)

The PXRD patterns were obtained using a Rigaku powder X-ray diffractometer (Rigaku, Japan), model MiniFlex 600, using a copper tube providing radiation CuK_{α}, λ = 1.5418 Å subjected to 40 kV, current of 15 mA. The samples were scanned in a 2θ angle range from 3° to 40°, in continuous scan mode, with a step size of 0.01° and scan speed of 5° min^{-1}. The samples were placed in round zero background holders with spin prior to analysis.

3.2.5 Dissolution rate study

The dissolution rate measurements were carried out in triplicate using a rotating disk apparatus (Wood's apparatus) coupled to a Sotax dissolution tester (SOTAX AG, Switzerland). 50 mg of crystalline NMS and selected systems were taken in the dissolution accessory and compressed to a 0.4 cm radius (0.5026 cm^2) stainless-steel disk using a hydraulic press (Specac press) at a pressure of 1.0 ton during 10 seconds. The accessory was placed in a jar of 900mL with phosphate buffer pH 7.4 with 2% of tween 80 (v/v) as dissolution media, pre-heated to 37 °C and stirred at 75 rpm. The experimental conditions follow the Brazilian Pharmacopeia for nimesulide tablets (ANVISA, 2019b).

NMS concentration was determined from the absorbance measured online in a Lambda 365 PerkinElmer UV-vis spectrophotometer every 5 minutes at 397 nm. A calibration curve for pure NMS, obtained at this wavelength, was used. Prior to the experiments, the selectivity of NMS determination by this procedure, relatively to the coformers, was evaluated (see Figures A.1 and A.2, in the Appendix section, for details). The remaining solids were analyzed by PXRD and no significant phase transition occurred due to the compression and dissolution processes.

3.3 RESULTS AND DISCUSSION

3.3.1 Nimesulide characterization

According to the TG-DTA analysis (Figure 16a), nimesulide is thermally stable up to 245 °C, suffering two steps of thermal decomposition. The first one occurring between 245 °C and 370 °C, correlated with a small exothermic peak at 340 °C on DTA curve. The second step occurs between 370 °C and 715 °C, associated to the exothermic event at 539 °C (GÁLICO et al., 2014). The DTA curve also presents an endothermic peak at 150.40 °C attributed to the nimesulide melting temperature. Afterwards, this event is also observed on the DSC curve (T_{onset}=149.0 °C; T_{peak}= 150.5 °C; ΔH= 98.7 J g^{-1}), as shown in Figure 16b. The results are in accordance with those reported by Gálico and co-workers (GÁLICO et al., 2014).

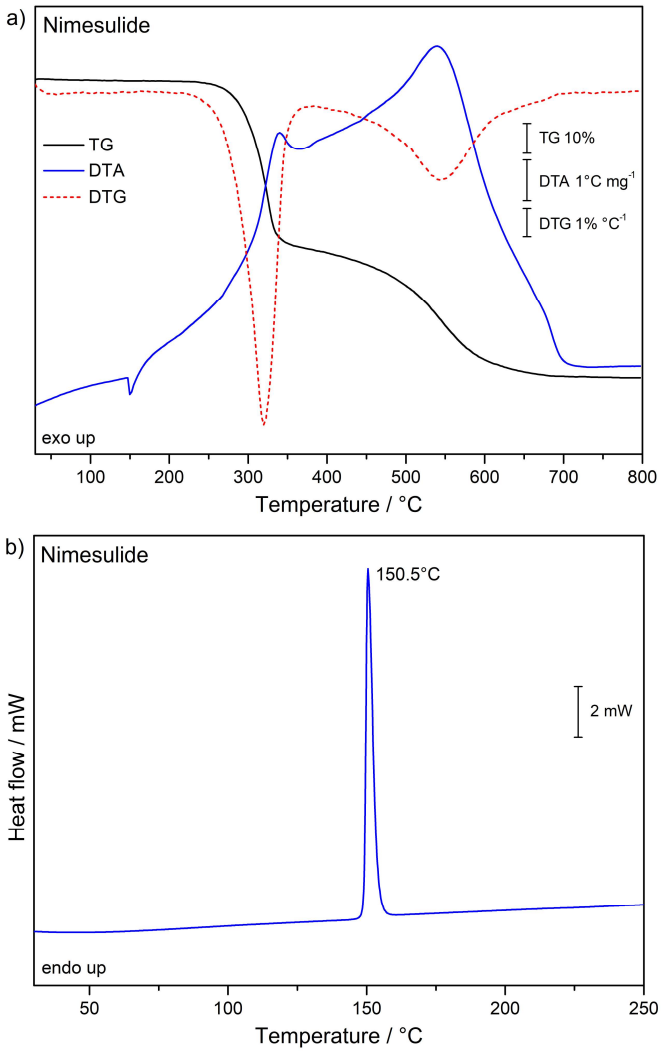


Figure 16 – TG-DTA-DTG (a) and DSC (b) curves of pure nimesulide.

Two polymorphic forms of nimesulide are reported in literature structures, the stable form I and the metastable form II (BARRIO et al., 2017; BERGESE et al., 2003; SANPHUI; SARMA; NANGIA, 2011). The PXRD diffractogram of NMS is presented in Figure 17a. The presence of characteristic peaks indicates the crystalline nature of the material and the diffraction pattern corresponds to the polymorph form I (BERGESE et al., 2003; SANPHUI; SARMA; NANGIA, 2011).

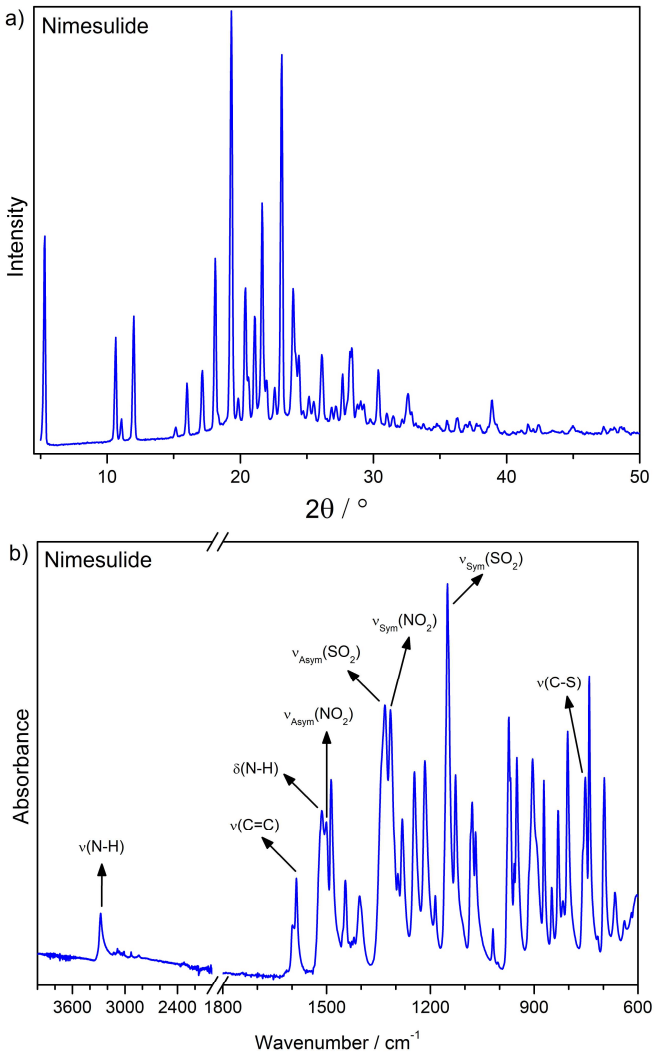


Figure 17 – PXRD pattern (a) and FTIR spectrum (b) of pure nimesulide.

The FTIR spectra of NMS is shown in Figure 17b. It reveals the main modes of vibration characteristics to N-H stretching at 3277 cm^{-1}, aromatic C=C stretching at 1587 cm^{-1}, N-H bending at 1513 cm^{-1}, symmetric and asymmetric NO_2 vibrations at 1318 cm^{-1} and 1501 cm^{-1}, respectively. Furthermore, strong

vibrational modes of sulfonyl group appears at 1331 cm^{-1} and 1150 cm^{-1} attributed to asymmetric and symmetric stretching, respectively (NUNES et al., 2016; PATEL et al., 2019).

3.3.2. Virtual-experimental cocrystal screening and coformers selection

Only one article reports obtaining NMS cocrystals (WANG et al., 2021a). In this regard we explored a combined virtual and experimental screening of NMS cocrystals.

The results obtained, using COSMOquick, for cocrystal screening of NMS with the 30 selected compounds, as well as with the coformers tested by Wang *et al.* (WANG et al., 2021a), are presented in Table A.2 (coformers are organized by structural similarities). It is worth remembering that the coformers were chosen in order to have different functional groups, systematic molecular diversity and/or a combination of desired therapeutic action with NMS. According to the COSMOquick software, the more negative the ΔH_{excess} and the lowest the F_{fit} values, the highest the probability of interaction between the precursors (BOLLA; SARMA; NANGIA, 2022; GUIDETTI et al., 2023; KUMAR; NANDA, 2021; PANTWALAWALKAR et al., 2021). Negative ΔH_{excess} were obtained for all the coformers tested by Wang *et al*. (WANG et al., 2021a). Among them, 1,3-bis(4-pyridyl)propane has the highest F_{fit} value and does not give rise to cocrystals. However, as observed in Table A.2, the ΔH_{excess} values for most of the coformers were positive or only slightly negative. This data indicates the low tendency of obtaining NMS cocrystals.

Despite *in silico* indications, all binary NMS mixtures were submitted to an experimental screening through mechanochemical processes. For some coformers, caffeine, ciprofloxacin, norfloxacin, piperazine, theobromine and theophylline, low negative ΔH_{excess} values were obtained, with different F_{fit}. Nimesulide binary systems with these coformers were also slurried in ethyl acetate and/or acetonitrile. Table A.2 (Appendix section) summarizes the virtual-experimental screening results. As a result of this combined screening approach, in addition to the already known NMS cocrystals with bipyridyl and its derivatives (WANG et al., 2021a), only a new cocrystal was identified, a NMS-PPZ 1-1

cocrystal (for this system ΔH_{excess} = -0.32; F_{fit} = 2.7), as will be shown in the next section.

When positive ΔH_{excess} are obtained the overall experimental results are in agreement with the virtual screening predictions, since cocrystal formation is not expected. For low negative values, as observed for several NMS coformers such as caffeine, theobromine, and ciprofloxacin, the results are not predictable and certainly depend on subtle association factors.

3.3.3 Nimesulide cocrystals

The DSC data, shown in Figure 18, gives an unequivocal proof of NMS-PPZ association since the mixture melts above the pure precursors (T_{onset}= 161.9 °C; T_{peak}= 164.9 °C; ΔH= 131.4 J g^{-1}). Nimesulide presents melting temperature around 149 °C (T_{onset}=149.0 °C; T_{peak}= 150.5 °C; ΔH= 98.7 J g^{-1}), while the DSC curve of piperazine presents two endothermic peaks related to water removal and melting/vaporization around 45–60 °C and at 85 °C, respectively (BISHNOI; ROCHELLE, 2002; GÁLICO et al., 2014; MOISESCU-GOIA; MURESAN-POP; SIMON, 2017; ZHANG et al., 2019).

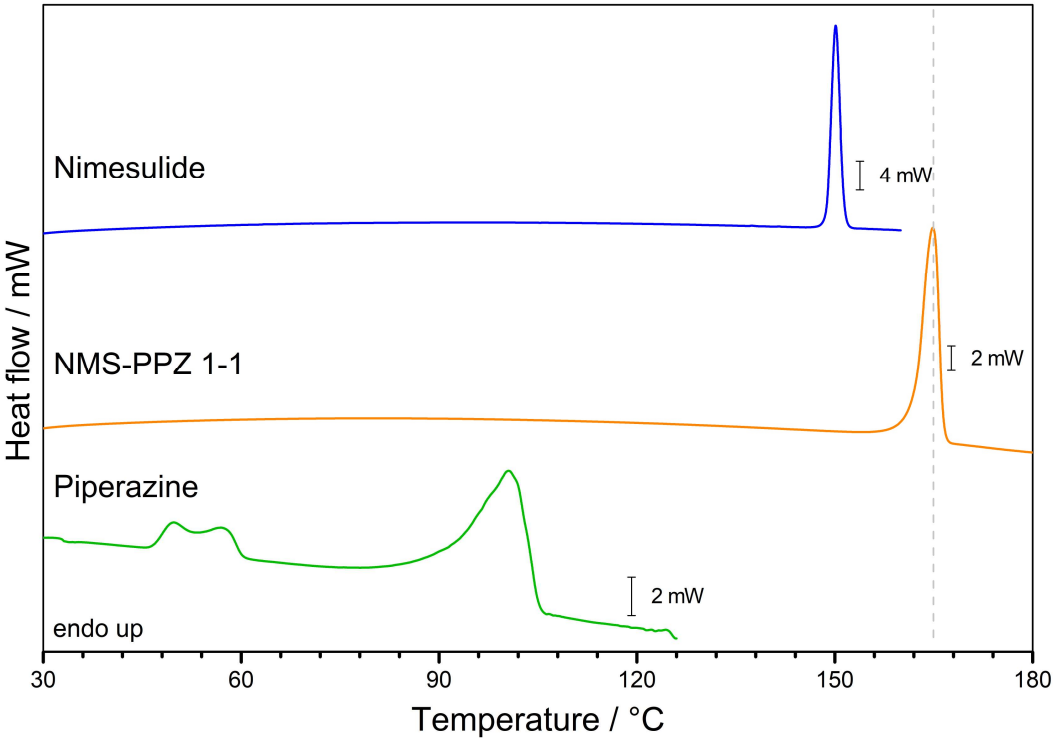


Figure 18 – DSC heating curves of NMS-PPZ equimolar system and pure compounds.

The formation of a novel multicomponent solid form is confirmed by PXRD and FTIR analyses, as observed in Figures 19a and 19b, respectively. The diffractograms of raw material correspond to the NMS polymorph form I (CCDC number: 773602) and PPZ monohydrated form (CCDC number: 1473720) (BARRIO et al., 2017; BERGESE et al., 2003; WANG et al., 2019; ZHANG et al., 2019). The NMS-PPZ 1-1 system shows a distinct PXRD pattern when compared to the starting compounds, with new peaks at 2θ = 4.27°, 8.56°, 13.38°, 17.17°, 20.01°, 20.87°, 22.31°, 25.88°, 26.94°, 28.86°. Characteristic reflections of the precursors are also absent, as expected.

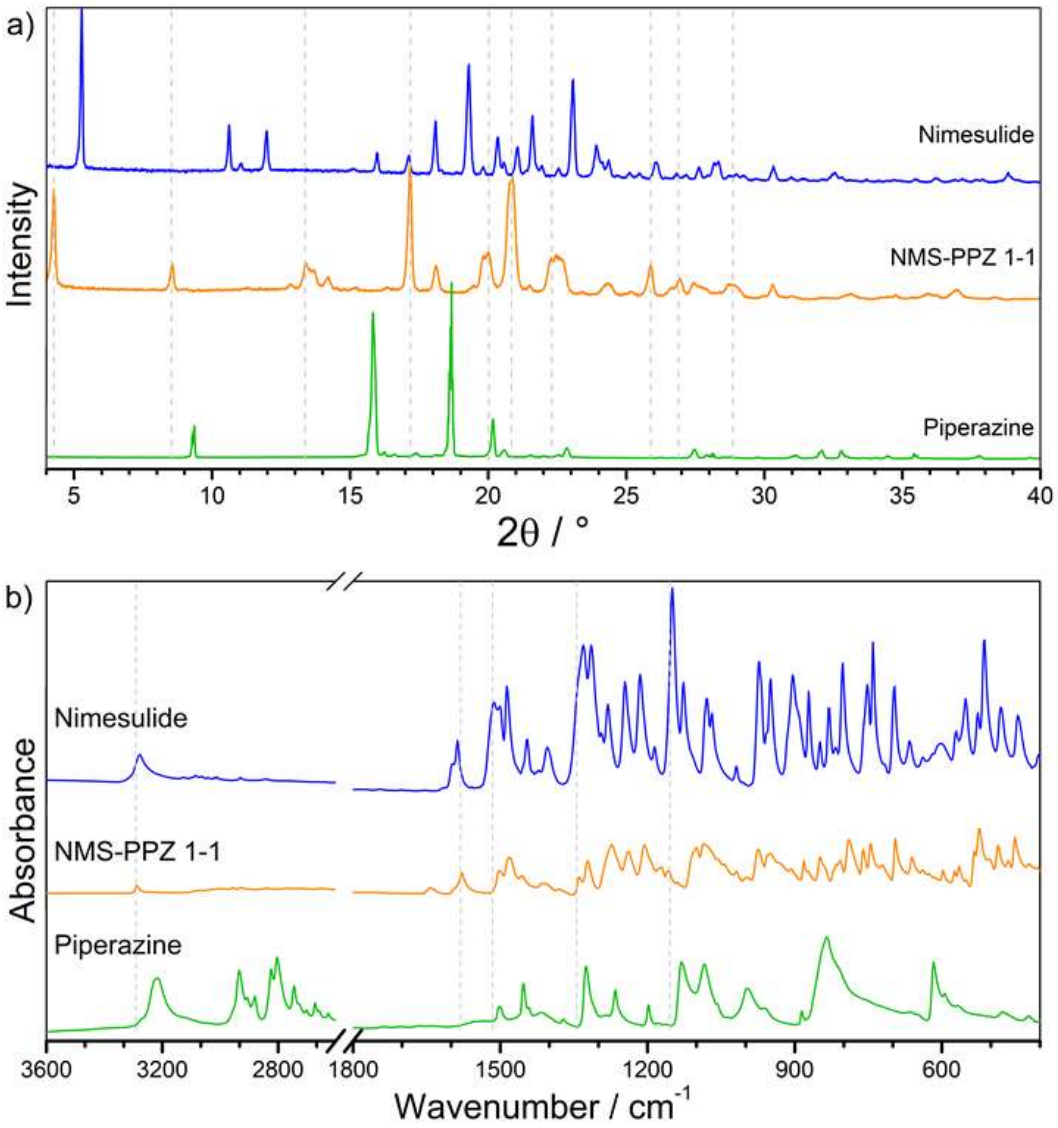


Figure 19 – PXRD pattern (a) and FTIR spectra (b) of NMS-PPZ equimolar system and pure compounds.

The FTIR spectrum of pure NMS was discussed above, while the main vibrational bands of PPZ are observed at 3287 cm^{-1} and 1501 cm^{-1} attributed to N-H stretching and bending, respectively (MOISESCU-GOIA; MURESAN-POP; SIMON, 2017).

On the other hand, the FTIR spectrum of NMS-PPZ 1-1 system presents evident changes related to the amine and sulfonyl groups. It is possible to verify a decrease of intensity and hypsochromic displacement of the N-H stretching vibrational mode of NMS and PPZ, respectively, from 3277 cm^{-1} and 3216 cm^{-1} to 3287 cm^{-1} in the mixture. Moreover, the symmetrical and asymmetrical stretches of SO_2 group are shifted to higher wavenumbers from 1150 cm^{-1} and 1331 cm^{-1} to 1156 cm^{-1} and 1340 cm^{-1}, respectively. The intensity of SO_2 bands also decreased (BOLLA; MITTAPALLI; NANGIA, 2015; MOISESCU-GOIA; MURESAN-POP; SIMON, 2017; WANG et al., 2019; ZHANG et al., 2019). Therefore, the hypsochromic displacements foremost suggest the formation of a new hydrogen bonding network involving NH and SO_2 groups, confirming the obtaining of a novel crystal structure. The main spectral assignment is summarized in Table 4.

Table 4 – Main FTIR vibrational modes of NMS-PPZ equimolar system and pure compounds.

Assignment	Wavenumber (cm^{-1})		
	NMS	**PPZ**	**NMS-PPZ 1:1**
ν (N-H)	3277	3216	3287
δ (N-H)	1513	1501	1501
ν_{Asym} (NO_2)	1501	-	1501
ν_{Sym} (NO_2)	1318	-	1321
ν_{Asym} (SO_2)	1331	-	1340
ν_{Sym} (SO_2)	1150	-	1156

Virtual screening pointed out to NMS-PPZ cocrystal formation, which was confirmed by the experimental results. Since the excess enthalpy (ΔH_{excess}) can be roughly approximated to the free energy of cocrystalization, NMS-PPZ

cocrystal formation could be favored (GUIDETTI et al., 2023; KUMAR; NANDA, 2021). Furthermore, the mechanochemical process can provide mechanical stress, through shear and friction forces, exposing the precursors surface, promoting molecules reorganization and leading to the interaction between NMS and the low molecular-weight coformer PPZ (BAZZO; PEZZINI; STULZER, 2020; FRIŠČIČ; JONES, 2009). On the other hand, apart from the good correlation between the virtual and experimental screening of the NMS-PPZ system, the other coformers tested experimentally did not form cocrystals with NMS, as expected. In these cases, the positive or slightly negative ΔH_{excess} values, as well as, the substantially high F_{fit} values indicate low tendency of cocrystalization (GUIDETTI et al., 2023; KUMAR; NANDA, 2021).

3.3.4 Nimesulide eutectic mixtures

Gentisic (GSA, or 2,5-dihydroxycarboxylic) acid, is a phenolic acid that has been associated as coformer in multicomponent solid approaches since it presents anti-inflammatory, antimicrobial, and antioxidant activities, among others (MASHHADI et al., 2021; SOKAL et al., 2017). On the other hand, isoniazid (INH) is an antibiotic drug widely used to treat tuberculosis (CARAZO et al., 2018; CHERUKUVADA; NANGIA, 2012; DINIZ et al., 2018). In this context, NMS-GSA and NMS-INH systems were explored due to their potential for combined therapy.

The DSC curves (Figures 20a and 20b) show that NMS-GSA and NMS-INH equimolar samples melt at 138.4 °C and 132.7 °C, respectively, a lower melting temperature than the starting material (NMS at 149.0 °C, GSA at 201.7°C and INH at 171.0 °C). Infrared spectra and PXRD shown in Figures A.3 and A.4 for the equimolar samples confirm that they are mixtures of the starting solid precursors.

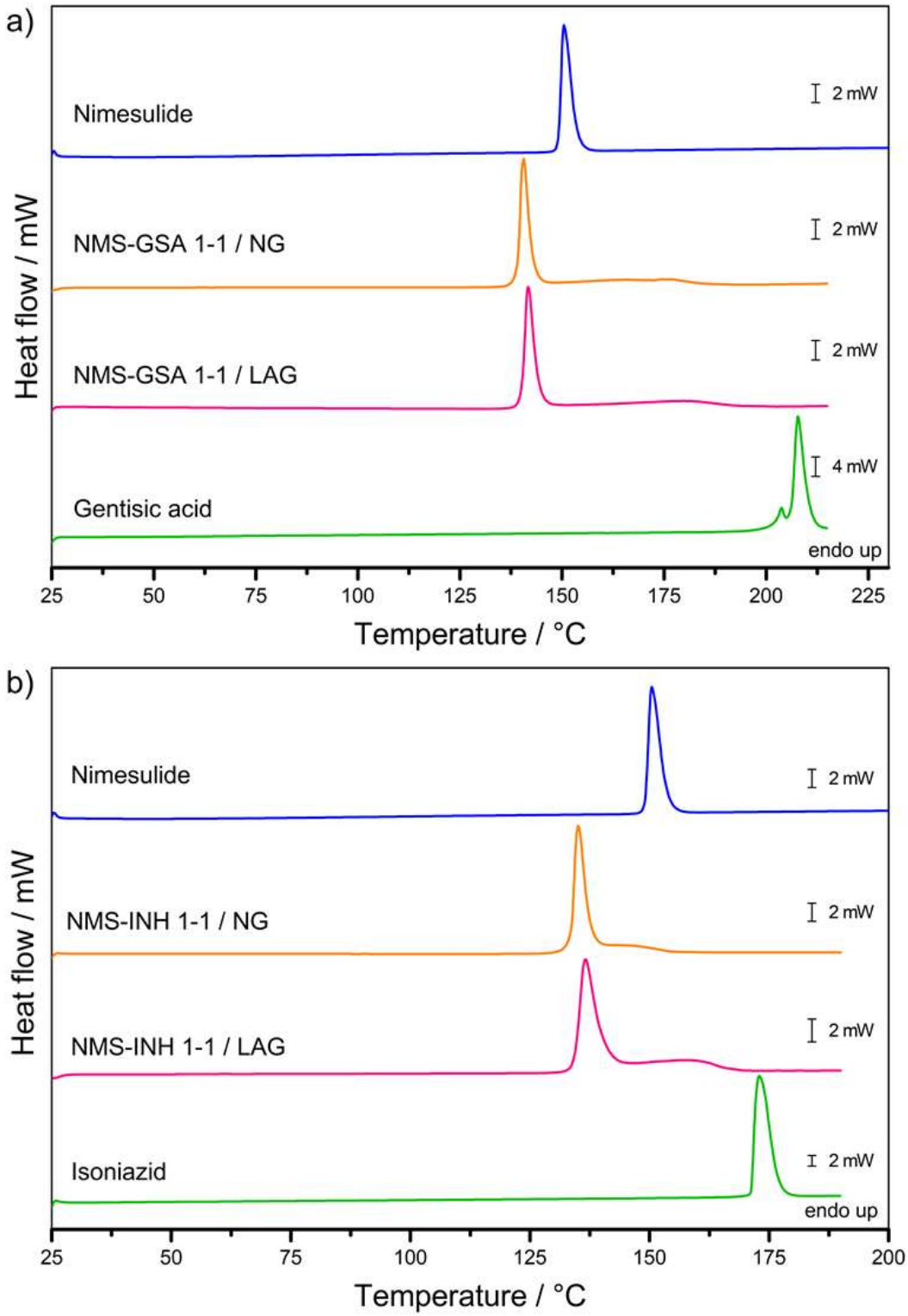


Figure 20 – DSC heating curves of NMS-GSA (a) and NMS-INH (b) equimolar systems and pure compounds, prepared by NG and by LAG.

Both systems show a profile of DSC heating curves, for different compositions, Figures 21a and 22a, that correspond to a typical binary system with a diagram of a simple eutectic. An invariant point – beginning of melting at

the same temperature – below the melting of pure compounds is observed at 138 °C to NMS-GSA mixtures and at 132 °C to NMS-INH mixtures (BAZZO; PEZZINI; STULZER, 2020; CORTESÃO et al., 2017). Furthermore, both experimental binary solid-liquid diagrams show some deviation from the respective theoretical diagrams, predicted using the Schroder-van Laar equation, that assumes ideality of the liquid mixtures (Figures 21b and 22b) (AGAFONOVA; MOSHCHENSKIY; TKACHENKO, 2014; BAZZO; PEZZINI; STULZER, 2020; PATEL et al., 2019; PRIGOGINE; DEFAY, 1954).

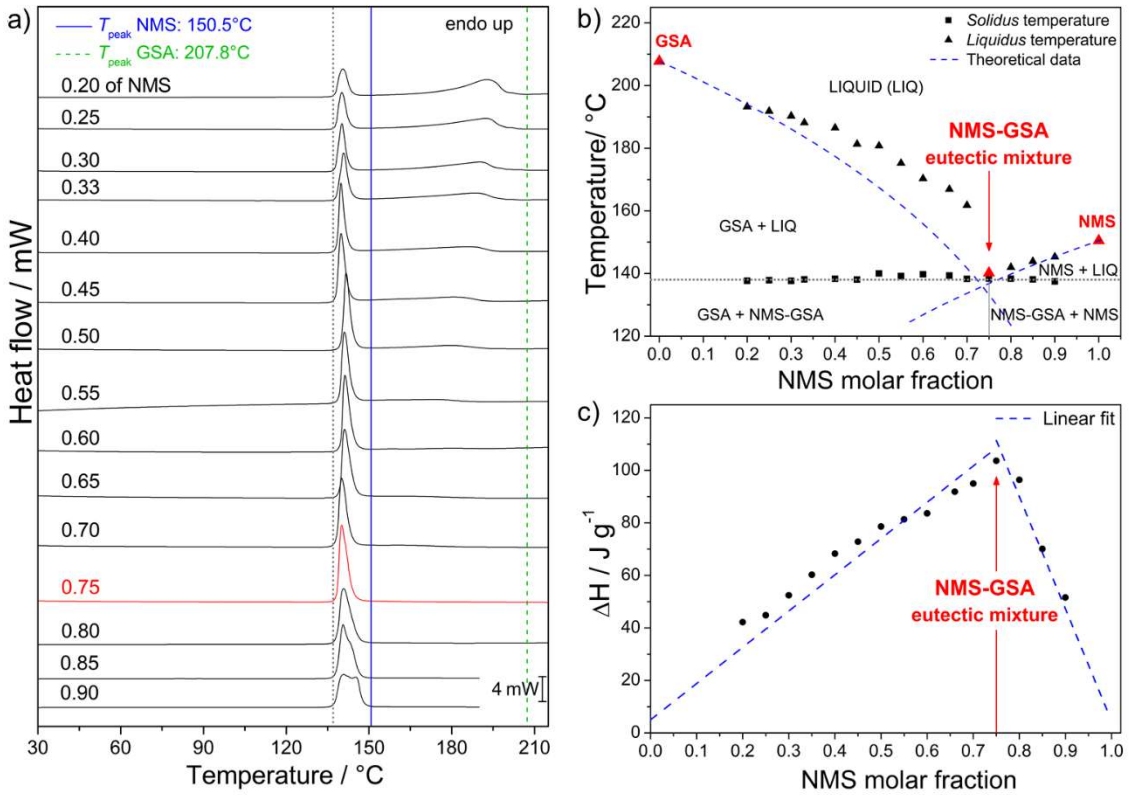


Figure 21 – DSC heating curves (a), binary solid-liquid phase diagram (b) and Tamman's triangle (c) of NMS-GSA system for different compositions. In the phase diagram, the dashed lines, correspond to the prediction of Schroder-van Laar equation (PRIGOGINE; DEFAY, 1954).

The phase diagrams give an indication of the eutectic compositions that were determined using the Tamman's plots (Figures 21c and 22c). Tamman's triangle was constructed by plotting the enthalpy of eutectic melting as a function of NMS molar fraction in the mixtures. Therefore, the intersection of the linear fits for hipo and hiper-eutectic compositions pointed out the NMS molar fractions in the eutectic mixture as 0.75 for NMS-GSA and 0.61 for NMS-INH, relative to the

mixture with highest enthalpy value (AGAFONOVA; MOSHCHENSKIY; TKACHENKO, 2014; BAZZO; PEZZINI; STULZER, 2020).

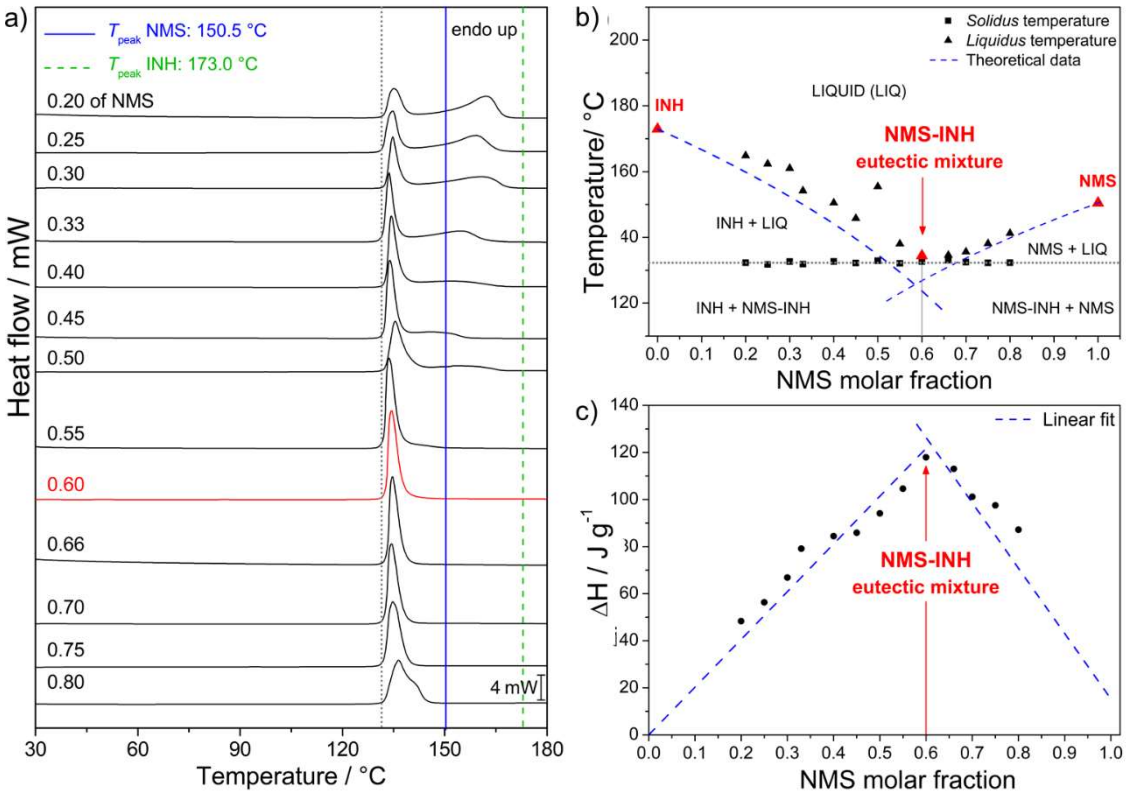


Figure 22 – DSC heating curves (a), binary solid-liquid phase diagram (b) and Tamman's triangle (c) of NMS-INH system for different compositions. In the phase diagram, the dashed lines, correspond to the prediction of Schroder-van Laar equation (PRIGOGINE; DEFAY, 1954).

3.3.5 Nimesulide coamorphous systems

Additionally, the present work also explored a coamorphization approach. As mentioned before, a set of APIs were selected focusing on an interesting association with NMS, in a dual-drug perspective. In the literature, only two articles recently report the investigation of NMS coamorphous systems with profen-analogues and indomethacin (WANG et al., 2020; ZHANG et al., 2021).

Coamorphous systems can be prepared via two different mechanisms, kinetic and thermodynamic disordering processes, such as mechanochemistry and quench cooling, respectively. In mechanochemical methods, the amorphous binary system can be formed directly from the crystalline solid-state by the continuous mechanical stresses. On the other hand, the quenching process

involves rapidly cooling the molten sample, a thermodynamically stable non-crystalline form (DENGALE et al., 2016; SHI; MOINUDDIN; CAI, 2019).

Equimolar NMS coamorphous systems were investigated through mechanochemistry and/or quench cooling processes. Novel NMS coamorphous systems were obtained with bicalutamide (glass-transition temperature, *T*g = 38 ºC), isoniazid (*T*g =15 ºC), metoclopramide (*T*g = 39 ºC), *p*-aminobenzoic acid (*T*g = 19 ºC), piracetam (*T*g = 10 ºC) and omeprazole (*T*g = 32 ºC), as shown in Figure A.5 (Appendix section). For amorphous nimesulide the glass-transition temperature is *T*g = 22 ºC, which is in agreement with literature (WANG et al., 2020; ZHANG et al., 2021). Some of these equimolar NMS coamorphous mixtures presented glass-transition temperature below that of NMS. Taking this into account, we decided to explore in more detail the NMS-OMP system using different mechanochemical approaches, and NMS-BICA system, using both mechanochemistry and quench cooling processes.

3.3.5.2 Nimesulide–omeprazole system

NMS is a preferential COX-2 inhibitor that can cause gastrointestinal disorders (KRESS et al., 2016; SZABÓ-RÉVÉSZ, 2018). In this regard, we selected omeprazole (OMP), an anti-acid drug widely used to treat gastric diseases (BENDAS; ABDELBARY, 2014; NOGUEIRA et al., 2021), due to the potential of pharmacological association between NMS and OMP.

Previously, into the cocrystal screening process, NMS-OMP equimolar mixture was prepared by mechanochemical method at 15 Hz during 30 minutes, with or without the addition of ethanol. Regarding the thermal analytical results (Figure 23) it is observed that both mixtures presented lower melting temperature compared to the isolated APIs.

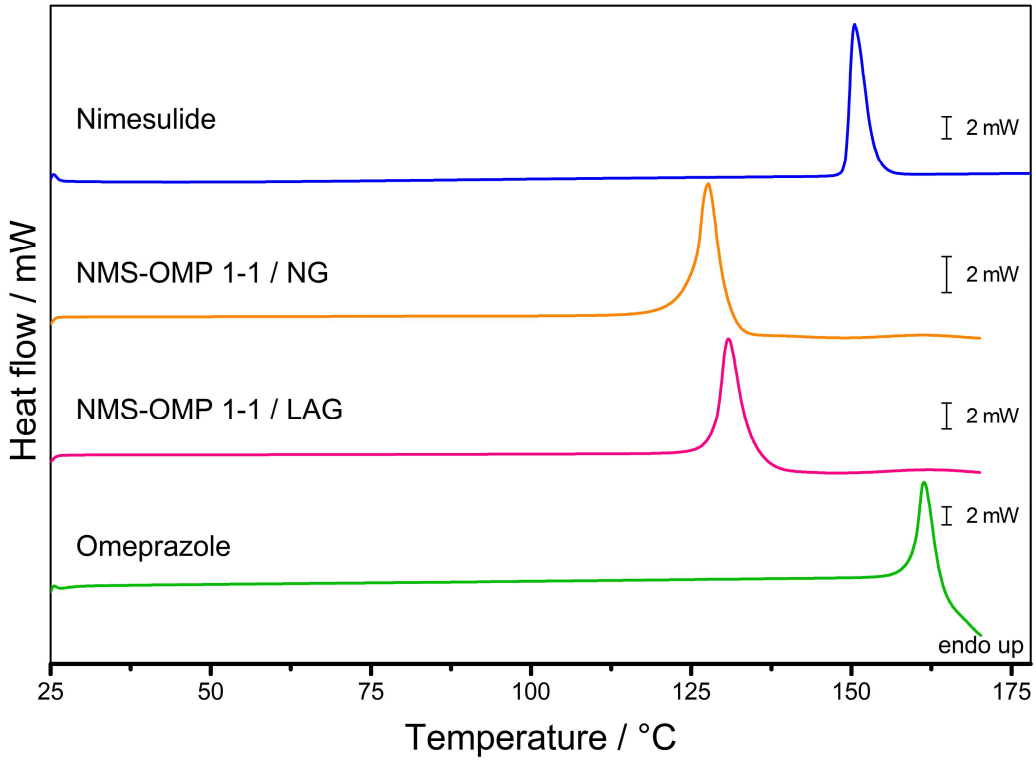


Figure 23 – DSC heating curves of NMS-OMP equimolar mixture and pure compounds, prepared by NG and by LAG.

Complementarily, both PXRD (Figure 24) and FTIR analyses (Figure A.6, in the Appendix section) showed a pattern corresponding to the sum of the starting materials profile, indicating that NMS and OMP formed a physical mixture. On the other hand, in the PXRD analysis, it was possible to see a halo of amorphization in the NMS-OMP 1-1 / NG sample. Then, in this regard, we performed a trial of coamorphization of this sample. It is worthy mention that coamorphization process was performed exclusively through mechanochemical methods since OMP degrades on melting (MURAKAMI et al., 2009), which makes the quench-cooling approach unfeasible.

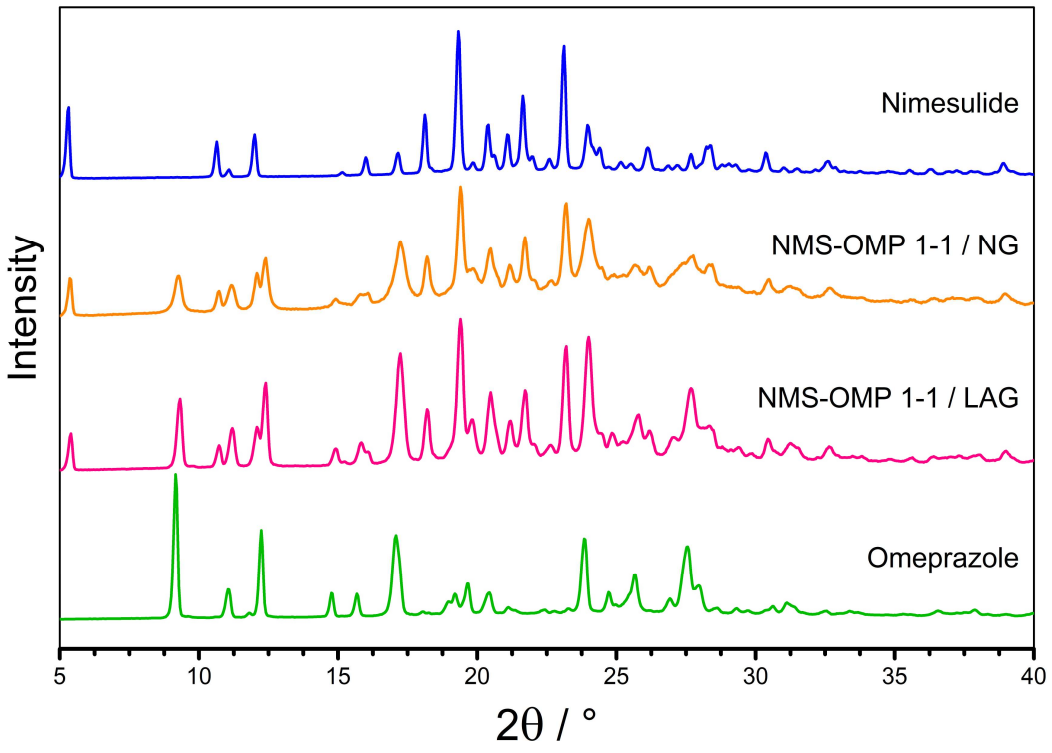


Figure 24 – PXRD pattern of NMS-OMP equimolar mixture and pure compounds, prepared by NG and by LAG.

Initially, the jars containing the NMS-OMP solid mixture were pre-cooled in the freezer for 1.5 hours prior to milling, as described in section 3.2.3.1. This process was named as “cold NG”. Furthermore, the cryomilling process was also performed. These samples were analyzed by DSC, shown in Figure 25. It is possible to observe a unique *T*g event in both DSC curves of NMS-OMP (Cryo) and NMS-OMP (cold NG) at 26 °C and 32 °C, respectively, indicating the coamorphization of samples through these two methodologies (SABERI et al., 2023). Moreover, during the heating on the DSC analysis, discrete exothermic events around 75 °C can be attributed to crystallization of part of material followed by slight endothermic event around 120 °C, close to melting of NMS-OMP NG physical mixture.

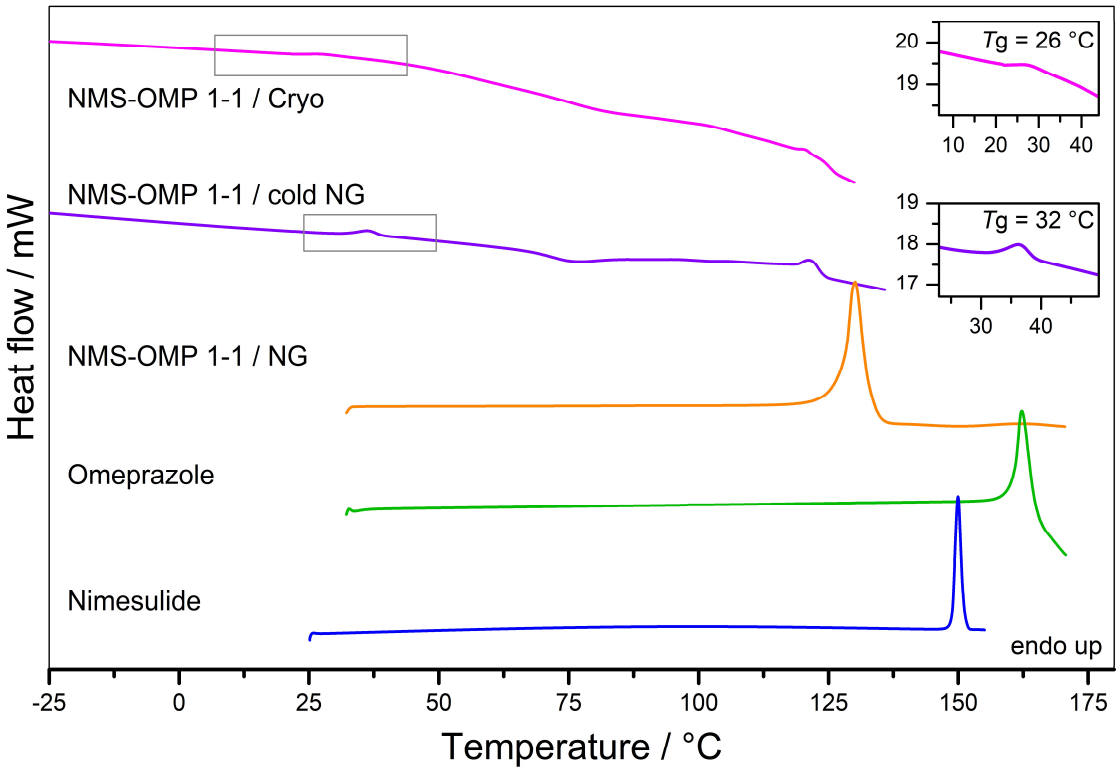


Figure 25 – DSC heating curves of coamorphized NMS-OMP equimolar system and pure compounds.

The PXRD of fresh cold NG and cryomilled samples, Figure 26, show totally amorphized pattern (HEALY et al., 2017). It is important to highlight that the binary coamorphous systems (stored under dry condition) were periodically analyzed by PXRD. Figure 26 also demonstrates the long-term stability of the coamorphized NMS-OMP systems. It can be inferred that the NMS-OMP cryomilled sample remained totally amorphized for at least 120 days (four months). The material coamorphized through cryomilling was more stable than that obtained by cold NG, since the mixture is cooled much lower than the glass transition temperature, favoring the formation of a disordered phase upon mechanical activation and preventing recrystallization of the sample.

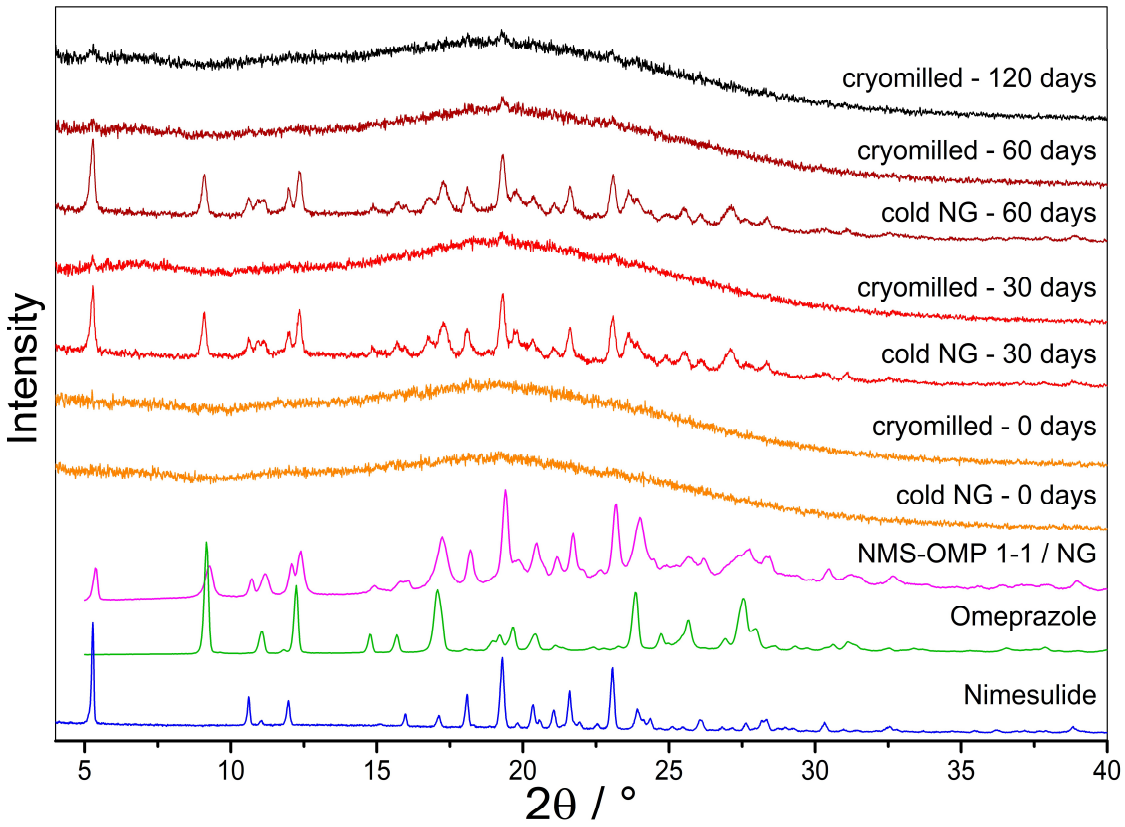


Figure 26 – PXRD pattern of coamorphized NMS-OMP equimolar system and pure compounds.

3.3.5.3 Nimesulide-bicalutamide

Bicalutamide (BICA) is a non-steroidal antiandrogenic drug used to treat prostate cancer (ESSA et al., 2019; SUROV et al., 2016), so its association with NMS could be pharmacological interesting. NMS-BICA equimolar mixture was studied through both mechanochemical and quench cooling approaches.

The NMS-BICA sample prepared by NG showed a PXRD pattern (Figure 27) corresponding to the sum of precursors. Meanwhile, a partial crystalline pattern of Cryo system and a complete amorphised profile for QC sample was observed. In this sense, PXRD results indicate that the quench cooling process is more prone to promoting total crystallinity breakdown (SHI; MOINUDDIN; CAI, 2019), being capable to produce a completely amorphous material. Furthermore, the FTIR analysis (Figure A.7) is in agreement with PXRD results: NMS-BICA 1-1 QC system presents broadening of spectral bands, characteristic of amorphous forms and shifting of maxima which indicates the presence of different

intermolecular interactions (CHAVAN et al., 2016; HEALY et al., 2017; SABERI et al., 2023).

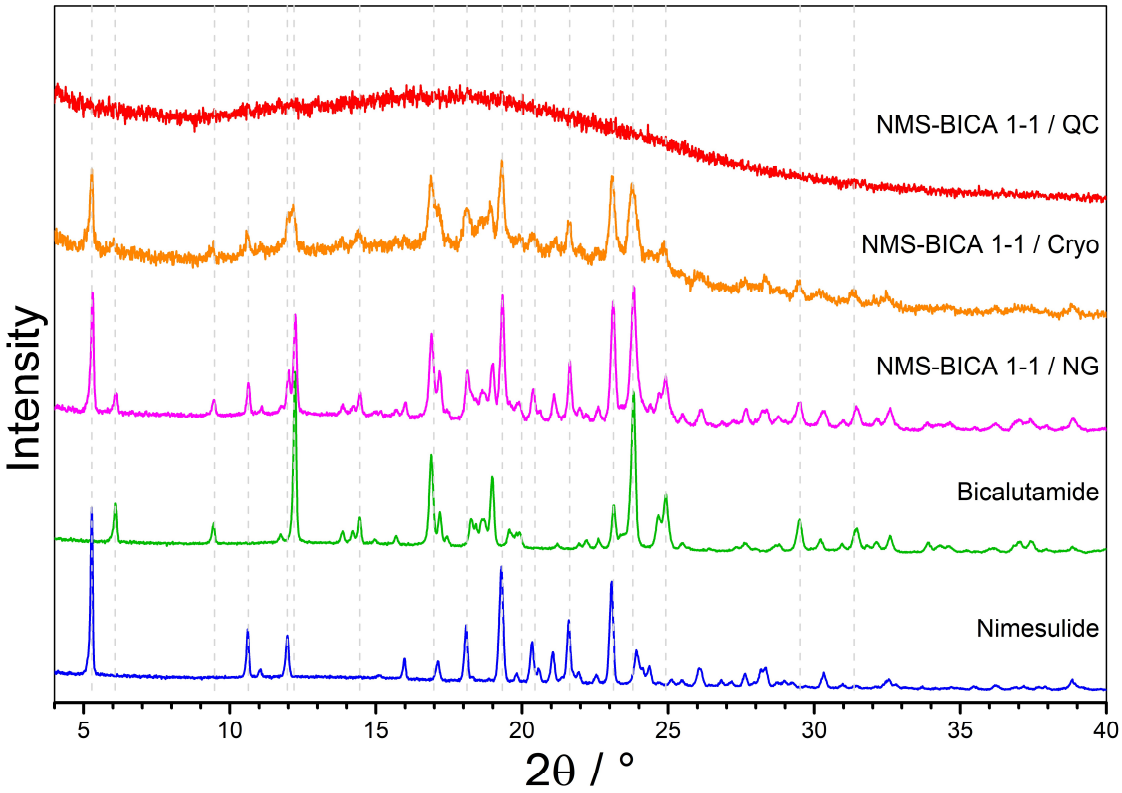


Figure 27 – PXRD pattern of NMS-BICA equimolar mixture and pure compounds.

Concerning to the DSC analysis, Figure 28, it can be inferred that NMS-BICA 1-1 QC sample presented *T*g value (38 °C) intermediate to the quench cooled NMS (22 °C) and BICA (57 °C) (ZHANG et al., 2021), and above room temperature. In addition, the NMS-BICA QC coamorphous does not crystallizes during the second heating step, which indicates that this mixture stabilizes the amorphous phase of both drugs.

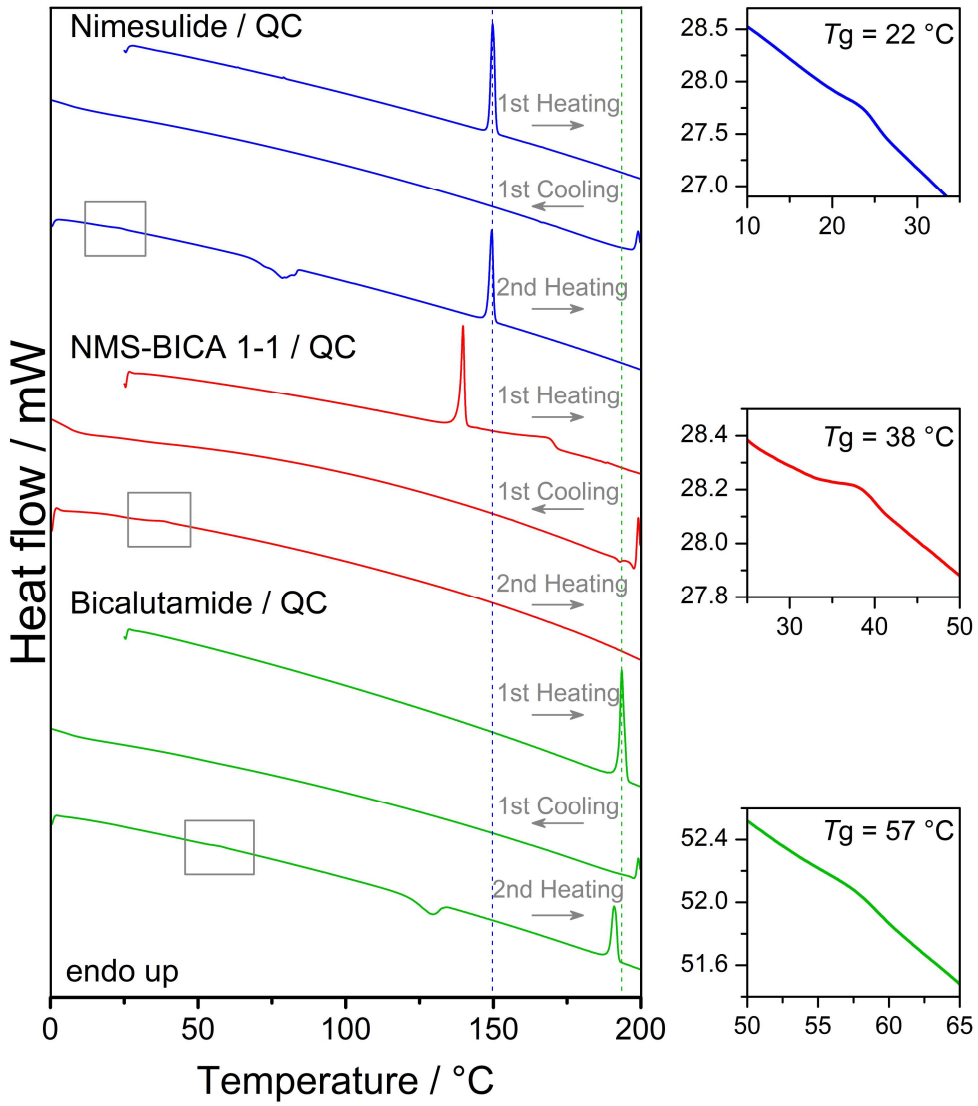


Figure 28 – DSC curves of quench cooled NMS-BICA equimolar mixture and pure compounds.

3.3.6 Dissolution rate study

The dissolution rate tests were performed for pure NMS and three systems, the eutectic samples NMS-INH 3-2 and NMS-GSA 3-1, and the investigated coamorphous system with the highest *T*g, NMS-BICA 1-1, an interesting drug-drug association. As shown in Figure 29, both NMS-BICA 1-1 coamorphous system and NMS-GSA 3-1 eutectic mixture presented higher dissolution profiles than the crystalline NMS in the first 25 and 35 minutes, respectively, while for the NMS-INH 3-2 eutectic mixture only a slight increase is observed. Taking into account the concentration of drug released in 25 min from tablets to the dissolution media, we calculated the increment of NMS released, in

percentage, for NMS-BICA coamorphous, for NMS-GSA and NMS-INH eutectic mixtures, relatively to pure nimesulide, that corresponded to 181%, 176% and 124%, respectively.

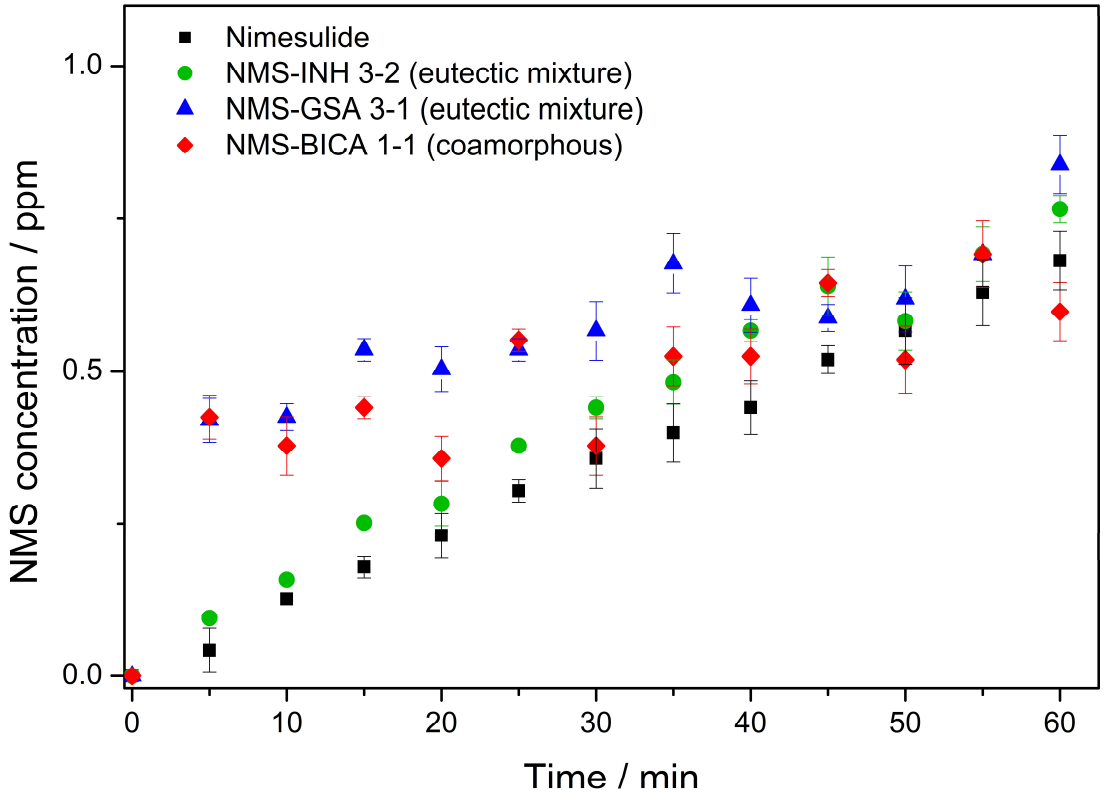


Figure 29 – Dissolution profile of pure NMS and selected multicomponent solid systems.

NMS from these multicomponent systems dissolve faster than the pure drug, with the rate of NMS-BICA ≈ NMS-GSA > NMS-INH > NMS. This results demonstrated that the coamorphous and eutectic systems showed improvement in the dissolution rates, at the initial stage, when compared to the respective original drug, which may favor and accelerate the NMS therapeutic effect (BANERJEE et al., 2022). Therefore, these novel multicomponent solid forms may have potential applicability for combined administration with nimesulide, since the three compounds could provide a complementary therapy associated with a non-steroidal anti-inflammatory drug (BANERJEE et al., 2022).

3.4 CONCLUSIONS

Using a selected set of coformers, differing in the functional groups and in molecular complexicity, both COSMOquick software and mechanochemical approaches point out a low tendency of NMS to form cocrystals. As a result, a novel NMS cocrystal could only be obtained with piperazine, a low molecular weight, simple coformer. Investigation of eutectic mixtures and coamorphous phases was also performed for the coformers with the potential for advantageous therapeutic combination with NMS. Binary solid-liquid phase diagrams and Tamman's triangle plots were constructed for NMS-GSA and NMS-INH systems, and the eutectic compositions determined as 75% and 61% (molar), respectively. Furthermore, several drug-drug coamorphous systems were effectively obtained through the employed methods, the most interesting being NMS-OMP and NMS-BICA. The cryomilled NMS-OMP (1-1) coamorphous solid was stable for at least 120 days in dry conditions. To conclude, dissolution rate tests were performed for NMS-BICA 1-1 coamorphous system, NMS-GSA 3-1 and NMS-INH 3-2 eutectic systems. The comparison of dissolution profiles revealed that, in general, these multicomponent solid systems show higher NMS dissolution rate compared to the pure drug.

CHAPTER 4

GENERAL CONCLUSIONS AND SCIENTIFIC CONTRIBUTIONS

4.1 GENERAL CONCLUSIONS

The present work depicted the prospection of new multicomponent solid forms of the poorly soluble NSAID nimesulide. A combined virtual-experimental cocrystal screening was performed using coformers with systematic molecular diversity and/or potential dual-drug association. In the range of tested compounds, both COSMOquick software and mechanochemical approaches indicated the low tendency of nimesulide to form cocrystals. As a result, in addition to the already known NMS cocrystals with bipyridyl and its derivatives, we obtained a novel NMS cocrystal with the low molecular weight piperazine coformer. It is worth mentioning that the virtual pre-screening method used, correctly predicted the success of cocrystallization for all coformers for which more negative ΔH_{excess} and lowest F_{fit} values were found. Positive or only slightly negative ΔH_{excess} values or high F_{fit} were associated with coformers for which cocrystas could not be obtained in the experimental screening.

Eutectic mixtures were also investigated. Binary solid-liquid phase diagrams and Tamman's triangle were constructed for NMS-GSA and NMS-INH systems. According to these complementary tools, the eutectic composition was determined as 75% and 61% of NMS in the NMS-GSA and NMS-INH systems, respectively.

Furthermore, drug-drug coamorphous systems were effectively obtained through the employed methods, especially with metoclopramide, omeprazole and bicalutamide. The cryomilled NMS-OMP coamorphous was stable for at least 120 days in dry conditions. In turn, quench cooling produced NMS-BICA coamorphous proved to be more stable than that obtained by cryomilling, presenting *T*g above the room temperature and a useful pharmacological stoichiometry.

Finally, dissolution rate tests were performed for selected multicomponent systems. The dissolution rate profiles revealed that these multicomponent solid systems showed higher dissolution rate compared to pure nimesulide within one hour.

As a final conclusion, it is worth noting that this multidisciplinary study presented an important contribution to the Material Science, Chemistry, Pharmaceutical and correlate areas.

4.2 SCIENTIFIC CONTRIBUTIONS

During this doctorate, some contributions were made to the scientific community through periodical publications and participation in national and international events. The PhD candidate also collaborated with other related projects that resulted in the publication of articles. Some of these contributions are described below.

4.2.1 Periodical Peer-Reviewed Publications

The detailed references of the publications in the literature periodicals are described following:

I. Porto, M. V.; Costa, G. P.; dos Santos, J. G.; **de Almeida, A. C.**; Caires, F. J. *Thermal analysis as a tool in the preparation and characterization of rosmarinic acid multicomponent systems with improved solubility*. Thermochimica Acta, 2025 (submitted for publication)

II. Ferreira, P. O.; Ferreira, L. T.; **de Almeida, A. C.**; Meneguin, A. B.; Chorilli, M.; Eusébio, M. E. S.; Castro, R. A. E.; Caires, F. J. *Thermoanalytical investigation of valsartan binary eutectic forming systems and low transition temperature mixtures (LTTM)*. Thermochimica Acta, 2025 (accepted for publication)

III. **de Almeida, A. C.**; Ferreira, P. O.; Porto, M. V.; Canotilho, J.; Castro, R. A. E.; Caires, F. J.; Eusébio, M. E. S. *Novel nimesulide multicomponent solid forms: Screening, synthesis, thermoanalytical study and characterization.* Journal of Thermal Analysis and Calorimetry, 2024. DOI: 10.1007/s10973-024-13189-2

IV. Ferreira, P. O.; **de Almeida, A. C.**; Costa, G. P.; Torquetti, C.; Baptista, J. A.; Eusébio, M. E. S.; Caires, F. J.; Castro, R. A. E. *Norfloxacin cocrystals: Mechanochemical synthesis and scale-up viability through solubility studies*. Journal of Pharmaceutical Sciences, 2023. DOI: 10.1016/j.xphs.2023.03.003

V. de Souza, F. Z. R.; **de Almeida, A. C.**; Ferreira, P. O.; Fernandes, R. P.; Caires, F. J. *Screening of coformers for quercetin cocrystals through mechanochemical*

methods. Eclética Química Journal, 2021. DOI:10.26850/1678-4618eqj.v47.1.2022.p64-75

VI. Ferreira, P. O.; de Moura, A.; **de Almeida, A. C.**; dos Santos, E. C.; Kogawa, A. C.; Caires, F. J. *Thermoanalytical study of a new polymorph of norfloxacin - saccharin cocrystal: Mechanochemical synthesis, characterization and solubility assays*. Journal of Thermal Analysis and Calorimetry, 2021. DOI: 10.1007/s10973-021-10658-w

VII. Torquetti, C.; Ferreira, P. O.; **de Almeida, A. C.**; Fernandes, R. P.; Caires, F. J. *Thermal study and characterization of new cocrystals of ciprofloxacin with picolinic acid*. Journal of Thermal Analysis and Calorimetry, 2020. DOI: 10.1007/s10973-020-10479-3

VIII. Ferreira, P. O.; **de Almeida, A. C.**; dos Santos, E. C.; Droppa, R.; Ferreira, F. F.; Kogawa, A. C.; Caires, F. J. *A norfloxacin-nicotinic acid cocrystal: mechanochemical synthesis, thermal and structural characterization and solubility assays*. Thermochimica Acta, 2020. DOI: 10.1016/j.tca.2020.178782

IX. Machado, R. G.; Gaglieri, C.; Alarcon, R. T.; de Moura, A.; **de Almeida, A. C.**; Caires, F. J.; Ionashiro, M. *Cobalt selenate pentahydrate: Thermal decomposition intermediates and their properties dependence on temperature changes*. Thermochimica Acta, 2020. DOI: 10.1016/j.tca.2020.178615

In the above referencing, the name of this author (**Amanda Cosmo de Almeida**) is highlighted to facilitate the spotting of the authorship and relative contribution to each work.

4.2.2 Event Participations

Besides the contribution in form of scientific periodic journal publications, the works from this project were also displayed and spread through congresses and other events. The specifics of such displays are the detailed following:

I. *Thermal analysis as a tool to prospect novel nimesulide dual-drug solid forms*. 16th Mediterranean Conference on Calorimetry and Thermal Analysis (MEDICTA), 2023, Porto, Portugal, oral communication.

II. *Binary diagrams of therapeutic deep eutectic solvents based on ketoprofen and terpenoids*. 16th Mediterranean Conference on Calorimetry and Thermal Analysis (MEDICTA), 2023, Porto, Portugal, poster presentation.

III. *Synthesis and characterization of nimesulide dual-drug co-amorphous systems*. Multiscale Phenomena in Condensed Matter Conference for young researchers (YOUNG MULTIS), 2023, Poland (online), oral communication.

IV. *Design and screening of nimesulide cocrystals.* 15° Encontro Nacional de Química Física (ENQF), 2023, Portugal (online), poster presentation.

V. *Cocrystallization through green mechanochemical synthesis: Na approach to improve solubility of drugs*. 9th IUPAC International Conference on green Chemistry (ICGC), 2022, Athens, Greece, poster presentation.

VI. *Síntese mecanoquímica e caracterização da mistura eutética tenoxicam-isoniazida.* 60º Congresso Brasileiro de Química (CBQ), 2021, Brazil (online), poster presentation.

The above-mentioned works were presented in the national or international scientific events by this author. Other contributions and information can be accessed in the ORCID and Lattes platforms.

- **Lattes:** http://lattes.cnpq.br/2300966590732336
- **ORCID:** https://orcid.org/0000-0002-0957-943X

4.2.3 Scholarship and internship

This work was possible thanks to the financial support from the Brazilian Federal Agency for Support and Evaluation of Graduate Education (CAPES), processes numbers 88887.495148/2020-00 and 88887.817528/2022-00.

Additionally, part of this study was performed in the *Laboratório de Termodinâmica e Química do Estado Sólido* (LTQES), University of Coimbra - Portugal, between August/2022 and July/2023, under supervision of Professor Maria Ermelinda da Silva Eusébio. The internship was carried out in the scope of the CAPES-PrInt Program, mobility number 88887.684961/2022-00.

REFERENCES

ABDELKADER, H. et al. Eutectic, monotectic and immiscibility systems of nimesulide with water-soluble carriers: Phase equilibria, solid-state characterisation and in-vivo/pharmacodynamic evaluation. **Journal of Pharmacy and Pharmacology**, v. 66, n. 10, p. 1439–1450, 2014.

ABDELQUADER, M. M. et al. Therapeutic deep eutectic solvents: A comprehensive review of their thermodynamics, microstructure and drug delivery applications. **European Journal of Pharmaceutics and Biopharmaceutics**, v. 186, p. 85–104, 1 May 2023.

ABRAMOV, Y. A.; LOSCHEN, C.; KLAMT, A. Rational Coformer or Solvent Selection for Pharmaceutical Cocrystallization or Desolvation. **Journal of Pharmaceutical Sciences**, v. 101, n. 10, p. 3687–3697, Oct. 2012.

AGAFONOVA, E. V.; MOSHCHENSKIY, Y. V.; TKACHENKO, M. L. DSC study and calculation of metronidazole and clarithromycin thermodynamic melting parameters for individual substances and for eutectic mixture. **Thermochimica Acta**, v. 580, p. 1–6, Mar. 2014.

AITIPAMULA, S. et al. Polymorphs, salts, and cocrystals: What's in a name? **Crystal Growth and Design**, v. 12, n. 5, p. 2147–2152, 2012.

ALLESØ, M. et al. Towards Effective Solid Form Screening. **Journal of Pharmaceutical Sciences**, v. 99, n. 9, p. 3711–3718, Sep. 2010.

ALVES, L. P. et al. A review on developments and prospects of anti-inflammatory in microemulsions. **Journal of Drug Delivery Science and Technology**, v. 60, p. 102008, 2020.

AMIDON, G. L. et al. A Theoretical Basis for a Biopharmaceutic Drug Classification: The Correlation of in vitro Drug product dissolution and in vivo bioavailability. **Pharmaceutical Researchaceutical**, v. 12, n. 3, p. 413–420, 1995.

ANVISA. **Anuário Estatístico do Mercado Farmacêutico 2017**. Brasília: Agência Nacional de Vigilância Sanitária, 2018.

ANVISA. **Anuário Estatístico do Mercado Farmacêtico 2018**. Brasília: Agência Nacional de Vigilância Sanitária, 2019a.

ANVISA. **Farmacopeia Brasileira**. 6. ed. Brasília: Agência Nacional de Vigilância Sanitária, 2019b. v. 1

ANVISA. **Anuário Estatístico do Mercado Farmacêtico 2022**. Brasília: Agência Nacional de Vigilância Sanitária, 2023.

ARAYA-SIBAJA, A. M. et al. Drug solubility enhancement through the preparation of multicomponent organic materials: Eutectics of lovastatin with carboxylic acids. **Pharmaceutics**, v. 11, n. 3, p. 1–16, 2019.

ARENAS-GARCÍA, J. I. et al. Interrelation of the dissolution behavior and solid-state features of acetazolamide cocrystals. **European Journal of Pharmaceutical Sciences**, v. 96, p. 299–308, Jan. 2017.

ASSALI, M. et al. Dexamethasone-diclofenac loaded polylactide nanoparticles: Preparation, release and anti-inflammatory activity. **European Journal of Pharmaceutical Sciences**, v. 122, p. 179–184, 2018.

BABU, N. J.; NANGIA, A. Solubility advantage of amorphous drugs and pharmaceutical cocrystals. **Crystal Growth and Design**, v. 11, n. 7, p. 2662–2679, 2011.

BADRI, W. et al. Encapsulation of NSAIDs for inflammation management: Overview, progress, challenges and prospects. **International Journal of Pharmaceutics**, v. 515, n. 1–2, p. 757–773, 2016.

BANERJEE, M. et al. Unlocking the potential of drug-drug cocrystals – A comprehensive review. **Journal of Controlled Release**, v. 348, n. March, p. 456–469, 2022.

BARNES, P. J. How corticosteroids control inflammation: Quintiles Prize Lecture 2005. **British Journal of Pharmacology**, v. 148, n. 3, p. 245–254, 2006.

BARRIO, M. et al. Pressure-temperature phase diagram of the dimorphism of the anti-inflammatory drug nimesulide. **International Journal of Pharmaceutics**, v. 525, n. 1, p. 54–59, 2017.

BAZZO, G. C.; PEZZINI, B. R.; STULZER, H. K. Eutectic mixtures as an approach to enhance solubility, dissolution rate and oral bioavailability of poorly water-soluble drugs. **International Journal of Pharmaceutics**, v. 588, p. 119741, 2020.

BENDAS, E. R.; ABDELBARY, A. A. Instantaneous enteric nano-encapsulation of omeprazole: Pharmaceutical and pharmacological evaluation. **International Journal of Pharmaceutics**, v. 468, n. 1–2, p. 97–104, 2014.

BERGESE, P. et al. Microstructural investigation of nimesulide-crospovidone composites by X-ray diffraction and thermal analysis. **Composites Science and Technology**, v. 63, n. 8, p. 1197–1201, 2003.

BERRY, D. J.; STEED, J. W. Pharmaceutical cocrystals, salts and multicomponent systems; intermolecular interactions and property based design. **Advanced Drug Delivery Reviews**, v. 117, p. 3–24, 2017.

BISHNOI, S.; ROCHELLE, G. T. Thermodynamics of piperazine/methyldiethanolamine/water/carbon dioxide. **Industrial and Engineering Chemistry Research**, v. 41, n. 3, p. 604–612, 2002.

BLAGDEN, N. et al. Crystal engineering of active pharmaceutical ingredients to improve solubility and dissolution rates. **Advanced drug delivery reviews**, v. 59, n. 7, p. 617–630, 2007.

BOLLA, G.; MITTAPALLI, S.; NANGIA, A. Modularity and three-dimensional isostructurality of novel synthons in sulfonamide-lactam cocrystals. **IUCrJ**, v. 2, p. 389–401, 2015.

BOLLA, G.; NANGIA, A. Pharmaceutical cocrystals: walking the talk. **Chemical Communications**, v. 52, n. 54, p. 8342–8360, 2016.

BOLLA, G.; SANPHUI, P.; NANGIA, A. Solubility advantage of tenoxicam phenolic cocrystals compared to salts. **Crystal Growth and Design**, v. 13, n. 5, p. 1988–2003, 2013.

BOLLA, G.; SARMA, B.; NANGIA, A. K. Crystal Engineering of Pharmaceutical Cocrystals in the Discovery and Development of Improved Drugs. **Chemical Reviews**, v. 122, n. 13, p. 11514–11603, 13 Jul. 2022.

CAIAZZO, E.; IALENTI, A.; CICALA, C. The relatively selective cyclooxygenase-2 inhibitor nimesulide: What's going on? **European Journal of Pharmacology**, v. 848, n. July 2018, p. 105–111, 2019.

CARAZO, E. et al. Kinetic and thermodynamic assessment on isoniazid/montmorillonite adsorption. **Applied Clay Science**, v. 165, n. June, p.

82–90, 2018.

CARNEIRO, R. L. et al. Mechanochemical synthesis and characterization of a novel AAs–Flucytosine drug–drug cocrystal: A versatile model system for green approaches. **Journal of Molecular Structure**, v. 1251, p. 132052, 2022.

CATARRO, M. et al. Nimesulide analogues: From anti-inflammatory to antitumor agents. **Bioorganic Chemistry**, v. 88, n. March, p. 102966, 2019.

CAVANAGH, K. L.; MAHESHWARI, C.; RODRÍGUEZ-HORNEDO, N. Understanding the Differences Between Cocrystal and Salt Aqueous Solubilities. **Journal of Pharmaceutical Sciences**, v. 107, n. 1, p. 113–120, 2018.

CHADHA, R. et al. Ciprofloxacin Hippurate Salt: Crystallization Tactics, Structural Aspects, and Biopharmaceutical Performance. **Crystal Growth and Design**, v. 16, n. 9, p. 4960–4967, 2016.

CHAVAN, R. B. et al. Co amorphous systems: A product development perspective. **International Journal of Pharmaceutics**, v. 515, n. 1–2, p. 403–415, 2016.

CHERUKUVADA, S.; GURU ROW, T. N. Comprehending the formation of eutectics and cocrystals in terms of design and their structural interrelationships. **Crystal Growth and Design**, v. 14, n. 8, p. 4187–4198, 2014.

CHERUKUVADA, S.; NANGIA, A. Fast dissolving eutectic compositions of two anti-tubercular drugs. **CrystEngComm**, v. 14, n. 7, p. 2579, 2012.

CHERUKUVADA, S.; NANGIA, A. Eutectics as improved pharmaceutical materials: Design, properties and characterization. **Chemical Communications**, v. 50, n. 8, p. 906–923, 2014.

CORTESÃO, A. M. et al. Binary phase diagrams of pyridinecarboxamide isomers. **Journal of Thermal Analysis and Calorimetry**, v. 130, n. 3, p. 1727–1733, 2017.

D'ANGELO, A. et al. Physico-chemical characterisation of three-component co-amorphous systems generated by a melt-quench method. **Journal of Thermal Analysis and Calorimetry**, v. 134, n. 1, p. 381–390, 2018.

DENGALE, S. J. et al. Recent advances in co-amorphous drug

formulations. **Advanced Drug Delivery Reviews**, v. 100, p. 116–125, 2016.

DESIRAJU, G. R. Supramolecular Synthons in Crystal Engineering— A New Organic Synthesis. **Angewandte Chemie International Edition in English**, v. 34, n. 21, p. 2311–2327, 1995.

DESIRAJU, G. R. Chemistry beyond the molecule. **Nature**, v. 412, n. 6845, p. 397–400, 2001.

DINIZ, L. F. et al. Modulating the water solubility and thermal stability of the anti-tuberculosis drug Isoniazid via multicomponent crystal formation. **Journal of Molecular Structure**, v. 1171, p. 223–232, 2018.

DUGGIRALA, N. K. et al. Pharmaceutical cocrystals: Along the path to improved medicines. **Chemical Communications**, v. 52, n. 4, p. 640–655, 2016.

DUGGIRALA, N. K. et al. Pharmaceutical Cocrystals: Formulation Approaches to Develop Robust Drug Products. **Crystal Growth and Design**, v. 20, n. 2, p. 617–626, 2020.

ESSA, E. A. et al. Co-crystallization for enhanced dissolution rate of bicalutamide: preparation and evaluation of rapidly disintegrating tablets. **Drug Development and Industrial Pharmacy**, v. 45, n. 8, p. 1215–1223, 2019.

FRIŠČIĆ, T. et al. The role of solvent in mechanochemical and sonochemical cocrystal formation: a solubility-based approach for predicting cocrystallisation outcome. **CrystEngComm**, v. 11, n. 3, p. 418–426, 2009.

FRIŠČIĆ, T.; JONES, W. Benefits of cocrystallisation in pharmaceutical materials science: An update. **Journal of Pharmacy and Pharmacology**, v. 62, n. 11, p. 1547–1559, 2010.

FRIŠČIČ, T.; JONES, W. Recent advances in understanding the mechanism of cocrystal formation via grinding. **Crystal Growth and Design**, v. 9, n. 3, p. 1621–1637, 2009.

FRIŠČIĆ, T.; MOTTILLO, C.; TITI, H. M. Mechanochemistry for Synthesis. **Angewandte Chemie - International Edition**, v. 59, n. 3, p. 1018–1029, 2020.

GADADE, D. D.; PEKAMWAR, S. S. Pharmaceutical cocrystals: Regulatory and strategic aspects, design and development. **Advanced**

Pharmaceutical Bulletin, v. 6, n. 4, p. 479–494, 2016.

GAJDA, M. et al. Continuous, one-step synthesis of pharmaceutical cocrystals via hot melt extrusion from neat to matrix-assisted processing – State of the art. **International Journal of Pharmaceutics**, v. 558, n. November 2018, p. 426–440, 2019.

GÁLICO, D. A. et al. Thermoanalytical study of nimesulide and their recrystallization products obtained from solutions of several alcohols. **Journal of Thermal Analysis and Calorimetry**, v. 115, n. 3, p. 2385–2390, 2014.

GEORGESCU, M. et al. Thermal Behavior of the Nimesulide-Salicylic Acid Eutectic Mixtures Prepared by Mechanosynthesis and Recrystallization. **Materials**, v. 14, n. 24, p. 7715, 2021.

GOPI, S. P.; BANIK, M.; DESIRAJU, G. R. New cocrystals of hydrochlorothiazide: Optimizing solubility and membrane diffusivity. **Crystal Growth and Design**, v. 17, n. 1, p. 308–316, 2017.

GUIDETTI, M. et al. Exploring the Cocrystal Landscape of Posaconazole by Combining High-Throughput Screening Experimentation with Computational Chemistry. **Crystal Growth & Design**, v. 23, n. 2, p. 842–852, 1 Feb. 2023.

GÜNGÖR, T. et al. New nimesulide derivatives with amide/sulfonamide moieties: Selective COX-2 inhibition and antitumor effects. **European Journal of Medicinal Chemistry**, v. 221, p. 113566, Oct. 2021.

GUO, M. et al. Pharmaceutical cocrystals: A review of preparations, physicochemical properties and applications. **Acta Pharmaceutica Sinica B**, v. 11, n. 8, p. 2537–2564, 2021.

HASKINS, M. M.; ZAWOROTKO, M. J. Screening and Preparation of Cocrystals: A Comparative Study of Mechanochemistry vs Slurry Methods. **Crystal Growth and Design**, v. 21, n. 7, p. 4141–4150, 2021.

HATANAKA, Y. et al. Improved solubility and permeability of both nifedipine and ketoconazole based on coamorphous formation with simultaneous dissolution behavior. **Journal of Drug Delivery Science and Technology**, v. 65, p. 102715, 2021.

HEALY, A. M. et al. Pharmaceutical solvates, hydrates and amorphous

forms: A special emphasis on cocrystals. **Advanced Drug Delivery Reviews**, v. 117, p. 25–46, 2017.

IONASHIRO, M.; CAIRES, F. J.; GOMES, D. J. C. **Giolito: fundamentos da termogravimetria e análise térmica diferencial / calorimetria exploratória diferencial**. 2. ed. São Paulo: Giz editorial e Livraria Ltda., 2014.

ISMAIL, S.; EL-MAHDY, M.; AL-KUBATI, S. S. Enhancement of solubility and dissolution of nimesulide using solubilization, solid dispersion and complexation techniques. **Bulletin of Pharmaceutical Sciences**, v. 32, n. PART 2, p. 321–338, 2009.

ISSA, N. **Towards more Efficient Screening of Pharmaceutical Cocrystals**. [s.l.] University College London, 2011.

IVASHENKO, A. V.; TITOV, V. V.; KOVSHEV, E. I. Liquid Crystalline Compounds: III On Applicability of Schröder-Van Laar Equations to Liquid Crystals Mixtures. **Molecular Crystals and Liquid Crystals**, v. 33, n. 3–4, p. 195–200, 28 Jan. 1976.

KARIMI-JAFARI, M. et al. Creating cocrystals: A review of pharmaceutical cocrystal preparation routes and applications. **Crystal Growth and Design**, v. 18, n. 10, p. 6370–6387, 2018.

KAUPP, G. Mechanochemistry: the varied applications of mechanical bond-breaking. **CrystEngComm**, v. 11, n. 3, p. 388–403, 2009.

KAVANAGH, O. N. et al. Pharmaceutical cocrystals: from serendipity to design to application. **Drug Discovery Today**, v. 24, n. 3, p. 796–804, 2019.

KOTBANTAO, G.; CHAROENCHAITRAKOOL, M. Processing of ketoconazole–4-aminobenzoic acid cocrystals using dense CO 2 as an antisolvent. **Journal of CO2 Utilization**, v. 17, p. 213–219, 2017.

KRESS, H. G. et al. Acute pain: A multifaceted challenge - The role of nimesulide. **Current Medical Research and Opinion**, v. 32, n. 1, p. 23–36, 2016.

KUMAR, A.; NANDA, A. In-silico methods of cocrystal screening: A review on tools for rational design of pharmaceutical cocrystals. **Journal of Drug Delivery Science and Technology**, v. 63, n. April, p. 102527, 2021.

LI, P. et al. Two Cocrystals of Berberine Chloride with Myricetin and Dihydromyricetin: Crystal Structures, Characterization, and Antitumor Activities. **Crystal Growth & Design**, v. 20, n. 1, p. 157–166, 2020a.

LI, W. et al. Eutectics and Salt of Dapsone With Hydroxybenzoic Acids: Binary Phase Diagrams, Characterization and Evaluation. **Journal of Pharmaceutical Sciences**, v. 109, n. 7, p. 2224–2236, 2020b.

LIU, M. et al. Development of a pharmaceutical cocrystal with solution crystallization technology: Preparation, characterization, and evaluation of myricetin-proline cocrystals. **European Journal of Pharmaceutics and Biopharmaceutics**, v. 107, p. 151–159, 2016.

LORENZ, H.; SEIDEL-MORGENSTERN, A. Binary and ternary phase diagrams of two enantiomers in solvent systems. **Thermochimica Acta**, v. 382, n. 1–2, p. 129–142, 2002.

LOSCHEN, C.; KLAMT, A. Solubility prediction, solvate and cocrystal screening as tools for rational crystal engineering. **Journal of Pharmacy and Pharmacology**, v. 67, n. 6, p. 803–811, 2015.

MACEDO, L. DE O. et al. Anti-inflammatory drug nanocrystals: state of art and regulatory perspective. **European Journal of Pharmaceutical Sciences**, v. 158, n. August 2020, p. 105654, Mar. 2021.

MALAMATARI, M. et al. Experimental cocrystal screening and solution based scale-up cocrystallization methods. **Advanced Drug Delivery Reviews**, v. 117, p. 162–177, 2017.

MANRIQUE-MORENO, M. et al. Biophysical study of the non-steroidal anti-inflammatory drugs (NSAID) ibuprofen, naproxen and diclofenac with phosphatidylserine bilayer membranes. **BBA - Biomembranes**, v. 1858, n. 9, p. 2123–2131, 2016.

MASHHADI, S. M. A. et al. Isoniazid-Gentisic acid cocrystallization: Solubility, Stability, Dissolution rate, Antioxidant and Flowability Properties Studies. **Journal of Molecular Structure**, v. 1226, p. 129388, Feb. 2021.

MESALLATI, H.; MUGHEIRBI, N. A.; TAJBER, L. Two Faces of Ciprofloxacin: Investigation of Proton Transfer in Solid State Transformations.

Crystal Growth and Design, v. 16, n. 11, p. 6574–6585, 2016.

MOHAMMAD, I. S. et al. Drug nanocrystals: Fabrication methods and promising therapeutic applications. **International Journal of Pharmaceutics**, v. 562, p. 187–202, 2019.

MOINUDDIN, S. M. et al. Facile formation of co-amorphous atenolol and hydrochlorothiazide mixtures via cryogenic-milling: Enhanced physical stability, dissolution and pharmacokinetic profile. **International Journal of Pharmaceutics**, v. 532, n. 1, p. 393–400, 2017.

MOISESCU-GOIA, C.; MURESAN-POP, M.; SIMON, V. New solid state forms of antineoplastic 5-fluorouracil with anthelmintic piperazine. **Journal of Molecular Structure**, v. 1150, p. 37–43, 2017.

MURAKAMI, F. S. et al. Physico-chemical solid-state characterization of omeprazole sodium: Thermal, spectroscopic and crystallinity studies. **Journal of Pharmaceutical and Biomedical Analysis**, v. 49, n. 1, p. 72–80, 2009.

NASCIMENTO, A. L. C. S. et al. Co-crystals of non-steroidal anti-inflammatory drugs (NSAIDs): Insight toward formation, methods, and drug enhancement. **Particuology**, v. 58, p. 227–241, 2021.

NOGUEIRA, R. C. et al. Omeprazole induces vascular remodeling by mechanisms involving xanthine oxidoreductase and matrix metalloproteinase activation. **Biochemical Pharmacology**, v. 190, n. May, p. 114633, 2021.

NUNES COSTA, R. et al. Optimization and comparison of statistical tools for the prediction of multicomponent forms of a molecule: the antiretroviral nevirapine as a case study. **CrystEngComm**, v. 22, n. 43, p. 7460–7474, 2020.

NUNES, J. H. B. et al. Synthesis, spectroscopic characterization, crystallographic studies and antibacterial assays of new copper(II) complexes with sulfathiazole and nimesulide. **Journal of Molecular Structure**, v. 1112, p. 14–20, 2016.

PANTWALAWALKAR, J. et al. Novel curcumin ascorbic acid cocrystal for improved solubility. **Journal of Drug Delivery Science and Technology**, v. 61, n. November 2020, p. 102233, 2021.

PATEL, R. D. et al. Functionality improvement of Nimesulide by eutectic

formation with nicotinamide: Exploration using temperature-composition phase diagram. **Advanced Powder Technology**, v. 30, n. 5, p. 961–973, 2019.

PINDELSKA, E.; SOKAL, A.; KOLODZIEJSKI, W. Pharmaceutical cocrystals , salts and polymorphs : Advanced characterization techniques. **Advanced Drug Delivery Reviews**, v. 117, p. 111–146, 2017.

PRASAD, R.; RAKESH, M. Pharmaceutical cocrystallization: a review. **Int J Pharm Chem …**, v. 1, n. 3, p. 725–736, 2012.

PRIGOGINE, I.; DEFAY, R. **Chemical thermodynamics**. Glasgow: Longmans, 1954.

PSOMAS, G. Copper(II) and zinc(II) coordination compounds of non-steroidal anti-inflammatory drugs: Structural features and antioxidant activity. **Coordination Chemistry Reviews**, v. 412, p. 213259, 2020.

QIAO, N. et al. Pharmaceutical cocrystals: An overview. **International Journal of Pharmaceutics**, v. 419, n. 1–2, p. 1–11, 2011.

RAJPUT, L.; SANPHUI, P.; DESIRAJU, G. R. New Solid Forms of the Anti-HIV Drug Etravirine: Salts, Cocrystals, and Solubility. **Crystal Growth & Design**, v. 13, n. 8, p. 3681–3690, 2013.

RAMAMOORTHY, S.; CIDLOWSKI, J. A. Corticosteroids. **Rheumatic Disease Clinics of North America**, v. 42, n. 1, p. 15–31, 2016.

RODRÍGUEZ-BARRIENTOS, D. et al. Determination of pKa values of tenoxicam from 1H NMR chemical shifts and of oxicams from electrophoretic mobilities (CZE) with the aid of programs SQUAD and HYPNMR. **Talanta**, v. 80, n. 2, p. 754–762, 2009.

SABERI, A. et al. Development, recent advances, and updates in binary, ternary co-amorphous systems, and ternary solid dispersions. **Journal of Drug Delivery Science and Technology**, v. 86, p. 104746, 2023.

SANPHUI, P.; SARMA, B.; NANGIA, A. Phase Transformation in Conformational Polymorphs of Nimesulide. **Journal of Pharmaceutical Sciences**, v. 100, n. 6, p. 2287–2299, Jun. 2011.

SARDANA, V. et al. Are non-steroidal anti-inflammatory drug injections an

alternative to steroid injections for musculoskeletal pain?: A systematic review. **Journal of Orthopaedics**, v. 15, n. 3, p. 812–816, 2018.

SATHISARAN, I.; DALVI, S. V. Engineering cocrystals of poorlywater-soluble drugs to enhance dissolution in aqueous medium. **Pharmaceutics**, v. 10, n. 3, p. 1–74, 2018.

SAVJANI, K. T.; GAJJAR, A. K.; SAVJANI, J. K. Drug Solubility: Importance and Enhancement Techniques. **ISRN Pharmaceutics**, v. 2012, p. 1–10, 2012.

SCHULTHEISS, N.; NEWMAN, A. Pharmaceutical cocrystals and their physicochemical properties. **Crystal Growth and Design**, v. 9, n. 6, p. 2950–2967, 2009.

SHAIKH, R. et al. Pharmaceutical Cocrystal Drug Products: An Outlook on Product Development. **Trends in Pharmacological Sciences**, v. 39, n. 12, p. 1033–1048, 2018.

SHI, Q.; MOINUDDIN, S. M.; CAI, T. Advances in coamorphous drug delivery systems. **Acta Pharmaceutica Sinica B**, v. 9, n. 1, p. 19–35, 2019.

SILVA, J. F. C.; ROSADO, M. T. S.; EUSÉBIO, M. E. S. Structure and energetics of intermolecular association in two lurasidone co-amorphous drug systems. **Journal of Molecular Structure**, v. 1242, p. 130709, 2021.

SOARES, F. L. F.; CARNEIRO, R. L. Evaluation of analytical tools and multivariate methods for quantification of co-former crystals in ibuprofen-nicotinamide co-crystals. **Journal of Pharmaceutical and Biomedical Analysis**, v. 89, p. 166–175, 2014.

SOKAL, A. et al. Pharmaceutical properties of two ethenzamide-gentisic acid cocrystal polymorphs: Drug release profiles, spectroscopic studies and theoretical calculations. **International Journal of Pharmaceutics**, v. 522, n. 1–2, p. 80–89, 2017.

SOLARES-BRIONES, M. et al. Mechanochemistry: A green approach in the preparation of pharmaceutical cocrystals. **Pharmaceutics**, v. 13, n. 6, p. 1–49, 2021.

STAREK, M.; KRZEK, J. A review of analytical techniques for

determination of oxicams, nimesulide and nabumetone. **Talanta**, v. 77, n. 3, p. 925–942, 2009.

SU, H. et al. Syntheses and characterizations of two curcumin-based cocrystals. **Inorganic Chemistry Communications**, v. 55, p. 92–95, 2015.

SUROV, A. O. et al. Cocrystals of the antiandrogenic drug bicalutamide: Screening, crystal structures, formation thermodynamics and lattice energies. **CrystEngComm**, v. 18, n. 25, p. 4818–4829, 2016.

SZABÓ-RÉVÉSZ, P. Modifying the physicochemical properties of NSAIDs for nasal and pulmonary administration. **Drug Discovery Today: Technologies**, v. 27, p. 87–93, 2018.

TASAKI, Y. et al. Oxicam structure in non-steroidal anti-inflammatory drugs is essential to exhibit Akt-mediated neuroprotection against 1-methyl-4-phenyl pyridinium-induced cytotoxicity. **European Journal of Pharmacology**, v. 676, n. 1–3, p. 57–63, 2012.

THAKURIA, R. et al. Pharmaceutical cocrystals and poorly soluble drugs. **International Journal of Pharmaceutics**, v. 453, n. 1, p. 101–125, 30 Aug. 2013.

TSUME, Y. et al. The Biopharmaceutics Classification System: Subclasses for in vivo predictive dissolution (IPD) methodology and IVIVC. **European Journal of Pharmaceutical Sciences**, v. 57, p. 152–163, 2014.

TUBIČ, B. et al. Dissolution profile of nimesulide from pharmaceutical preparations for oral use. **Acta Chimica Slovenica**, v. 63, n. 1, p. 193–199, 2016.

UPPALA, S. et al. Exploring the utility of co-amorphous materials to concurrently improve the solubility and permeability of Fexofenadine. **Journal of Drug Delivery Science and Technology**, v. 72, p. 103431, 2022.

VISHWESHWAR, P. et al. Pharmaceutical co-crystals. **Journal of Pharmaceutical Sciences**, v. 95, n. 3, p. 499–516, 2006.

WANG, M. et al. Exploring the physical stability of three nimesulide–indomethacin co-amorphous systems from the perspective of molecular aggregates. **European Journal of Pharmaceutical Sciences**, v. 147, p. 105294, 2020.

WANG, M. et al. Similar but Not the Same: Difference in the Ability to Form Cocrystals between Nimesulide and the Pyridine Analogues. **Crystal Growth and Design**, v. 21, n. 1, p. 287–296, 2021a.

WANG, N. et al. Consistency and variability of cocrystals containing positional isomers: The self-assembly evolution mechanism of supramolecular synthons of cresol-piperazine. **IUCrJ**, v. 6, p. 1064–1073, 2019.

WANG, R. et al. Structural features and interactions of new sulfamethazine salt and cocrystal. **Journal of Molecular Structure**, v. 1229, p. 129596, 2021b.

WARD, A.; BROGDEN, R. N. Nimesulide: A Preliminary Review of its Pharmacological Properties and Therapeutic Efficacy in Inflammation and Pain States. **Drugs**, v. 36, n. 6, p. 732–753, 1988.

YADAV, A. et al. Co-crystals: A novel approach to modify physicochemical properties of active pharmaceutical ingredients. **Indian Journal of Pharmaceutical Sciences**, v. 71, n. 4, p. 359, 2009.

YANG, Z. et al. Drug-drug eutectic mixtures of celecoxib with tapentadol and milnacipran which could improve analgesic and antidepressant efficacy. **Journal of Drug Delivery Science and Technology**, v. 67, n. November 2021, 2022.

ZHANG, J. et al. Crystallization kinetics and molecular dynamics of binary coamorphous systems of nimesulide and profen analogs. **International Journal of Pharmaceutics**, v. 610, p. 121235, 2021.

ZHANG, Y.-X. et al. The comparative study of cocrystal/salt in simultaneously improving solubility and permeability of acetazolamide. **Journal of Molecular Structure**, v. 1184, p. 225–232, May 2019.

Appendix section

Table A.1 – Materials, and respective abbreviation, supplier, molecular weight, purity and CAS number.

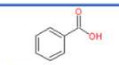
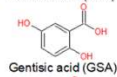
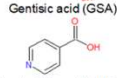
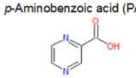
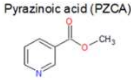
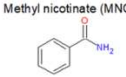
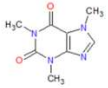
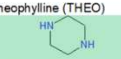
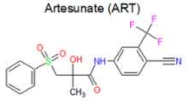
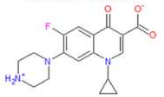
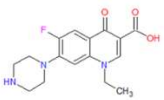
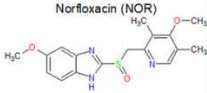
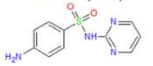
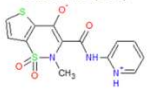
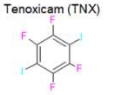
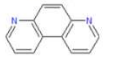
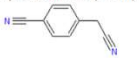
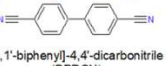
Compound	Acronym	Supplier	Molar weight (g/mol)	Purity (%)	CAS Number	Lot
Nimesulide	NMS	Local laboratory, Bauru, BR	308,31	≥98	51803-78-2	
Tenoxicam	TNX	Pharma Nostra, Araraquara, BR	337,37	≥98	59804-37-4	16J01-B001010799
Coformers						
[1,1'-biphenyl]-4,4'-dicarbonitrile	BPDCN	BLD Pharmatech GmbH	204,23	98	1591-30-6	DKY398
1,4-diiodotetrafluorobenzene	DITFB	Fluorochem	401,87		392-57-4	FCB112754
4-(cyanomethyl)benzonitrile	CMBN	BLD Pharmatech GmbH	142,16	95	876-31-3	BKC632
4,7-phenanthroline	PHEN	BLD Pharmatech GmbH	180,21	98	230-07-9	APC475
Artesunate	ART	BLD Pharmatech GmbH	384,42	98	88495-63-0	BGS257
Benzamide	BA	Sigma Aldrich	121,14	99,9	55-21-0	
Benzoic acid	BZA	Riedel-de Haen	122,12	99,9	65-85-0	11280
Bicalutamide	BICA	BLD Pharmatech GmbH	430,37	98	90357-06-5	BRY737
Caffeine	CAF	Fluka (Sigma Aldrich)	194,19	≥99	58-08-2	1428211
Ciprofloxacin	CIP	Sigma Aldrich	331,34	≥98	85721-33-1	
Gentisic acid	GSA	Sigma Aldrich	154,12	98	490-79-9	BCBM4330V
Hydrochlorothiazide	HCTZ	Sigma Aldrich	297,74	≥99	58-93-5	BCBL6365
Isoniazid	INH	Sigma Aldrich	137,14	≥99	54-85-3	MKCJ5583
Isonicotinic acid	INCA	Sigma Aldrich	123,11	99	55-22-1	STBG8975
Methyl nicotinate	MNCT	Sigma Aldrich	137,14	99	93-60-7	STBK5302
Metoclopramide	MET	BLD Pharmatech GmbH	299,8	99,96	364-62-5	RQC700
Nicotinamide	NA	Sigma Aldrich	122,12	≥99,5	98-92-0	BCBF9698V

Nicotinic acid	NCA	Sigma Aldrich	123,11	≥99,5	59-67-6	BCBS7378V
Norfloxacin	NOR	Local drugstore	319,33	≥98	70458-96-7	
Omeprazole	OMP	Tokyo Chemical Industry Co.	345,42	≥98	73590-58-6	E50MH-MC
***p*-Aminobenzoic acid**	PABA	Sigma Aldrich	137,14	≥99	150-13-0	MKCP140
Piperazine	PPZ	Sigma Aldrich	86,14	99	110-85-0	S62826-189
Piracetam	PIRA	Local drugstore (Portugal)	142,16		7491-74-9	
Proline	PRO	Sigma Aldrich	115,13	99	147-85-3	SHBL7134
Pyrazinoic acid	PZCA	Sigma Aldrich	124,1	99	98-97-5	S74693V
Saccharin	SAC	Sigma Aldrich	183,19	≥98	81-07-2	04336-087
Salicylamide	SLA	Fluka (Sigma Aldrich)	137,14	≥99	65-45-2	1284232
Sulfadiazine	SDZ	Flagron Ltda.	250,28	99,7	68-35-9	
Theobromine	TBM	BLD Pharmatech GmbH	180,16	98	83-67-0	BKP911
Theophylline	THEO	Sigma Aldrich	180,16	99	58-55-9	040M0069
trans-1,2-bis(4-pyridyl)ethylene	BPE	BLD Pharmatech GmbH	182,22	99,57	13362-78-2	CLA254
Tryptophan	TRYP	Sigma Aldrich	204,23	≥99,5	73-22-3	1400132V

Solvents / others

Acetonitrile	ACN	Merck Millipore, Germany	41,05	≥99,9	75-05-8	I0931130802
Ethanol	EtOH	Fisher Chemical, UK	49,07	≥99,8	64-17-5	1864185
Ethyl acetate	EA	Fisher Chemical, UK	88,11	≥99,8	141-78-6	1868743
Tween 80 (polysorbate 80)	P80	Sigma Aldrich	1310,00	d=1,064 g cm^{-3}	9005-65-6	BCCK0668
Sodium hydroxide	NaOH	JTBaker	40,00	98,7	1310-73-2	

Table A.2 – Virtual-experimental nimesulide screening results. (**CC** = cocrystal, **E** = a mixture with a eutectic composition; **A*** = coamorphous system obtained through quench cooling and/or cryomilling methods; **X =** no cocrystal formed). *Dashed section: Coformers used in the work of Wang et al. (2021).*

Coformer	COSMOquick prediction			Experimental results	
	Ranking	ΔH_{excess}	F_fit	Mechanochemical	Slurry
 Benzoic acid (BZA)	19	0,2865	3,8579	E	–
 Gentisic acid (GSA)	31	0,1784	4,7702	E	–
 Isonicotinic acid (INCA)	20	0,3459	3,9173	E	–
 Nicotinic acid (NCA)	21	0,3505	3,9219	E	–
 *p*-Aminobenzoic acid (PABA)	28	0,2619	4,3435	E / A *	–
 Pyrazinoic acid (PZCA)	22	0,3858	3,9572	E / A *	–
 Methyl nicotinate (MNCT)	13	-0,2443	3,3271	E	–
 Benzamide (BA)	18	0,1853	3,7567	E	–
 Salicylamide (SLA)	26	0,1275	4,2091	E	–
 Saccharin (SAC)	11	0,0463	3,1075	E	–
 Proline (PRO)	14	-0,1442	3,4272	E	–
 Tryptophan (TRYP)	33	0,0956	5,1976	E	–
 Caffeine (CAF)	3	-0,3348	2,7264	E	E
 Theobromine (TBM)	7	-0,1086	2,9526	E	E
 Theophylline (THEO)	10	-0,0033	3,0579	E	E
 Piperazine (PPZ)	4	-0,3236	2,7376	CC	CC
 Artesunate (ART)	34	0,2304	5,8426	E	–
 Bicalutamide (BICA)	35	0,1293	6,2517	E / A *	–
 Ciprofloxacin (CIP)	25	-0,4362	4,1556	E	E
 Isoniazid (INH)	27	0,12996	4,2116	E / A *	–
 Metoclopramide (MET)	36	0,0322	7,175	E / A *	–
 Norfloxacin (NOR)	24	-0,4634	4,1284	CC	CC
 Omeprazole (OMP)	32	-0,0746	5,0274	E / A *	–
 Piracetam (PIRA)	17	-0,3358	3,7458	E / A *	–
 Sulfadiazine (SDZ)	30	0,0595	4,6513	E	–
 Tenoxicam (TNX)	29	0,0087	4,6005	A *	–
 1,4-diiodotetrafluorobenzene (DITFB)	16	0,5293	3,5905	E	–
 4,7-phenanthroline (PHEN)	6	-0,2453	2,8159	E	–
 4-(cyanomethyl)benzonitrile (CMBN)	9	-0,0768	2,9844	E	–
 [1,1'-biphenyl]-4,4'-dicarbonitrile (BPDCN)	8	-0,1012	2,96002	E	–
pyrazine (PYE)	5	-0,2591	2,8021	X	X
4,4'-bipyridine (BP)	1	-0,4363	2,6249	CC	CC
trans-1,2-bis(4-pyridyl)ethene (BPE)	12	-0,4508	3,1206	CC	CC
1,2-bis(4- pyridyl)ethyne (BPY)	2	-0,3558	2,7054	CC	CC
1,2-bis(4-pyridyl)ethane (BPA)	15	-0,583	3,4986	CC	CC
1,3-bis(4-pyridyl)propane (BPP)	23	-0,5917	4,0001	X	X

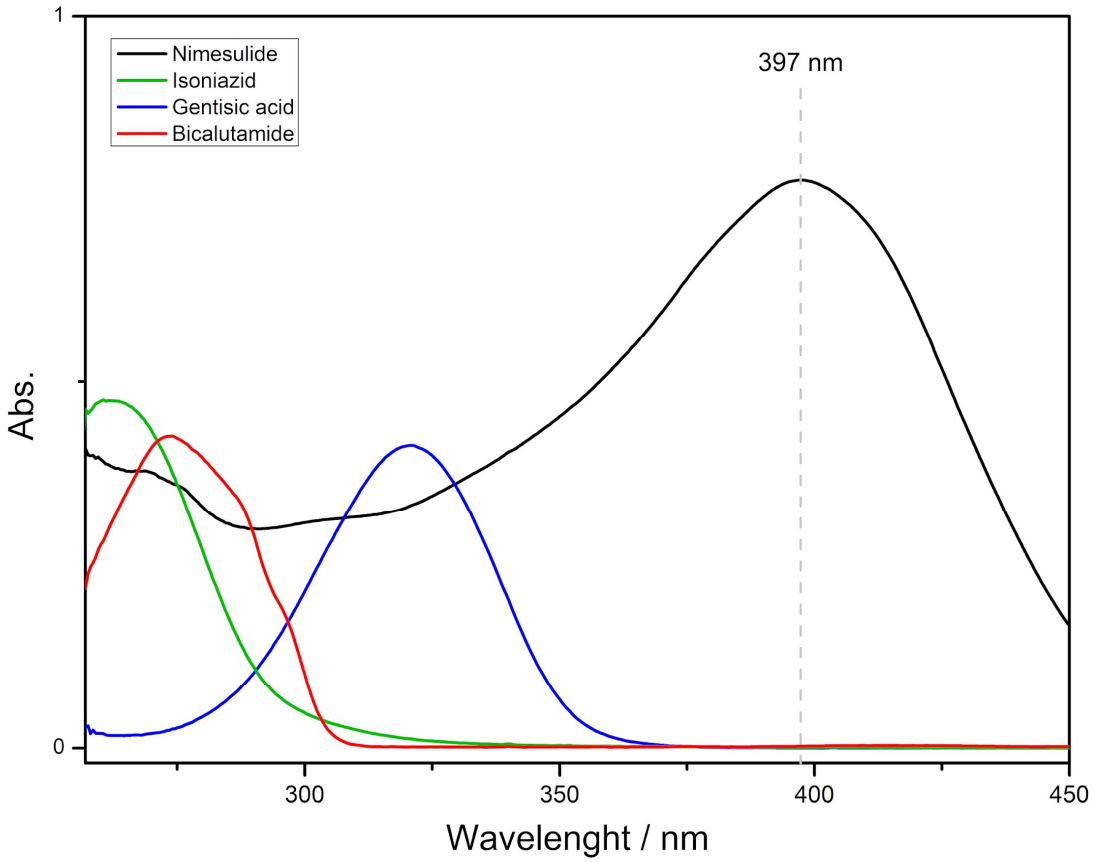


Figure A.1 – Selectivity essay of NMS, BICA, GSA and INH in phosphate buffer pH 7.4 with 2% (v/v) of tween 80.

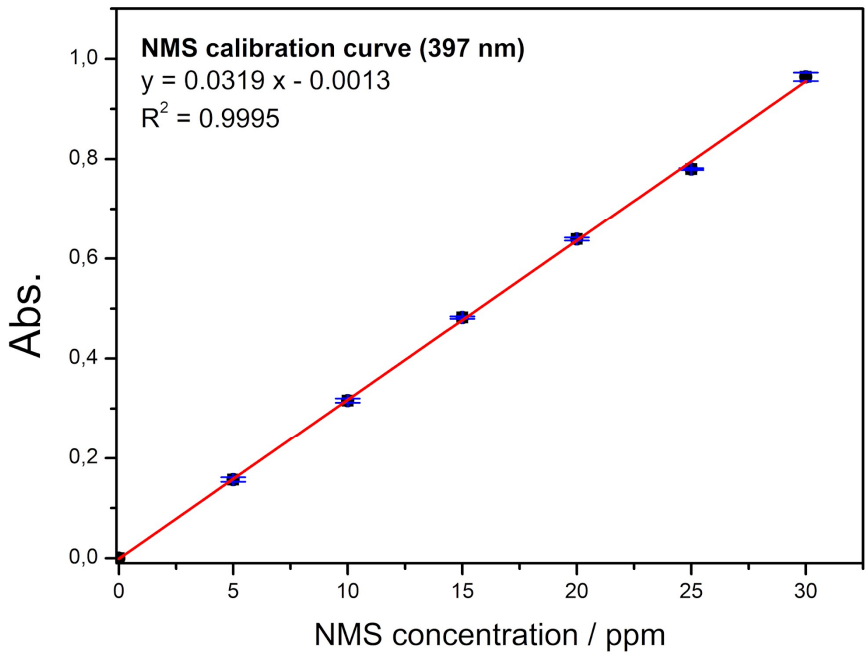


Figure A.2 – Calibration curves of pure NMS in phosphate buffer pH 7.4 with 2% (v/v) of tween 80 (prepared at 397 nm).

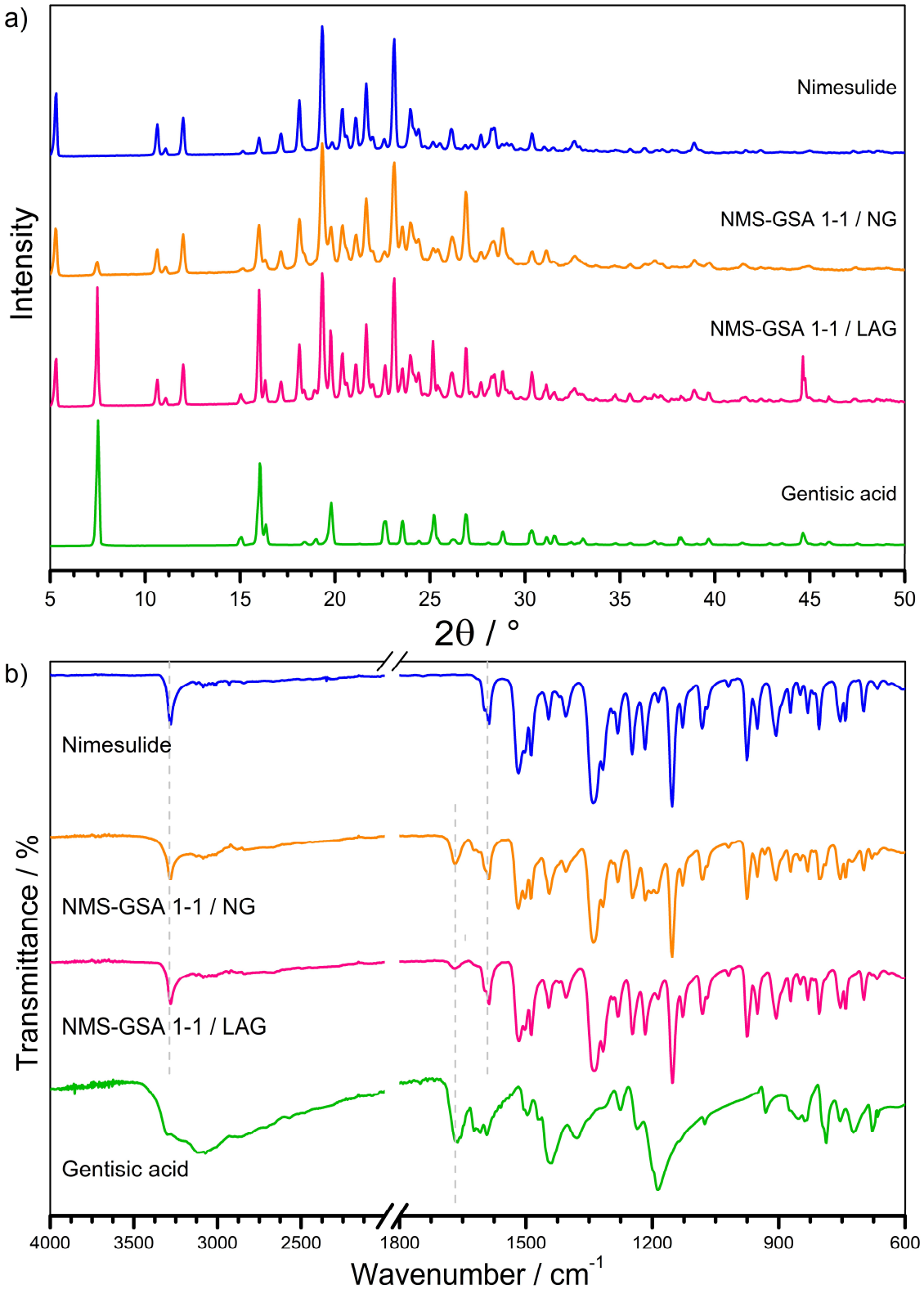


Figure A.3 – PXRD pattern (a) and FTIR spectra (b) of NMS-GSA equimolar system and pure compounds.

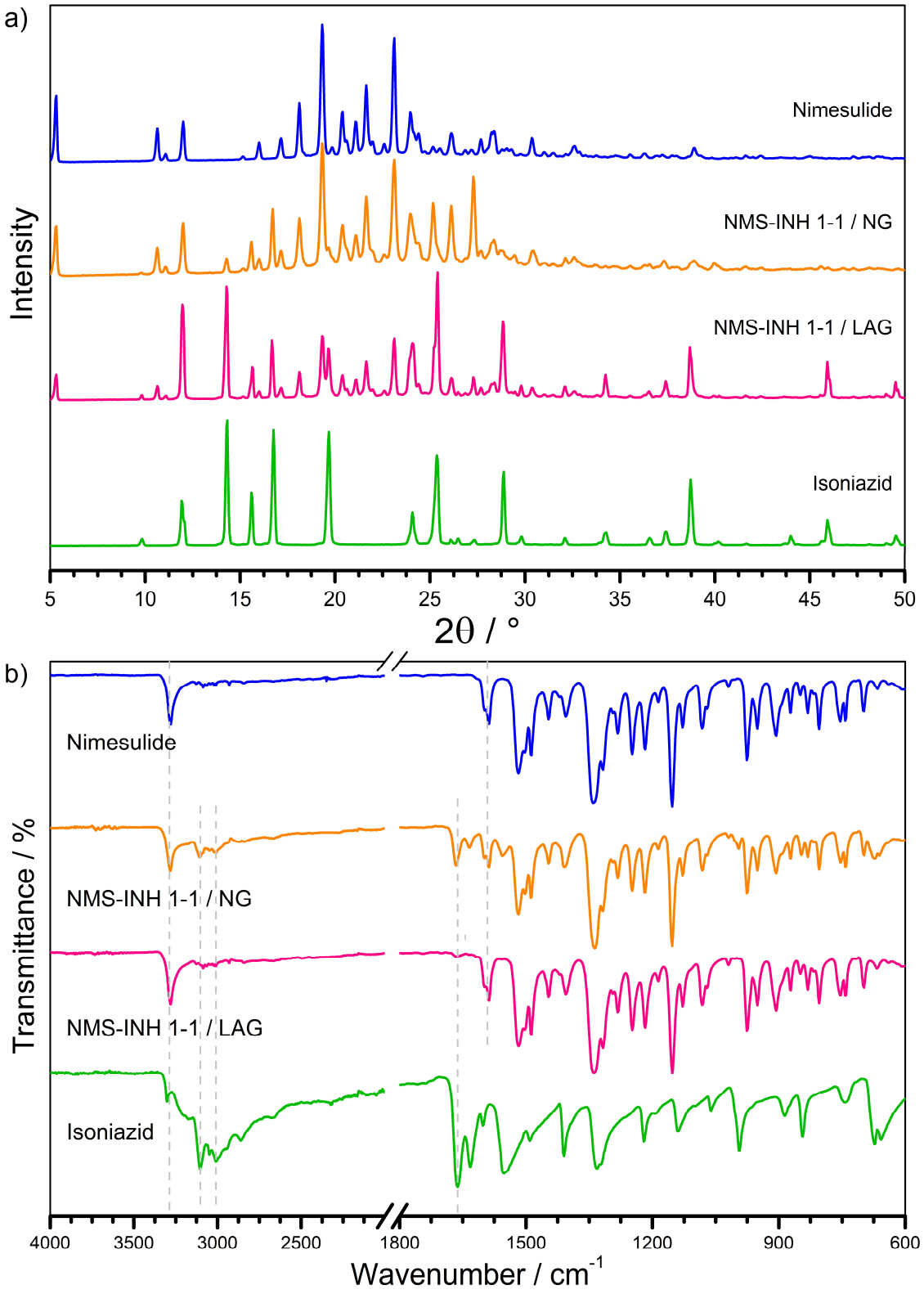


Figure A.4 – PXRD pattern (a) and FTIR spectra (b) of NMS-INH equimolar system and pure compounds.

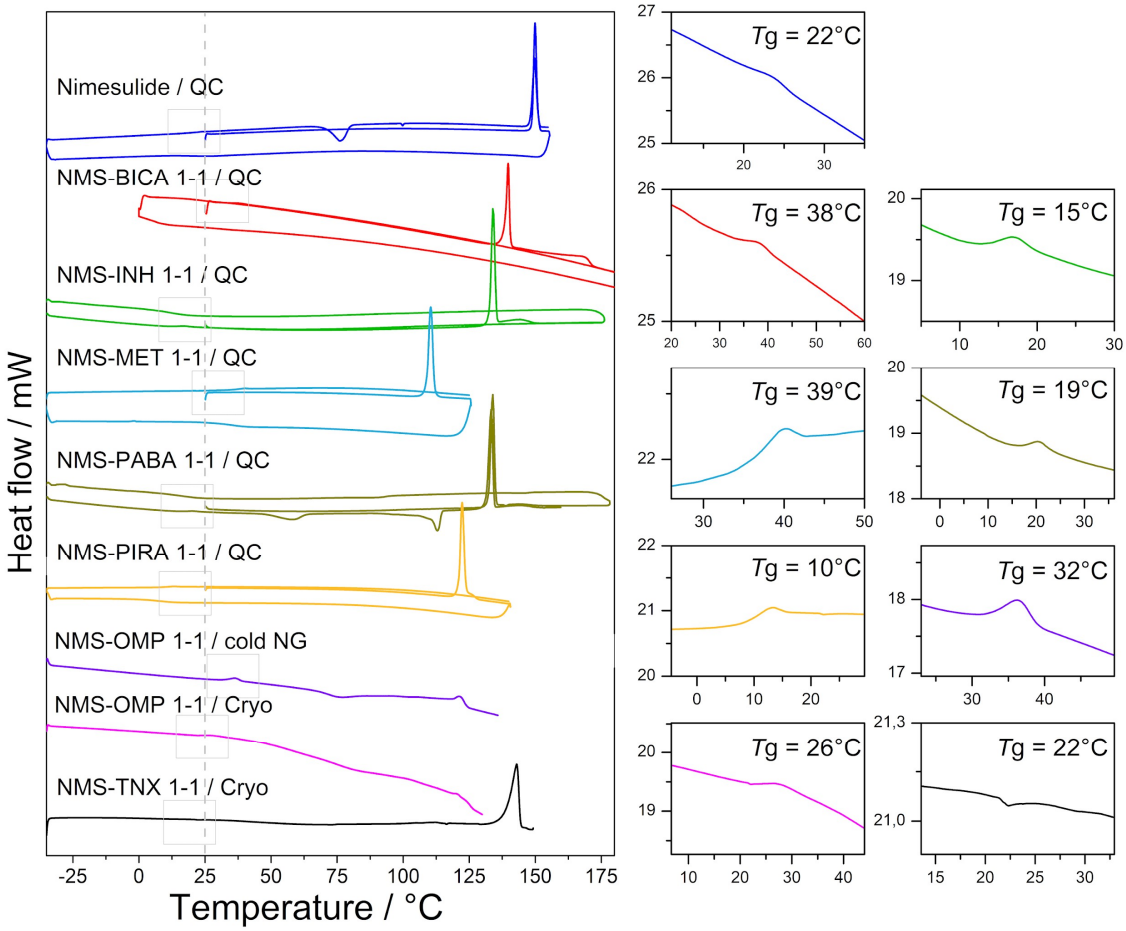


Figure A.5 – DSC curves of NMS coamorphous systems obtained *via* quench cooling (QC), cryomilling (Cryo) and/or “cold NG”.

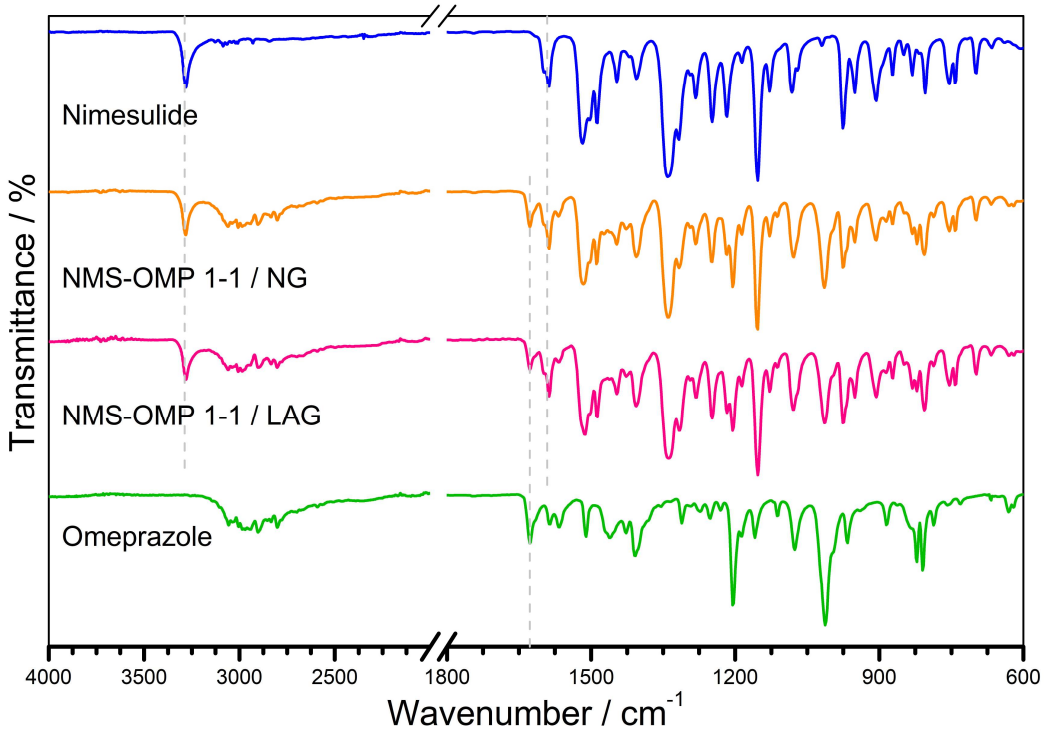


Figure A.6 – FTIR spectra of NMS-OMP equimolar system and pure compounds.

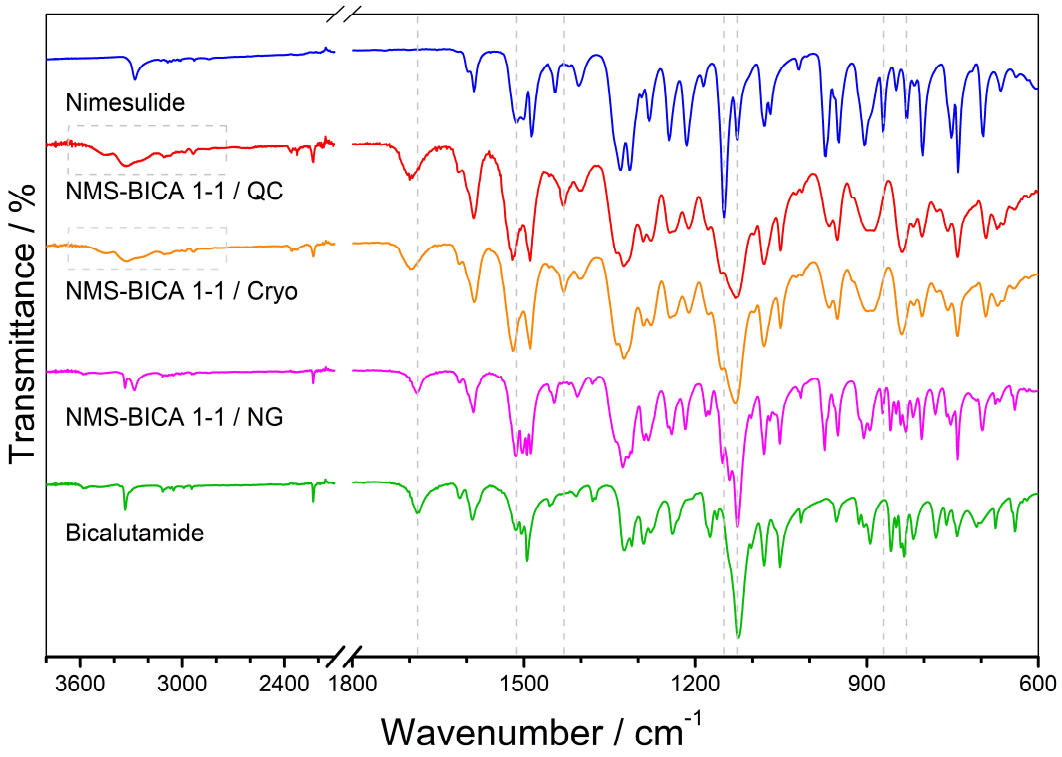


Figure A.7 – FTIR spectra of NMS-BICA equimolar mixture and pure compounds.